Titre: Title:	Characterization of porous nickel-titanium alloys for medical applications
Auteur: Author:	Rommy Hernandez Tenorio
Date:	2008
Type:	Mémoire ou thèse / Dissertation or Thesis
Référence: Citation:	Hernandez Tenorio, R. (2008). Characterization of porous nickel-titanium alloys for medical applications [Thèse de doctorat, École Polytechnique de Montréal]. PolyPublie. https://publications.polymtl.ca/8135/

URL de PolyPublie: PolyPublie URL:	https://publications.polymtl.ca/8135/
Directeurs de recherche: Advisors:	L'Hocine Yahia, & Oumarou Savadogo
Programme: Program:	Génie biomédical

UNIVERSITÉ DE MONTRÉAL

CHARACTERIZATION OF POROUS NICKEL-TITANIUM ALLOYS FOR MEDICAL APPLICATIONS

ROMMY HERNANDEZ TENORIO

INSTITUT DE GÉNIE BIOMEDICAL

ÉCOLE POLYTECHNIQUE DE MONTREAL

THÈSE PRÉSENTÉE EN VUE DE L'OBTENTION

DU DIPLÔME DE PHILOSOPHIAE DOCTOR (Ph.D.)

(GÉNIE BIOMEDICAL)

AVRIL 2008

UNIVERSITÉ DE MONTRÉAL

ÉCOLE POLYTECHNIQUE DE MONTRÉAL

Cette thèse intitulée:

CHARACTERIZATION OF POROUS NICKEL-TITANIUM
ALLOYS FOR MEDICAL APPLICATIONS

présentée par : HERNANDEZ TENORIO Rommy
en vue de l'obtention du diplôme de: Philosophiae Doctor
a été dûment acceptée par le jury d'examen constitué de:

M. AUBIN Carl-Eric, Ph.D., président
M. YAHIA L'Hocine, Ph.D., membre et directeur de recherche
M. SAVADOGO, Oumarou, D. d'État, membre et codirecteur de recherche
M. L'ESPERANCE Gilles, Ph.D., membre
M. ASSAD Michel, Ph.D., membre

Dedicated to my parents, Elisa Tenorio Márquez y Antonio Hernández Montes,

my brother, Antonio Hernández Tenorio,

my grandmother Catalina Márquez Martínez,

my aunt Olga Tenorio Márquez

and Andrew Stairs

Acknowledgments

I owe my warmest appreciation to my advisor, Professor L'Hocine Yahia, for proposing this interesting project and introducing me to the scientific research and community.

I express my special recognition to my coadvisor, Professor Oumarou Savadogo, without his support and supervision this work could not been taken to term.

I am grateful to Professor Sylvain Turenne for his scientific advice and criticism.

During these years the support of all the students at the LIAB and the neighbours laboratories has been particularly valuable, they provided with a nice and warm environment and their candid support. I would like to express my warmest thanks to Benjamin Boyer for his cell's drawings. Thank you all.

Through out this project I had the opportunity to collaborate with people in different laboratories, Suzie Poulin and Marie France Pepin, were patient and kind enough to help me with the XSP analyses. I am also thankful to all the personal at the $(CM)^2$ for the time they dedicated to facilitate my investigations and José Laviolette for her great pictures. I wish to thank Carole Massicotte, for her precious assistance and friendship.

I am deeply grateful to Teko Napporn, not only because of his scientific guidance, tolerance and encouragement, but also for his invaluable friendship through these past years. The bill keeps growing!

I would like also to thank Huimin, Cissé, Youcef, Javier, Fréderic, Kentaro, Marc and Rafael for their significant help and warmest welcome in their laboratory.

My loving thanks to my parents, Elisa and Antonio, and my brother, as well as my grandmother and Mechas, for their support and encouragement throughout my life. Their love and confidence despite the distance made this possible.

I wish to thank Andrew, for his optimism and encouragement that help me to conclude this project. You walked me through this important stage and taught me how strong I am. I couldn't make it with out you!

I would like to express my sincere gratitude, to the members of the jury for taking the time to review this work. I could not forget Mrs. Cournoyer who advised me through the process of the deposition.

Abstract

Porous NiTi alloys are a promising material for bone replacement, due to their mechanical properties and porous structure. The use of these alloys to fabricate medical devices has been slow down by the scientific community due to the high content of Ni. Solid NiTi alloys have been used for several decades in medical applications in particular for the fabrication of cardiovascular and dental devices. Recent studies showed visible signs of corrosion on cardiovascular implants at an early stage of implantation (5 months), this fact can be regarded as the beginning of material failure. Therefore the understanding and evaluation of the corrosion resistance of these alloys is needed. The purpose of this study is to investigate the electrochemical behaviour of porous NiTi alloys provided by different sources. In order to achieve this goal, a systematic characterization of the physical and chemical properties by different techniques and new approaches were conducted. The martensite-austenite phase transition was determined by the use of the Differential scanning Calorimetry (DSC). The morphological characteristics (porosity and roughness) were measured with the Scanning Electron Microscopy (SEM). The surface chemical composition of the samples was identified by the use of X-ray Photoelectron Spectroscopy (XPS) and Auger Electron Spectroscopy (AES).

The corrosion was evaluated by the used of the Voltammetry (Potentiodynamic mode) and the In-situ Fourier Transformed Infrared Reflectance Spectroscopy coupled to the voltammetry technique (Spectroelectrochemistry). In fact this is the first time that the spectroelectrochemistry technique is used to investigate the electrochemical behaviour of NiTi alloys. This *in situ* method allows the determination of the resulting chemical reactions due to the interaction between the material and its environment. The use of solid NiTi alloy as reference allowed us to compare and better understand the corrosion resistance of the porous samples.

In the case of porous material the biomechanical compatibility is closely related to the porosity distribution of the sample. To describe appropriately the influence of this parameter on the properties of NiTi, four types of materials provided by different sources were analyzed. The samples were produced by Self-propagating High-temperature Synthesis (SHS) procedure. A heat treatment was applied in order to release internal stress created during forming processes, one series of specimens from each type was submitted to an annealing process during 30 min at 550°C in an air atmosphere. Its influence on the properties of the materials was also evaluated.

Our first results showed that despite the fact that all the materials present different pore size, all the samples exhibited an open and interconnected porosity that promotes a good fixation and bone ingrowth within their structure. The thermal analysis showed that the temperature of the inception of the martensite-austenite phase transition occurs at 60°C, which is greater than the body temperature by 20°C. The microscopic analysis for the samples revealed that the heat treatment did not generate any morphological changes. The XPS study indicated that the surface oxidation occurs after the heat treatment. This oxide layer has a different thickness for the materials in the range of 310 - 3990 Å.

The evaluation of the corrosion resistance of the four porous NiTi alloys showed a correlation between the chemical composition, pore size and the electrochemical behaviour. In particular it was found that the corrosion resistance is related to the surface chemical composition of the electrodes rather than to their surface morphology. First we observed that the impact of the annealing process varies with the type of sample. The non-treated samples showed higher breakdown potentials and also bigger pores. The materials with a pore size in the range of 80-120μm showed different behaviours, one material (B) showed no visible effect while the other two (A and C) exhibited a decrease of the breakdown potential value. The material with the smallest pore size 35-50μm showed an important improvement after the heat treatment. Therefore, we can conclude,

that the surface treatment used in our investigations led to an improvement of the corrosion resistance for small pores whereas a decrease was observed for bigger pores.

On the other hand the lower corrosion rates observed on treated samples are an indication of the high corrosion resistance compare to those non-treated. In this case we observed that the one material (B) exhibited the highest corrosion rate presented a difference in the chemical composition as shown by XPS analysis. Moreover, the absence of intermediate titanium oxides (Ti^{2+} and Ti^{3+}) was observed. As these oxides were identified in the other materials (A, C and D) we conclude that the presence of intermediate titanium oxides on surface chemical composition of the samples results on better corrosion rates and improved corrosion resistance.

The Spectroelectrochemistry evaluation showed that solid electropolished sample and solid mechanopolished samples exhibited a better corrosion resistance than porous mechanopolished samples. However the solid mechanopolished sample exhibits a higher corrosion rate almost as high as the one showed by the porous sample. On the other hand a higher breakdown potential was measured porous samples compared to previous studies. However this sample shows a higher susceptibility for pitting and crevice corrosion. This can be explained by the porous structure of the sample. The FTIR results showed the interactions between the solution and the samples. It can be observed that each sample exhibit a particular behaviour. The porous sample as well as the solid samples showed Ti-OH interactions. Moreover both solid samples exhibited another peak corresponding to the OTi(OH)CCH interaction, which is explained by the chemical composition of the electrolyte, in this case the Hank's solution that has a certain amount of glucose. However an inversion of the peak is observed in both samples, this direction change can be attributed to the surface treatment. The electropolished sample showed a more stable behaviour mean while the mechanopolished sample exhibited a change during the reverse scan.

Résumé

Les alliages poreux de NiTi sont des matériaux très prometteurs pour le replacement de l'os, à cause de leurs propriétés mécaniques et leur structure poreuse. Toutefois le pourcentage élevé de Ni contenu dans l'alliage inquiète encore la communauté scientifique et freine considérablement l'introduction de ce biomatériau. Les alliages de NiTi solides sont déjà utilisés pour la fabrication des implants médicaux particulièrement pour des applications cardiovasculaires et dentaires. Cependant, des études récentes ont montré après l'implantation l'apparition de corrosion sur les dispositifs cardiovasculaires plutôt que prévu. En conséquence une évaluation et une compréhension approfondies de la résistance à la corrosion de ces alliages sont nécessaires. Ainsi l'objectif de cette étude est de caractériser les alliages de NiTi poreux à travers une étude de leur résistance à la corrosion en utilisant de nouvelles approches. La voltammétrie ou polarisation, la Spectroscopie Photoélectronique par rayons-X (XPS), la Spectroscopie Auger (AES), la Calorimétrie Différentielle (DSC), la Microscopie Électronique à Balayage (SEM) et la Spectroscopie Infrarouge à Transformée de Fourrier FTIR *in situ* sont autant de techniques qui sont utilisées pour atteindre notre objectif.

La corrosion de ces matériaux a été réalisée par la Voltammetrie simple en mode potentiodynamique puis *in situ* en la couplant avec la Spectroscopie Infrarouge de Réflexion à Transformée de Fourier (Spectroelectrochimie). D'ailleurs, c'est la première fois que cette méthode est utilisée pour caractériser ces alliages. Elle permet de déterminer les espèces issues de l'interaction entre le matériau et son environnement en fonction du potentiel.

Dans le cas de matériaux poreux, la biocompatibilité mécanique est étroitement reliée à sa porosité. Pour bien décrire l'influence de ce paramètre sur les propriétés des alliages NiTi, quatre types de matériaux fournis par différents laboratoires ont été analysés. Les échantillons ont été fabriqués avec la méthode de synthèse par combustion (SHS), suivi

d'un traitement thermique à 550°C pendant 30 min dans l'air pour supprimer les contraintes internes provenant du procédé de fabrication et pour optimiser leur comportement mécanique et leur biocompatibilité.

Les résultats ont montré que malgré une taille de pore différente, tous les échantillons présentent, des pores ouvertes et interconnectés qui favorisent une meilleure fixation biologique et la croissance de l'os dans le réseau des canaux. Les analyses thermiques ont indiqué que la température du début de la transition de phase martensite-austenite, se produit à 60°C, laquelle est 20°C plus élevée que la température du corps humain. Aussi, le traitement thermique appliqué n'a pas généré des changements au niveau de la porosité des échantillons. L'analyse XPS des quatre types de matériaux indique que la surface subit une oxydation lors du traitement thermique. La couche d'oxyde présente différentes épaisseurs pour les matériaux dans une plage de 310 - 3990 Å.

L'étude de la corrosion de ces quatre types d'échantillons a permis de faire une corrélation entre leur comportement électrochimique, leur composition chimique et la taille de leurs pores. Plus particulièrement, nous avons montré que la résistance à la corrosion est reliée à la composition chimique des électrodes plutôt qu'à la morphologie de leur surface. Dans un premier temps nous avons observé que l'influence du traitement thermique sur la résistance à la corrosion varie en fonction de la morphologie de l'échantillon. Les potentiels de ruptures mesurés étaient plus élevés pour les échantillons non traités ayant une grande taille de pores. Les matériaux ayant une taille de pores dans une plage de 80-120µm ont montré différents comportements : sur un matériau (B) il n'a pas eu d'effet, tandis que dans les deux autres (A et C) une diminution de la valeur du potentiel de rupture a été constatée. Une amélioration importante a été observée sur le matériau (D) ayant la plus petite taille de pores (35-50µm).

Par conséquent, nous avons conclu que l'application du traitement de surface a un effet positif sur les échantillons ayant une petite taille de pores. Aussi il est observé un taux de

corrosion plus faible pour les échantillons traités. Ce qui indique que leur résistance à la corrosion est plus élevé. En effet le matériau B qui exhibait le taux de corrosion plus élevé présentait l'absence de certaines espèces d'oxydes de titane II (Ti^{2+}) ou III (Ti^{3+}). Ayant pu identifier ces espèces dans les autres échantillons (A, C et D), nous en déduisons que la présence des espèces intermédiaires d'oxyde de titane dans l'échantillon entraîne des meilleurs taux de corrosion ainsi que l'amélioration de sa résistance à la corrosion. L'étude par spectroélectrochimie a montré que les échantillons solides possèdent une meilleure résistance à la corrosion que l'échantillon poreux. Cependant, l'échantillon solide poli mécaniquement présente un taux de corrosion aussi élevé que celui du poreux. Nous avons observé que les potentiels de rupture mesurés pour ce dernier sont supérieurs à ceux qui sont mentionnés dans la littérature. Par contre, sa prédisposition à la corrosion par piqûration et crevasse reste élevée. Ceci peut être expliqué par la structure poreuse de l'échantillon. Les résultats de l'étude infrarouge ont aussi montré que chaque type d'échantillon interagit d'une façon particulière. Des interactions Ti-OH ont été observées sur l'échantillon poreux. Il en est de même pour les autres échantillons solides. Sur ces derniers, un pic correspondant à l'interaction OTi(OH)CCH a été observé. Ceci se justifie par le fait que la solution de Hank's qui est notre électrolyte contient du glucose. Cependant une inversion du pic est observée avec les échantillons solides. Ce changement pourrait être dû au traitement de surface. L'échantillon poli par électrochimie présente un comportement plus stable tandis que l'échantillon mécaniquement poli montre un changement de comportement pendant la variation négative de potentiel.

En conclusion, les résultats ont montré que la composition chimique en plus de la taille de pore, à un rôle important sur la résistance à la corrosion, autrement dit sur la biocompatibilité. La résistance à la corrosion d'un alliage poreux de NiTi a été étudiée puis comparée à celle des alliages solides. Il a été observé que les alliages du NiTi poreux présente une prédisposition à la corrosion par piqûration et crevasse élevée.

Condensé en français

1. Introduction

Des alliages Nickel-Titane ayant une structure interne poreuse ont été déjà utilisés depuis approximativement une décennie dans la chirurgie maxillo-faciale [33] et dans d'autres procédures orthopédiques [5, 34-36] sur des milliers de patients en Russie [6-7] et en Chine [5,8]. Cependant, l'intérêt de l'utilisation de ces matériaux augmente toujours dans plusieurs secteurs du domaine biomédical, comme par exemple le développement d'implant à mémoire de forme de conception spéciale. Dans ce contexte, de nouvelles connaissances sont nécessaires pour comprendre le rapport entre les propriétés fondamentales des matériaux et la réponse du dispositif biomédical utilisé. Les facteurs clés identifiés dans l'utilisation de ces alliages comme des matériaux pour implants, sont leur propriété capillaire et la compatibilité biomécanique (i. e. module élastique et capacité d'amortissement proches de celui de l'os). Le comportement capillaire dépend fortement de la structure interne du matériau. En effet, la force capillaire contrôle le transport du liquide à travers les canaux des pores connectés et la mouillabilité du matériau, à cause de l'influence exercée sur la vitesse et la hauteur maximale atteinte par le liquide dans les capillaires [37-38]. La combinaison optimale de ces deux caractéristiques favorise la pénétration de la moelle osseuse et des cellules dans la structure interne de l'implant. Cela offre une meilleure fixation biologique (ostéointégration) de l'implant NiTi poreux dans différents types de tissu.

Une porosité interconnectée est essentielle pour assurer la croissance de l'os dans le réseau des canaux près de la surface entretenant la vascularisation, la viabilité à long terme, et la possibilité d'une fixation désirable. Il a été trouvé que la taille de pore optimale se situe dans la gamme de 100-400 μm [39].

La porosité affecte aussi le comportement mécanique du matériau [40]. Une bonne correspondance entre le module d'élasticité de Young de l'os (20 GPa) et celui de l'implant est nécessaire. Les alliages de NiTi ont montré des valeurs plus proches de celles de l'os dans la phase martensite (28-41 GPa). Une structure interne caractérisée par une porosité de 50 %, diminue cette plage de valeur ; des valeurs du module d'élasticité entre 14-20 GPa permettent la possibilité d'une croissance osseuse significative.

Les alliages de NiTi poreux peuvent être produits par divers procédés de métallurgie des poudres. Nous avons choisi la synthèse par combustion solide (Self-propagating High-temperature Synthesis (SHS)) ou frittage réactif qui permet de contrôler le gradient de porosité, ajuster la taille des pores connectés et de créer une morphologie semblable à celle de l'os. Les échantillons ont été fournis par nos collaborateurs, Prof. Moore (Colorado School of Mines), Prof. Victor E. Gjunter (Institute of Medical Materials and Shape Memory Implants), Prof. B. Silberstein (Institute of Medical Materials and Shape Memory Implants), Dr. Tae-Hyun Nam (Division of Materials Science and Engineering) Ils ont été fabriqués dans leur laboratoires en utilisant des réacteurs de synthèse.

La biocompatibilité de NiTi poreux a été démontrée comparable à celle de l'acier inoxydable, du chrome, du cobalt et du titane. Shabalovskaya *et al*, ont effectué une étude *in vitro* et ont conclu que le NiTi poreux ou solide, est aussi bien accepté par des tissus humains que le Titane pur [49]. Basé sur des études *in vitro* et *in vivo*, Rhalmi *et al*., sont parvenus aux mêmes résultats et ils ont observé une croissance de l'os dans les pores de l'implant trois semaines après son implantation [50]. Toutefois le pourcentage élevé de Ni inquiète encore la communauté scientifique et freine considérablement l'introduction de ce biomatériau. Comme la libération des ions Ni est reliée à la résistance à la corrosion cette thèse vise à élucider le comportement en corrosion de ces alliages.

L'objectif de cette étude est de caractériser des alliages de NiTi poreux et de fournir une meilleure compréhension à la résistance à la corrosion de ces alliages par l'utilisation de nouvelles approches. La couche d'oxyde sera considérée comme le facteur le plus important. Dans un premier temps une caractérisation systématique d'alliage de NiTi poreux pour déterminer les propriétés physiques et les caractéristiques de surface sera réalisée. Pour décrire convenablement l'influence des caractéristiques de ces NiTi sur les propriétés à mémoire de forme, quatre types de matériaux fournis par différentes laboratoires préparés par la méthode de synthèse par combustion (SHS) seront analysés. Pour optimiser le comportement mécanique et la biocompatibilité du matériau et pour supprimer les contraintes internes provenant du procédé de fabrication nous avons utilisé des traitements thermiques (550°C pendant 30 min dans l'air). L'analyse thermique montrera les changements produits sur la température de transformation de l'échantillon par le traitement thermique.

Une étude du comportement électrochimique a été réalisée sur les différents échantillons. L'influence du traitement thermique sur la résistance à la corrosion et la composition chimique sera analysée. Notre hypothèse est que la composition chimique de la surface ainsi que la porosité jouent un rôle important sur le comportement électrochimique des alliages NiTi poreux étudiés. Une caractérisation a été réalisée in situ en utilisant la technique de Spectroscopie Infrarouge de Réflexion à Transformée de Fourier. Cette caractérisation devrait nous conduire à une meilleure compréhension des interactions entre la surface de l'électrode et le milieu utilisé. Trois échantillons différents ont été étudiés : un échantillon poreux poli mécaniquement, un échantillon solide poli mécaniquement et un échantillon solide poli électrochimiquement. Les échantillons ayant subi un traitement de polissage électrochimique sont bien connus par leur résistance élevée à la corrosion. La comparaison permettra donc une meilleure compréhension du comportement électrochimique des alliages de NiTi.

2. Procédure Expérimentale

2.1 Matériaux

Les différents échantillons poreux ont été nommés A, B, C et D en fonction du fournisseur. Les spécimens cylindriques, avec une épaisseur de 5 millimètres et un diamètre de 10 millimètres ont été coupés à partir de tiges poreuses avec une scie à diamant pour éviter de modifier leur structure interne. Ils ont été nettoyés pendant 10 minutes par ultrason en utilisant de l'acétone et par la suite du méthanol grâce à un appareil Branson, le Modèle 2510.

Des échantillons solides de NiTi ont été aussi fournis par Dr. Ming Wu de la compagnie Memry. Les échantillons ont suivi deux différents types de traitement de surface: le polissage mécanique et l'électropolissage. Ces traitements ont été réalisés par le fournisseur.

2.2 Méthodes

Les techniques expérimentales utilisées ont mené à une caractérisation de : la température de transformation, la morphologie, la surface de nos alliages. De plus, une étude électrochimique a été réalisée pour évaluer la résistance à la corrosion. Une série de spécimens de chaque échantillon a été soumis à un traitement thermique pendant 30 minutes à 550°C dans l'air [77]. Le nettoyage a été effectué après le traitement.

3. Résultats

3.1 Propriétés physiques et caractéristiques de surface

Le matériau A, présente une taille de pore de 80-120 µm tel que révélé par observation en Microscopie Électronique à Balayage (SEM). Dans le cas du matériau B, nous avons observé une distribution homogène des pores, avec une taille de 100 µm pour les pores isolés. Les observations sur le matériau C montrent une taille de pores de 100 µm. La porosité du matériau D est différente par rapport aux trois autres types d'échantillons. Les pores présentent un diamètre de 35-50 µm. Aucun changement de la porosité n'a été observé après le traitement thermique. La taille des pores moyens (100-120 µm) révèle une structure interne favorable aux phénomènes capillaires [39]. Tous les matériaux présentent une structure connectée qui augmente la croissance de l'os ainsi qu'une bonne fixation de l'implant.

Les résultats des analyses thermiques (DSC) effectuées sur les différents matériaux ont révélé un profil de courbe ne changeant pas entre 0 et 50°C, donc nous concluons que les échantillons se trouvent dans la phase martensite à la température du corps. Aucune différence significative dans le comportement thermal n'a été observée avant et après le traitement thermique, sauf pour le matériau A où un nouveau pic est apparu ce. qui pourrait correspondre à la phase R, semblablement apparu suite au traitement thermique étant donne qu'il s'agit d'une alliage equiatomique. Il reste à confirmer l'apparition de la phase R par la microscopie à transmission et la diffraction des rayons X.

L'analyse XPS indique que la surface subit une oxydation après le traitement thermique pour tous les quatre types de matériau. La surface des échantillons est principalement composée d'oxyde de Titane et d'oxyde de Nickel en quantité moins élevée. Les résultats de l'analyse AES, permettent de calculer l'épaisseur ainsi que la composition chimique de

la couche d'oxyde. Les résultats ont montré que le traitement thermique a augmenté la couche d'oxyde.

3.2 Caractérisation électrochimique

Les résultats de la caractérisation électrochimique montrent que l'échantillon A non traité montre un potentiel de rupture plus élevé que celui de l'échantillon traité. En ce qui concerne le matériau B, les deux échantillons (traités et non traités) suivent le même comportement, la différence entre les valeurs du potentiel de rupture étant négligeable. L'échantillon traité C a une valeur plus faible. Le matériau C suit à peu près le même comportement que le matériau A. Cependant les valeurs du potentiel de corrosion sont semblables pour les échantillons traités et non-traités. Contrairement au matériau précédent, l'échantillon D traité montre un potentiel de rupture plus élevé par rapport au matériel non-traité.

Les analyses microscopiques montrent que tous les échantillons présentent des changements dans leur porosité après les tests de corrosion. De fait, les bords des pores sont plus affectés. Il est même possible d'observer que la corrosion se fait en surface mais aussi en profondeur.

3.3 Spectroscopie Infrarouge de Réflexion in situ à Transformée de Fourier

L'étude par spectroélectrochimie a montré que les échantillons solides possèdent une meilleure résistance à la corrosion que l'échantillon poreux. Cependant, l'échantillon solide poli mécaniquement présente un taux de corrosion aussi élevé que celui du poreux.

Nous avons observé que les potentiels de rupture mesurés pour ce dernier sont supérieurs à ceux qui sont mentionnés dans la littérature. Par contre, sa prédisposition à la corrosion par piqûration et crevasse reste élevée. Ceci peut être expliqué par la structure poreuse de l'échantillon. Les résultats de l'étude infrarouge ont aussi montré que chaque type d'échantillon interagit d'une façon particulière. Des interactions Ti-OH ont été observées sur l'échantillon poreux. Il en est de même pour les autres échantillons solides. Sur ces derniers, un pic correspondant à l'interaction OTi(OH)CCH a été observé. Ceci se justifie par le fait que la solution de Hank's qui est notre électrolyte contient du glucose. Cependant une inversion du pic est observée avec les échantillons solides. Ce changement pourrait être dû au traitement de surface. L'échantillon poli par électrochimie présente un comportement plus stable tandis que l'échantillon mécaniquement poli montre un changement de comportement pendant la variation négative de potentiel.

4. Discussion

Dans un premier temps la caractérisation physico-chimique des différents matériaux a montré que la taille des pores moyens (100-120 µm) révèle une structure interne favorable aux phénomènes capillaires [39]. Tous les matériaux étudiés présentent une structure connectée qui augmente la croissance de l'os et la bonne fixation de l'implant. Les échantillons se trouvent dans la phase martensite à la température du corps humain. Le traitement thermique n'a pas eu d'influence sur les transformations de phase des échantillons excepté pour un matériau où l'apparition de la phase R a été observée. Les études de XPS effectuées avant le traitement thermique révèlent la présence d'ions de Ni. Après le traitement thermique la surface subit une oxydation dans tous les cas des matériaux, tel que confirmé par la disparition des traces d'ions de Ni.

Les études électrochimiques ont montré que le traitement thermique diminue la résistance à la corrosion des matériaux A et C. Des valeurs négatives pour le potentiel de rupture ont été observées pour le matériau B et l'échantillon D non traité, ce qui montre que la rupture de la couche protectrice d'oxyde se produit rapidement. Le traitement thermique a amélioré la résistance à la corrosion seulement pour le matériau D. Ceci peut être expliqué par la petite taille des pores qui produisent une surface lisse.

Les matériaux A, B et C ont une porosité élevée, mais les échantillons non traités A et C montrent les valeurs de potentiel de rupture les plus élevés. Ceci nous amène à penser que la taille de pores n'est pas le seul facteur ayant une influence sur la résistance à la corrosion. La composition chimique pourrait être un autre facteur important sur la corrosion des échantillons. Le traitement a un effet positif sur le taux de corrosion, qui est plus faible pour les échantillons traités. Les taux de corrosion diminuent dans l'ordre suivant : B>A>C>D pour les échantillons traités et non traités. Le ratio du taux de corrosion des échantillons non traités sur les électrodes traités augmente dans l'ordre: D<A<C<B. Ceci indique que le traitement thermique dans l'air a eu un effet plus important sur l'échantillon B. Ce comportement doit être étroitement relié à la surface de l'échantillon.

Les analyses XPS ont montré que les concentrations d'oxygène augmentent pour les échantillons traités. Les faibles taux de corrosion observés pour les échantillons traités sont une indication de sa résistance à la corrosion élevée par rapport à ceux non-traités. Ceci s'explique par la présence des espèces d'oxydes de titane intermédiaire. La présence d'autres éléments : Na, Cl, Ca (< 2 %) est justifiée selon la composition chimique de la solution de Hank's. Les analyses AES ont montré la formation d'une couche de repassivation. Etant donné la nature poreuse de l'échantillon, on ne peut pas conclure si la couche est homogène car elle peut présenter des défauts au bord des pores.

La résistance à la corrosion d'un alliage poreux de NiTi a été étudiée puis comparée à celle des alliages solides. Nos résultats ont montré que les échantillons solides possèdent une meilleure résistance à la corrosion. De plus le plus petit taux de corrosion a été mesuré pour l'échantillon poli par électrochimie. Il est rapporté dans la littérature que ce type d'échantillon exhibe une bonne biocompatibilité et résistance à la corrosion [2-3, 24, 97]. Il a été observé que l'échantillon poreux présente une prédisposition à la corrosion par piqûration et crevasse élevée. Cependant, l'échantillon solide mécaniquement poli présente un taux de corrosion aussi élevé que celui du poreux. Les résultats obtenus par FTIR ont montré des interactions Ti-OH pour tous les échantillons. De plus une autre interaction a été observée sur les échantillons solides. Ceci peut être expliqué par la différente nature de chaque surface crée par le traitement de surface appliqué.

De par leurs propriétés, les alliages du NiTi poreux demeurent un matériau prometteur pour le remplacement osseux. D'autres matériaux poreux comme le Titane et le Tantale n'offrent pas les mêmes avantages. Le Titane est un matériau biocompatible, mais ces propriétés mécaniques sont plus élevées que celles de l'os, sa porosité est limitée à quelques couches et ne possède pas les propriétés de mémoire de forme ni la superélasticité. De plus, les alliages du NiTi poreux ont une capacité d'amortissement qui est recherchée pour certaines applications telles que le remplacement des disques vertébraux. Ces matériaux montrent aussi une capillarité qui améliore la croissance de l'os à l'intérieur de l'implant. Ce qui ne se retrouve pas chez les autres matériaux comme le Titane et le Tantale.

5. CONCLUSION

Pour tous les matériaux, la taille des pores interconnectés de 100-120 µm, révèle une structure interne favorable aux phénomènes capillaires [12]. Les matériaux étudiés présentent une structure connectée qui augmente la croissance de l'os et favorise la bonne

fixation de l'implant. Le profil des thermogrammes n'ayant pas changé entre 0 et 50°C ; nous en concluons que tous les échantillons se trouvent dans la phase martensite à la température du corps humain. La surface a subi une oxydation après le traitement thermique (dans l'air à 550°C pendant 30 mins.) pour les quatre types de matériaux ce qui prouve que le traitement thermique a augmenté la couche d'oxyde à la surface.

La caractérisation électrochimique a montré que la résistance à la corrosion des alliages de NiTi poreux est plus faible que celle des alliages NiTi solides. Le traitement thermique appliqué pour cette étude conduit à une amélioration de la résistance à la corrosion pour des échantillons ayant une taille de pores petits, mais une réduction est observée pour une taille de pores plus grande. La présence d'espèces d'oxydes de titane intermédiaire produit des meilleurs taux de corrosion. La surface des échantillons ne présente pas d'ions de Ni dans sa composition chimique. En conclusion, le traitement a montré que la composition chimique en plus de la taille de pore, à un rôle important sur la résistance à la corrosion, autrement dit sur la biocompatibilité.

La résistance à la corrosion d'un alliage poreux de NiTi a été étudiée puis comparée à celle des alliages solides. Il a été observé que les alliages du NiTi poreux présente une prédisposition à la corrosion par piqûration et crevasse élevée. Cependant, l'échantillon solide mécaniquement poli présente un taux de corrosion aussi élevé que celui du poreux. Bien que les résultats obtenus par FTIR aient montré des interactions pour chaque échantillon, aucune interaction particulière avec l'électrolyte (Solution de Hank's) n'a été observée aux potentiels critiques.

Table of contents

List of tables

List of figures

List of annexes

Nomenclature

AES	Auger Electron Spectroscopy
A_f	Austenite finish temperature
A_s	Austenite start temperature
Co-Cr-Mo	Cobalt-Chromium-Molybdenum
DSC	Differential Scanning Calorimetry
FDA	United States Food and Drug Administration
FTIR	Fourier Transformed InfraRed Reflectance
M_f	Martensite finish temperature
M_s	Martensite start temperature
Ni	Nickel
NiTi	Nickel-titanium shape memory alloy (also Nitinol)
OCP	Open circuit potential
SEM	Scanning Electron Microscopy
SHS	Self-propagating High-Temperature Synthesis
SMA	Shape memory alloy
SME	Shape memory effect
Ti	Titanium
Ti-6Al-4V	Titanium-aluminum(6%)-vanadium(4%) alloy
XPS	X-Ray Photoelectron Spectroscopy

CHAPTER I. Introduction

Several metals have been used over the years in medical applications. Each material was chosen due to a particular reason for a specific application. However, through development of new materials, a special material has been proposed, an equiatomic Nickel-Titanium alloy (NiTi). This new alloy presents a few unique features, such as shape memory effect, superelasticity, damping capacity and good biocompatibility. It was first discovered by Buehler *et al*, [1] in the 1960's at a naval facility. The applications for this alloy have been numerous, for example in orthopedics (staples), dentistry (dental wires) and cardiovascular surgery (stents). Obviously, as with all biomaterials, its biocompatibility and corrosion resistance have had to be evaluated. During the last decades, the results of these evaluations have been published; however these studies do not offer conclusive results. Although it has been pointed out that the TiO_2 at the material's surface offers a good biocompatibility for these alloys [2], its corrosion resistance remains controversial. The surface of these alloys has an important role and it is not yet well understood. A small variation on the chemical composition, a surface treatment, and even a sterilization procedure can change its behavior [3]. More attention needs to be paid to *in vivo* results, some of the medical devices have been used in humans for a few decades, and stents are the most common internal device nowadays [4].

In the quest to improve the fixation of biomaterials to bone, a porous NiTi alloy has been proposed. The porous interconnected structure allows bone ingrowth. Its mechanical properties seemed to better match those of the bone, therefore bone resorption is avoided. This is important because the quality of the surrounding tissues has an influence on the implant performance. Porous implants, however present a larger area that can be subjected to corrosion. Therefore the concern of an increment of a possible ion nickel released is increased. The biocompatibility of these alloys have been studied and found to be acceptable. They have even been used in Russia and China in thousands of patients [5-8]. The authors reported favorable results. However, despite the use of these alloys, there

is still a lack of information on these alloys. The corrosion resistance has been evaluated in a few studies [9-11]. More information is needed to understand the influence of the porous structure on its electrochemical behavior.

1.1 Structure of the project

The purpose of this study is to characterize the porous NiTi alloys and to provide a better understanding of the corrosion resistance of these alloys using new approaches. The most important consideration will be the study of the oxide layer. The chapters fifth and the annex A described the physical and chemical characterization of four different types of porous NiTi alloys prepared by Self-propagating High-Temperature Synthesis (SHS) technique. The influence of an annealing treatment, used to release stresses caused during processing, is studied. The thermal evaluation will determine any changes on the transformation temperatures of the sample. In chapter 6th the electrochemical evaluation of the different porous NiTi alloys is presented. The influence on the corrosion resistance of the heat treatment on the surface chemical composition is analyzed. We believe that the surface chemical composition as well as its porosity may play an important role on the electrochemical behaviour of the studied porous NiTi alloy. The chapter 7th is dedicated to the Fourier Transformed Infrared Reflectance Spectroscopy *in situ*. This evaluation was carried out in order to better understand the interaction between the electrode surface and its environment. Three different samples were studied a mechanopolished porous sample, a solid mechanopolished sample and an electropolished sample. The solid samples are used as references. The electropolished samples are well known for their good corrosion resistance. Therefore the comparison will permit a better understanding of their electrochemical behaviour.

CHAPTER II. Literature review

2.1 Shape Memory Alloys (SMA)

NiTi shape memory alloy has two different temperature-dependent crystal structures (phases) called *martensite* (lower temperature) and *austenite* (higher temperature or parent phase) [1]. The phase transformation can be induced by changing the temperature, when martensite NiTi is heated, it transforms into austenite. The temperature at which this phenomenon starts is called *austenite start temperature* (As) and the temperature at which is completed is called *austenite finish temperature* (Af). On the other hand, when austenite NiTi is cooled, it changes onto martensite. The temperature at which this phenomenon starts is called *martensite start temperature* (Ms) and the temperature at which martensite is again completely reverted is called *martensite finish temperature* (Mf).

Each phase presents different properties and the phase transformation temperatures strongly depend on the chemical composition of the alloy. The material at its martensite form can be easily deform because is soft and ductile. At its super-elastic form (a stress-induce martensite) is highly elastic. The austenite form is strong and hard. NiTi alloys present all these properties, depending on the desired application the temperature at which is used will be chosen. Shape memory alloys are characterize by interesting features: the shape memory effect, superelasticity and damping capacity.

2. 1.1 Shape Memory Effect

The shape memory effect (SME) is the ability of a material to remember a preprogrammed structure. The material is deformed at the martensite phase at a lower temperature, and will recover its initial shape upon heating to a higher temperature, at the

austenite phase. (Figure 2.1) This is called the one way shape memory effect. It is important to mention that the deformation can be completely recover as long as it does not over pass the strain limit of 8%. The two-way memory effect refers to the memorization of two shapes. This can be obtained after a thermo-mechanical treatment, called training [12].
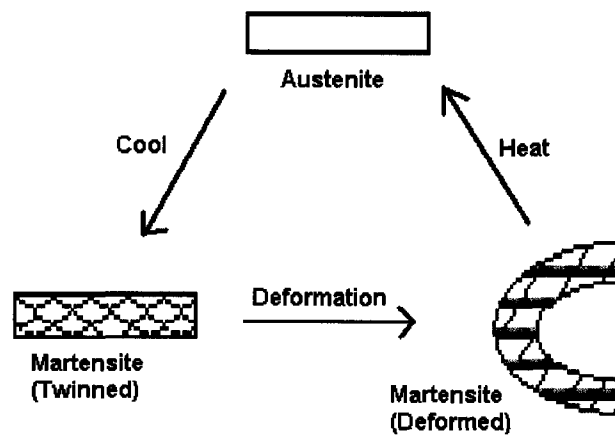
Figure 2.1 Schematic representation of the shape memory effect. [13]

2. 1. 2 Superelasticity

This particular property, in contrast to the shape memory effect, does not require temperature changes. So it refers to the ability to return to its original shape upon unloading after a reversible deformation (up to 8%) under isothermal conditions [12, 14]. The transformation occurs when the stresses are released.

2. 1. 3 Damping Capacity

Shape memory alloys also present a high damping capacity in the martensitic state. These alloys show in the cold shape condition a strong amplitude-dependent internal friction. For impact loads, the specific damping capacity can be as high as 90% [12]. In the hot

shape energy is dissipated during superelastic loading and unloading. This property has been used in the space-craft and also for earth quake damping and isolation purposes.

2. 2 Corrosion

2. 2. 1 General

The corrosion of a material can be defined as a fast degradation of a material that could produce its destruction; under the attack of the environment due to a chemical or electrochemical process. This phenomenon occurs as a result of the surface interactions at the interface between a material and its surroundings. It can affect metals, polymers and ceramics.

There are different types of corrosion such as [15]:

a) Uniform attack: the most common type, it is characterize by a large material lost

b) Galvanic corrosion: produce when two different metals are in contact in the presence of a electrolyte (conductive solution).

c) Grain Boundary attack: occurs at the grain boundaries, basically in regions with different behavior.

d) Crevice corrosion: locally aggravated in the cracks, etc. basically in close spaces of small dimensions.

e) Fatigue-corrosion: combination of two effects, in which the corrosion is increase under repeated stress.

f) Pitting corrosion: cavities appear at the surface that eventually might cause the perforation of the material.

In the physiological environment there are some conditions than can accelerate the corrosion process. This is an aggressive medium because of the high oxygen content, proteins, chloride ions, etc.

The surface of the implant plays an important role on its corrosion resistance. In fact, it most acts as a barrier protection at the metal/tissue interface. Their properties such as roughness, chemical composition, an even its mechanical properties are important.

2. 3 Solid Nickel-Titanium

2.3.1 Corrosion resistance

Solid NiTi alloys are characterize for a good corrosion resistance. Its surface presents a titanium oxide layer very protective and stable in a biological environment at a pH≈7. The nickel-ion release is a concern; therefore many studies have been carried out to investigate the corrosion resistance of these alloys.

Ryhanen reported that most of the knowledge on NiTi alloys was obtained from dental wires at the time [14]. Compared to others materials such as Co-Cr-Mo, 316L and Ti-6Al-4V, NiTi alloys seemed to have a similar corrosion resistance. However in some cases the Nickel ion release was up to three times higher than for stainless steel for simulating fluids. Although there was a concern regarding the ion release the corrosion resistance seemed to be acceptable. The studies performed in dogs and sheep were more encouraging, no presence of trace metals from NiTi was found in the distant organs.

As we mention before the body is an aggressive corrosion environment, Shabalovskaya points out that some body fluids present a high acidity making them hostile for metallic implants [3]. In fact acidity can increase locally around an implant due to inflammatory

responses. The pH can also be altered by the design of the implant. *In vitro* evaluation is performed with the use of simulating fluids, such as artificial saliva, Hank's and Ringer Solution. These fluids are far for reality, many cells can be involved in the immunitary system, making them more or less aggressive to the implant, and should be taken under consideration. The surface of NiTi has been modified to improve its corrosion resistance however there are not standards on this matter. NiTi alloys can present a different behavior due to small changes in the chemical composition or surface in consequence its behavior lacks of predictability. Basically most of the corrosion tests are conducted under static conditions but in the body implants are subject to stress, loading, etc., therefore in a dynamic environment. Even in those some studies where a dynamic condition was incorporated, do not provide enough information to understand these alloys.

In vivo studies show no signs of corrosion after long term implantation [14]. There are however a few cases where some failures have appeared. In most cases the absence of visual changes does not mean that no degradation occurred. Ni ion released has been observed specially in blood and some times in remote organs.

In order to improve the performance of these alloys a few solutions have been proposed, surface treatments, coatings, etc.

2. 3.2 Surface Modification

Surface modification of materials for medical applications presents the possibility of combining the ideal bulk properties with the desired surface properties [16]. In order to achieve this purpose, many authors have proposed surface treatments in order to improve the corrosion resistance of NiTi alloys [17-24]. Such as electropolishing, mechanical polishing, chemical etching and heat treatments among others. These treatments have as an objective to create a TiO_2 oxide layer on the surface of the sample. A brief description of some treatments is given:

A) Thermal Oxidation: When titanium is heated in air between 500 and 800°C for 2 to 10 minutes, a protective thermal oxide of rutile (TiO_2) is formed. It improves resistance to dilute reducing acids but long-term performance has not been fully demonstrated. On the other hand it does not improve resistance in highly alkaline or oxidizing aqueous media. Thermal oxide films may exhibit limitations at higher temperatures and in low-pH brine. Strain must be avoided for effective performance.

B) High-temperature salt baths: Operate between 370 to 480°C. It produces rapid reaction for oxide film. In fact, the major advantage of high-temperature oxidizing or reducing salt baths for titanium scale removal is their great speed in removing extremely tenacious scale. After treatment in salt baths (5 to 20 min for oxidizing salt baths and 1 to 5 min for reducing salt baths), the titanium alloy is generally rinsed or quenched in water, and immerse in acid solution for cleaning.

Types of acid cleaning (may vary greatly with manufacturer):

1. Sulfuric acid 10 to 40 vol% for 2 to 5 min at 50 to 60°C
2. Solution of 35% nitric acid and 3.5% hydrofluoric acid for 1 min at 20°C.

C) Aqueous caustic descaling baths: to remove light scale from titanium. Descaling require from 5 to 30 min. Examples of aqueous caustic solutions are:

1. 40 to 50% sodium hydroxide (temperature near boiling point, i.e. 125°C)
2. Solution of copper sulfate or sodium sulfate with sodium hydroxide (ex of comp.: 50% sodium hydroxide,
3. 10% copper sulfate pentahydrate ($CuSO_45H_2O$) and 40% water) at temperature near 105°C.

D) Low-temperature baths: not as aggressive as high-temperature baths. They operate between 200 and 220°C. Cycling of the acid between salt and acid is common. Typical bath compositions:

1. 30% sulfuric acid
2. 30% nitric acid, 3% hydrofluoric acid.

E) Acid passivation (include chemical passivation):

Chemical or acid passivation is obtained by the use of one of the six chemical cleaning methods:

1. Circulation: flow of the solution through the equipment (or the equipment through the solution).
2. Fill and soak cleaning: involves filling the equipment with the solution and draining it after a set period of time.
3. Cascade cleaning: only applied to column with trays.
4. Foamed cleaning: uses a static foam generator that employs air or nitrogen to produce foamed solvent.
5. Vapor phase organic cleaning: when the equipment is difficult to clean with liquid.
6. Steam-injected cleaning: injection of a concentrated mixture of cleaning chemical into a steam fast-moving steam.

Types of acid used for cleaning or passivation of titanium are:

a) Hydrochloric acid: concentration from 5 to 15% and temperature from 50 to 80°C. Its applicability for cleaning titanium alloys depends on the oxidizing contaminants present in the acid. Titanium alloys shall never be exposed to HCl containing NH_4HF_2.

b) Although titanium has limited resistance to HCl, it is, unlike other metals, passivated rather than corroded by the presence of dissolved oxygen, Fe^{3+}

and Cu^{2+} ions, nitrates, chromates, chlorine, and other oxidizing impurities.

c) Nitric acid (HNO_3): Even if this acid is rarely used because of handling difficulties, it is one of the acids commonly used for titanium alloys passivation. It is mainly used to remove iron contamination: for mild contamination, a use of a mixture of 1% each of citric acid and HNO_3 is recommended, but for persistent contamination, strong HNO_3 solutions must be used.

d) Citric acid: Is used at 3% and 65°C to clean iron oxide deposits from titanium

Note that small chlorine with small amounts of moisture can passivate titanium. In dry chlorine, at temperatures as low as 18°C, titanium will ignite.

These surface treatments have been applied to samples of solid NiTi, wires, stents, etc. Several studies have been conducted in order to verify its performance. A few are cited below.

Shabalovskaya et al. studied the surface and corrosion for NiTi alloys with different surface treatments [22]. They performed XPS and an electrochemical evaluation on mechanically polished to mirror, chemically etched and boiled-in-water, H_2O_2-treated and electropolished (trifflic acid and methanol) NiTi wires from different sources. Surface analysis showed the presence of some contaminants prior to treatment due to wire processing. Chemical etching removes the defect surface material and results in the formation of a uniformly amorphous surface. The electropolished surfaces presented a high level of organic contamination. The measured low corrosion potentials of raw materials confirmed the need for surface improvement. Chemically etched samples showed the highest corrosion resistance, greater to that one of stainless steel and Co-Cr alloys. They concluded that the final decision for an appropriate set of surface-treatment procedures depends on the biological response that range surface on a different scale.

The study perform by Su and Raman, confirmed that the surface quality is very important [25]. They point out based on their observations that the as received samples presented different surface defects, such as: cracks, inclusions, lap defects, and a heavy and non-uniform layer oxide, giving as a result a poor quality surface. A passivation process was carried out to obtain a better surface. However the details are not given. The samples were tested in a Ringer's solution. The electrochemical behaviour of the samples indicated the possibility of crevice corrosion. They reported that an amorphous oxide layer on the surface seemed to better protect the sample against corrosion. The chemical composition of this layer was not studied, more information is needed to compare this results.

A more complete study involving surface analysis was performed on NiTi plates with different surface treatments (mechanical polishing, electropolishing, chemical and plasma etching) [26]. The surface roughness has an effect on the corrosion resistance of the samples; smoothest surfaces exhibit higher corrosion susceptibility. This result was not expected and was observed on mechanical and electropolished samples. Although the oxide layers had similar thickness its chemical composition was different. Electropolished samples presented an enriched Ti layer, meanwhile mechanically polished presented Ni as the principal element. They conclude that rougher surfaces produced by chemical or gas plasma etching showed a higher corrosion resistance. They point out that a passive surface to corrosive environments and Ti enriched to prevent Ni ion release is desired in all medical applications.

On the contrary, another study demonstrated that smoother surfaces obtained by electropolishing exhibit higher corrosion resistance over porous an irregular layers [24]. This study was performed in stents, a cardiovascular device. All the samples follow the same treatment prior to other treatment, in fact all the samples were mechanically polished, follow by chemical polishing and finally electropolished. After this treatment some samples were heat treated and some chemically passivated. According to their

results oxide layer thickness has a direct influence on the corrosion resistance rather than surface uniformity. They observed a better corrosion resistance on electropolished and chemically polished samples, they presented a thinner oxide layer. They conclude that electropolishing increases the corrosion resistance of NiTi alloys. Although they reported that they are not able to establish a relation between the oxide layer composition and its corrosion resistance.

Another treatment was proposed an oxidation treatment on a low-oxygen pressure atmosphere [27]. This treatment showed a surface with a very low Ni surface concentration and a thick oxide layer. There is no influence on the shape memory properties of the alloy. Even though the corrosion evaluation was not performed, an ion release evaluation was performed. According to the results the treatment decreases the release of Ni compared to untreated samples.

The effects of the sterilization process on NiTi alloys needs to be study. As we mention before any changes on the surface chemical composition can have an influence on its behaviour. The sterilization process could modify the surface. A study was carried out to evaluate the effect of this process. The samples were NiTi discs mechanically polished and electropolished, they were sterilized by ethylene oxide, steam autoclaved, and sterilized with peracetic acid and by hydrogen peroxide plasma. Stainless steel and Ti6Al4V discs were used as control materials [2]. The results showed that electropolished samples presented higher and more reproducible breakdown potentials. The sterilization process seemed to have weakening the oxide surface layer, producing localized corrosion on some samples. The chemical composition and topography of the samples seemed to be modified by the sterilization process. However the authors believed, based on their observations, that electropolishing might reduce the effects of sterilization process on both surface characteristics and its electrochemical behaviour.

The evaluation of surface treatments is controversial. However it is clear that the surface is very important and plays an important role on the performance of the alloy. The fact that not all the authors detailed described the applied treatments difficult the comparison.

More studies are needed to determine the influence of chemical composition, surface roughness, the design of the material on the surface resistance to corrosion.

2. 3. 3 Biocompatibility

The biocompatibility of a material is the response of the body or human tissues. This reaction is closely related to its corrosion resistance and surfaces characteristics. The study of the biocompatibility of NiTi alloys is very important in order to enlarge its medical applications.

NiTi is one of the most innovative concepts to have appeared in the field of metallic biomaterials in recent years but its biocompatibility remains controversial [28]. Due to the high content of nickel the biocompatibility of NiTi has been studied. The cytotoxicity and genotoxicity was evaluated to measure the short-term biological safety of NiTi alloy [29]. The results showed that the response to NiTi was similar to AISI 316 LMV stainless steel, it will be useful to point out that no cytotoxic, allergic or genotoxic activity was observed. The promising behavior of NiTi alloys might be due to a minimal ion release. The fact that some of the studies are controversial and contradictories could be related to the possibility of different alloy composition or surface preparation. As they conclude that NiTi has a good short-term biological response, they underline that this result was observed under the chosen test conditions. They agreed to other authors on the potential for these alloys in clinical applications.

Similar results were obtained in a study performed to evaluate the *in vitro* and *in vivo* biocompatibility of NiTi alloy [30]. As we mention before surface treatments are used to

improve the corrosion resistance and biocompatibility, this study aimed to evaluate different treatments. On the contrary to a previous study were electropolished samples were found to exhibit the higher corrosion resistance, in this study they provoked a slight decrease of cell proliferation. In fact passivated, air aged and heat treated samples seemed to have a similar behavior and double the number of fibroblast cells with reference to the control. The *in vivo* tests were performed in rabbit paramuscular muscle. They showed a good response to the treated samples. A low value of the fibrocellular capsule indicated that the resulted surface after the treatments was relatively inert. As there are no significant differences on the results between the treatments, they conclude that heat treatment or nitric acid passivation is not necessary after electropolishing. Electropolishing was used in all samples prior to other treatment.

Ryhanen studied the biocompatibility of NiTi for orthopedics applications. He and his team evaluated the response to osteoblasts and fibroblast [14]. They found that the NiTi alloys posses a good *in vitro* biocompatibility, there were no presence of toxic effects or decrease in cell proliferation. The inflammatory response of muscular tissue to NiTi was similar to that of stainless steel and Ti6Al4V. The bone and soft tissue histology findings showed good acceptance in a 26 week follow up. In a 60 weeks implantation period, NiTi intramedullary rod presented slight marks of surface corrosion, in fact fewer that those ones on the stainless steel rod. Its conclusion is that Nitinol appears to have an excellent potential for clinical used due to its good biocompatibility.

On the contrary, another study reveals that NiTi showed a slower osteogenesis process, no close contact between the implant and bone was observed [28]. This study was performed in rabbits and the control materials were titanium, austenitic-ferretic stainless steel and stainless steel 316L. The study aimed for qualitative observations; however the results are explained by a cytotoxic effect. It has already point out that chemical composition and surface conditions, and even the experiment conditions (culture cells,

implant shape, site implantation, etc.) have an influence in the results. Therefore NiTi results could be contradictory.

The haemocompatibility of NiTi with surface modification was evaluated. The surface characteristics chemical composition and roughness were identified [31]. This study provides more information on the influence of these parameters on the biocompatibility of NiTi. The control samples were pure titanium and 316L stainless steel, the nickel titanium samples were mechanically polished follow by electropolishing, shot-peening or annealing. The cytotoxicity test showed no toxic effects and no difference between the studied samples. According to the authors surface chemistry has a more significant influence on the platelet behavior. The Ni content seemed to be a determinant characteristic. More information will be needed to understand the biological response to NiTi.

Good results were also obtained on a thrombogenicity study in an ex vivo porcine model [32]. The presence of thrombus within the stent struts is a major concern in the coronary stenting. In order to evaluate this phenomenon Nitinol stents were cut to the same geometry of stainless steel Palmaz® for comparison purposes. The results showed a fewer presence of thrombus on the Nitinol stent. The rich titanium oxide surface might have an influence on these results. However no surface characterization was carried out. It was also pointed out that the ex vivo porcine model does not reproduce the coagulation process. But it is used in the evaluation of cardiovascular devices.

A recent study on 48 explanted endovascular grafts showing controversial results has raised some important questions [4]. The time of implantation was 30 ± 14 months (range 5-50 months). The devices were examined and pits with a size in the range of 10-25 μm in diameter were observed in all the specimens. Other types of damages were observed: map-shape craters, large surface deficiencies and fractures on the wire. The fact that corrosion signs were observed as soon as 5 months of implantation was unexpected. This

might be the beginning of material failure. Complete fractures were present in seven devices. The authors underlined that the titanium oxide layer must resist cracking in the pulsatile oscillation. The *in vivo* conditions are more complex that we expect and static tests do not allow obtaining all the necessary information. More information is needed to prove the consistency of long-term stent metals. The authors also recommend to pay attention to other materials such as Elgiloy and stainless steel.

The study of the biocompatibility of NiTi alloys is controversial and some studies show contradictory results. It will be important to have information to fully understand the role of the surface condition and properties on its corrosion resistance and biocompatibility. *In vitro* and *in vivo* implantations can give an idea about the behavior of the alloy but they cannot mimic human conditions, some parameters are left on the side and its influence seemed to be important.

Nickel Titanium alloys represent a new generation of interesting materials, its mechanical properties as well as unique properties made them a good candidate to replace other materials. Until its biocompatibility and corrosion resistance will be understood its medical applications will be restrain to short-term implantations.

2. 3. 4 Medical applications

NiTi shape memory alloy has been used in several medical applications such as: dental, cardiovascular, and orthopedics, an extensive list of the medical devices has been made by Van Humbeeck et al. [12]. A brief review will be presented to give an idea of the endless possibilities for shape memory alloys on biomedical applications.

The most common dental applications are orthodontic archwires, in fact these are the first medical application. NiTi superelastic properties are an advantage for this application. Other dental devices are dental root implants, adjustable telescopic head gears, tension

and compression springs, heavy suture expanders and adjustable orthodontic brackets, just to mention a few.

Cardiovascular devices are also fabricated with NiTi alloys. Self expandable intravascular scaffolding generally called stents have demonstrated great advantages over stainless steel.

There are also some orthopedic applications for solid NiTi alloys, for example, miniature bone anchors, cerclage wires, intramedullary fixation nails with self-expanding memory metal, ostheosynthesis bone staples, tools for the removal of broken bone screws, superelastic rods for gradual correction of scoliosis and external fixators with a high grade of adjustability.

The information above is just to show how solid shape memory alloys are used in the fabrication and development of medical devices, its shape memory effect and superelastic properties made them superior to other materials. Their biocompatibility and corrosion resistance have been evaluated and even if they are controversial, most of the studies show good results. Therefore more applications might be explored.

2. 4 Porous Nickel-Titanium

2. 4. 1 General

NiTi alloys with a porous internal structure have already been used for approximately a decade, in maxillofacial surgeries [33] and other orthopedic procedures [5, 34-36] involving thousands of patients in Russia [6-7] and China [5, 8]. However, the interest for

these materials is still increasing in many areas of the biomedical field, such as, in the development of shape memory implant of special design. Therefore, further knowledge is needed concerning the relationship between, on one hand, the phase constituent and the factors determining the internal structure of the material, and on the other, the fundamental material properties and the response of the biomedical device used.

The key factors identified to play a determinant role, for the use of these alloys as materials for implants, are their capillary property and biomechanical compatibility (low elastic modulus, damping capacity). The capillarity behavior strongly depends on the internal structure of the material. In fact, the capillary force controls the transport of fluid through interconnected pore channels and the material wetability influences the velocity and height of rise fluid in capillaries [37-38]. The optimal combination of both features encourages the bone marrow penetration within the internal structure of the implant. This results in a good attachment between any contacting tissue and the porous NiTi implant.

An interconnected porosity is very important because the bone will grow within the interconnected pore channels near the surface maintaining its vascularity as well as long-term viability and providing a desirable firm fixation. It has been found that the optimal pore size is in the range of 100-400 μm. [39]. Besides their opened porous structure allows bone tissue ingrowth into the body of the implant and thus provides the desirable firm fixation.

The porosity affects also the mechanical behavior of the material [40]. A good matching between the elastic modulus of the bone (20 GPa) and that one of the implant is needed. The closer values have been shown by NiTi alloys in the martensite phase (28-41 GPa). Moreover, if the material has an internal structure of 50% porosity, it exhibits a lower modulus (14-20 GPa), which allows the possibility of significant bone ingrowth at this matching value.

2. 4. 2 Fabrication Methods

Porous NiTi can be produced by various manufacturing processes. We can mention, for instance, Powder Metallurgy and Self-propagating High-temperature Synthesis (SHS) [40-41]. Powder metallurgy process NiTi alloys consist in the compactation and sintering of Titanium and Nickel powders [42]. The investigation of their properties and behaviors, including crystal structure, phase composition, mechanical properties and shape memory parameters, started to be carried out in the late 1970's [40]. From these studies, it has been reported that the properties of the sintered alloys are extremely sensitive to the sintering conditions. The SHS method, also called ignition synthesis, is based on the utilization of the exothermic heat formation upon interaction of various elements. There are two kinds of SHS: layer burning and heat explosion. In the former, heat is initially released due to localized exothermic reaction in some regions. It is then absorbed by the neighboring layers of powder, causing reactions and thereby shifting the reaction zone. In this case, a chemical reaction takes places only in a thin-layer wave of burning but not in the whole volume at the same time. In the latter, the increase of the temperature in the whole volume of the reacting system leads to a self-ignition that is similar to an explosion. In the reacting zones the maximum temperature values reached in both techniques are similar. These temperatures can be lower, equal, or even a little higher than the melting point of NiTi [40]. Both methods can be used efficiently to control the porosity range and thus providing appropriately sized and interconnected pores, in order to create similar bone morphology.

Various parameters are involved in the production of porous samples with SHS method, Chenglin *et al.* established that preheating temperature of the green compact is a key parameter that define the shape and distribution of the bores [43]. They found that a preheating temperature lower than 250°C will result in uniform distributed stripes. At a temperature between 250-400°C the pores are spherical and homogeneously distributed. Above 400°C, the pores are spherical but distributing heterogeneously. They measured

the compressive strength at a 70% porosity to be up to 100MPa and the recovery percentage of 92%. Although pore distribution is important, they do not mention being able to control the porosity of the final product.

2. 4. 3 Mechanical properties

In order to have a good implant their mechanical properties most match those ones of the bone, this is called mechanical biocompatibility. It is very important because most of the materials that are used nowadays do not respect this issue; the biggest consequence is the possibility of bone resorption around the implant. The bone needs a mechanical charge to renew itself, when a material that has a higher elastic modulus is used to replace bone the mechanical charges will go through the implant, avoiding the natural regeneration process of the bone. In the last few decades more research has been done to study this particular matter. The mechanical properties of porous alloys have been investigated and evaluated in order to reach this important mechanical match.

The mechanical properties of porous NiTi alloys produce by sintering or SHS depend on different parameters, such as porosity and sintering temperature. In fact Shabalovskaya *et al.* carried out a study to compare the mechanical properties of porous samples produce by both methods [44]. They observed that the superelasticity and shape memory properties where present and depend on the sintering conditions. Other properties such as yield strength and recoverable strain seemed to be controlled by the porosity. For example, on solid samples of NiTi it is possible to apply up to an 8% deformation and as mention before by heating at the right temperature it will recover its shape. It is necessary to be careful not to exceed the 8% limit otherwise irreversible dislocations can appear. Deformations applied to porous samples are not uniform and regions with a 10% deformation can be found, therefore the percent of recoverable strain can not be greater than 70%. They observed that an increase in the porosity from 20-60% increases the volume recovery. The authors point out that porous NiTi alloys are very sensitive to any

changes in composition or thermo-mechanical treatment. In fact in order to obtain the optimal characteristics in any application a control of these parameters has to be achieved.

In another study performed by Martynova *et al.* a new feature is integrated, something they called volume memory effect [45]. The mechanical properties of porous NiTi alloys were investigated; the results show that the reversible deformation material exceeds the one of non porous alloys. This is a contradiction to the study of Shabalovskaya. In fact they associated the heterogeneity of the sample to this behavior. They explained that the deformation goes together with macroscopic volume changes; in consequence the shape recovery in the matrix provides the initial volume body; which they called volume memory effect. Regarding the porosity they observed that the recovery degree is proportional to the porosity, so for lower porosities lower recovery degree. The same effect was measured under compression loading; the maximum value was obtained for higher porosities. A 100% recovery was observed after a few loading-unloading cycles, the higher the porosity the more cycles were needed, however the reversible deformation value decrease considerably. They conclude that the functional capacities of porous alloys expands the SME alloys due to a wider range of permissible macroscopic deformations and also because powder metallurgy methods are useful when manufacturing complex parts.

On the other hand Li *et al.* studied the compressive strength of porous NiTi alloys produced by combustion synthesis [46]. They used several samples with different porosities. The porosity was three-dimensionally interconnected; therefore good for bone ingrowth. The pore size ranged from 200-600 μm, which met the demands for a cancellous bone replacement. They reported three main regions on the stress-strain curve: an apparent linear elastic phase, an increasing steeply stress yield phase then the maximum was reach and a fracture failure appears. Even thought the stress-strain curve for cancellous bone presents also three portions, it is obvious that the behavior is

completely different. However the compressive strength of the porous NiTi alloys was found in the same range as that one of the cancellous bone at the corresponding porosity. They found that by increasing the porosity the compressive strength and strain decrease. Secondary electron images allow the evaluation of the fracture morphology; they conclude that it was a ductile fracture. In another study, the same authors were able to evaluate the Young's modulus and recovery strain. They compare porous NiTi alloys to bulk NiTi and stainless steel. They observed that the porous samples presented a lower Young's modulus that match the value of cancellous bone and a higher recovery strain after loading. They conclude that porous NiTi with 60% porosity has a better mechanical-compatibility than solid NiTi and stainless steel.

As we can see porosity plays an important role in the mechanical properties of porous NiTi alloys. The porosity and pore size will be defined by the medical application. It seems that the fabrication methods are controlled successfully to produce the desired porosity. It is important to mention that interconnected porosity is required for a material that will replace bone. In fact this feature will facilitate bone ingrowth and good fixation of medical devices.

2. 4.4 Corrosion resistance

Once the mechanical properties have been met, it will be important to determine the corrosion resistance of porous NiTi alloys for medical applications. There is concern about the metal ion release, especially for Nickel ions. As we pointed out already solid NiTi exhibits a good corrosion resistance and biocompatibility. As we will find the same oxide layer on the surface of porous NiTi alloys we expect that its electrochemical behaviour will be similar. However there is a concern regarding its porosity which gives a non homogenous surface. We could think that the oxide layer will present some

morphologic defects but in terms of chemical composition we do not suspect any differences.

Despite the interest that has been pointed to these alloys a few studies have been carried out regarding its corrosion resistance. In one such study, Abiko *et al.* studied the corrosion resistance of different samples, a polish plate, a porous specimen and a thin film [9]. Their objective was also to evaluate the biological response of MC3T3-E1 and human fibroblast. Surface analysis demonstrated the presence of a TiO_2 layer without Ni oxides for the three specimens, although the thickness was different. They observed that even after polishing the plate presented some defects, therefore a non-uniform surface. The porous samples seemed to be actively corrosive in saline solution, a breakdown potential of 60 mV for porous NiTi was measured. In fact the thin film specimen presented the higher breakdown value and lower current density. This might be due to the fact that the oxide layer was uniform on this sample. Even though the results seemed to be better for this sample there is a contradiction with other studies, because thin films presented a thicker oxide layer. The results found for porous samples could be explained by the inhomogeneous surface structure. There is no mention on how the active surface of porous specimens was calculated. Becker and Bolton performed a study on three porous materials, stainless steel 316L, Ti-6Al-4V and Co-29Cr-6Mo [47]. They conclude that porous sintered 316L exhibited the worst anodic behaviour while Ti-6Al-4V exhibited the best behaviour. They identify pore geometry, especially pore size and compositional variations having a significant effect on corrosion behaviour. They also pointed out that all elements released from three materials can cause toxic reactions from surrounding body tissue. They recommended further studies in order to minimise the corrosion of such materials.

Yong_Hua Li *et al.* conducted a study on porous NiTi alloys recently [10-11]. They compare a porous sample filled with resin and as received sample. They found that the porous sample exhibited passive characteristics; however its corrosion resistance was

lower than the one of solid NiTi. They concluded that pores have a significant effect on corrosion. In another study the same authors compare porous samples with different porosities. They conclude that the corrosion resistance of porous NiTi decreased with the increase of porosity, but it is still less resistant than solid NiTi. They indicated that this behavior could result from the interconnected and permeable porous structure of the samples. There is no mention on these articles about the measurement of the active surface area for the corrosion evaluation.

Another factor that may reduce the corrosion rate in an alloy is related to its lower surface area due to higher portion of big sized pores [33]. Thus, alteration of the corrosion behavior of porous Nitinol by the manufacturing process is possible and merits further research.

Further studies are necessary because porous materials present some difficulties in their electrochemical studies, such as the measurement of the active surface. There are some techniques that allow measuring the specific surface of porous materials such as Brunauer–Emmett–Teller (BET). However this technique does not provide accurate information regarding the activity of the surface during the corrosion process.

2.4.5 Biocompatibility

Good surface properties and biocompatibility are crucial to porous NiTi used in medical implants as possible nickel release from these alloys may cause deleterious effects in the human body [48]. The evaluation of the biocompatibility of porous NiTi has not been widely studied, there are some studies that point out that these alloys present an acceptable biocompatibility. For instance, Shabalovskaya *et al.* carried out an *in vitro* study and concluded that the porous as well as the solid phases of NiTi are well accepted by human tissues as nearly as pure Titanium is [49]. The nickel surface concentration seemed to be quite similar for solid and porous NiTi from the results of surface analysis.

Lymphosytes-T cells were chosen for this study, due to their important role on the immune system. The proliferation rate for the cell exposed to porous NiTi was found to be about 60-100% compare to that one of solid alloys. Ni specimens were used as control sample; the proliferation cell was very low as expected because of its toxicity.

In the study by Abiko *et al.*, mention before they pointed out that cell growth was difficult to evaluate due to cell growth in the interior of the pores [9]. They did not find a difference of the number cells present on the three specimens. However porous samples presented a reduce biocompatibility; probably due to its low corrosion resistance.

Based on *in vitro* and *in vivo* experiments, Rhalmi *et al.* evaluated the muscle and bone reaction to porous NiTi [50]. A cell culture was performed prior to implantation. L-929 fibroblasts were used. After 3 days incubation period, they manage to grow inside and around the porous specimens. No cytotoxic effect was observed. The porous implants seemed to be well attached to the soft tissue and they did not cause any adverse effects. A normal inflammatory reaction was observed. They observed bone ingrowth within the pores of the implants three weeks after implantation. In fact there was an increment of bone inside the pores in implants close to the cortex with increasing implantation time. So that at 3 month period the pores of the porous specimens were filled at about 80%. No adverse tissue reaction was observed at the bone implantation site. The authors conclude that they results indicate a good biocompatibility of porous NiTi alloys, and suggested further bone implantation studies most likely in vertebrae.

Kang *et al.* also found that bone ingrowth in porous NiTi increases with implantation time [51]. They measured a 78.3 ± 9.7 bone ingrowth after 6 weeks implantation, much faster than Rhalmi *et al.* results and higher compare to other porous materials. There was no presence of inflammation or foreign body reaction. Therefore they conclude that the biocompatibility of porous NiTi is excellent and it is an ideal bone substitute.

The bone ingrowth on bones has also been measured by other authors. Simske and Sachdeva, and Ayers et al. were able to demonstrate bone ingrowth into porous Nitinol in the crania of rabbits was evident as early as six weeks and that bone contact is made with the surrounding cranial hard tissue. [51-52]

Porous NiTi alloys seemed to be accepted by the human body tissues. Their porosity and mechanical biocompatibility made them good candidates for bone substitution. We could mostly suggest orthopedic and dental applications. However there are still a few features that have not been fully investigated. We already mention the capillarity property, which was also, mention by authors of ref. 50 regarding the high tissue attachment and penetration. This property needs to be studied to be better understood in order to explain good fixation. Others porous materials have been studied but they do not present these faster results, so we could assume that the implant architecture might not be the only reason for good tissue ingrowth.

2. 4.6 Medical Applications

Porous NiTi have recently attracted attention in clinical surgery because they are a very interesting alternative to more brittle and less machinable conventional porous CA-based ceramics [54]. Ideally porous NiTi alloys are used for bone replacement, due to their porosity, mechanical properties. In fact in some countries like Russia and China, they have been used for several decades in orthopedics and maxillofacial applications; showing no significant detrimental effects of implanted devices [5-8].

In North America, solid NiTi alloys have been use in cardiovascular and dental applications, such as stents, filters [24, 55] and dental wires [56-57]. Their shape memory effect, superelasticity and biocompatibility have been a great advantage over other materials. There is still concern over nickel ion release and corrosion resistance.

Lately a Canadian company fabricated a disc spine replacement made with porous NiTi, produced by SHS method, the company called it Actipore™. Basically they aimed orthopedics applications; among their products we found a vertebral disc replacement. In order to evaluate its biocompatibility a study was carried out on lumbar on two lumbar levels on sheep [58-59]. A NiTi intervertebral implant was compared to a titanium cage system. The results indicated a better osseointegration on the NiTi implants. They pointed out that the implant structure and shape have an influence on its functionality but their biocompatibility is comparable.

The study of the surface of these implants was carried out to evaluate the nickel ion release [60]. There was no evident data of surface corrosion observed either prior or postimplantation. Inductively coupled plasma-mass spectrometry (ICP-MS) was used to evaluate the nickel ion release. The results showed that blood nickel levels were found to be within acceptable levels. The authors concluded that porous titanium-nickel demonstrates resistance to both *in vivo* surface corrosion and nickel ion release and compared very well with a conventional titanium implant. The evaluation was carried out in a course of 12-months.

There are other medical applications that can be taken into account, recently a proposition of a stent fabricated from an ultra flat porous NiTi sheet [61]. Their advantage relies on a low delivery profile, variable coverage and superelastic properties. Attachment of a polymer coating seemed to be improved by using this kind of material, as well as precise positioning. The fluid dynamics are superior. An 81% success rate was measured. This concept appears to be very attractive and could be applied to exclude aneurysms and provide a cure for artero-venous fistulas.

2. 5 Other Porous materials

2. 5. 1 General

Several materials have been used over the years to replace and repair bone such as stainless steel, pure titanium, Ti6Al4V, and cobalt-chrome for metallic materials. Basically surface treatments have been performed to obtain a porous surface, for example the use of plasma spray. Porous surfaces are important in bone replacement because of desirable bone ingrowth. However machining of these materials is not always easy. There are new emerging porous materials like tantalum.

2. 5. 2 Titanium

Titanium is a well-known implant material widely and successfully used in medicine. The primary reason for using titanium in medical applications is its biocompatibility [62]. The biocompatibility of this alloy relies on a native passive titanium oxide layer. The basic corrosion and biodegradation properties of Ti have been studied by *in vivo* and *in vitro* evaluations [63].

Titanium and its alloys possess suitable mechanical properties such as strength, bend strength and fatigue resistance to be used in orthopedics and dental applications. It can be used under load-bearing conditions [64]; however their poor fatigue resistance has been reported [65].

As we mention before porous surfaces are better candidates to replace bone because they allow a better bone ingrowth and tissue attachment. The textured surface can be achieved by the application of sintered beads, meshes or plasma-spray coatings to the surface [66].

In order to evaluate the possibility of using porous titanium for spine applications a study was conducted by Takemoto *et al.* [67]. Porous titanium implants sintered with volatile spacer particles (50% porosity, average pore size 303 μm) were subjected to chemical and thermal treatments to produce a bioactive microporous titania layer on the titanium surface. Dogs were the animals used in this study at a one lumbar lever (L6-7). After three months implantation histological examination demonstrated a large amount of new bone formation on the treated samples. The non treated samples presented a fibrous tissue formation on the surface. Therefore, bioactive treatment effectively enhanced the fusion ability of the porous titanium implants.

Although metallic devices were selected due to their stable oxide film, it has been observed that sterilization process have an influence on their electrochemical behavior [68-69]. It has been reported that the oxide layer on pure titanium implants, retrieved form human tissues has increased two to three times. Therefore the material undergoes an electrochemical process under physiological conditions [69].

Even thought the corrosion resistance of Titanium is well established and found to be excellent, some treatment had been applied to titanium surfaces to evaluate their behavior. For example, titanium plasma spray, hydroxyapatite coatings, sandblasted and acid etched. Some of the treatments are also applied to generate a porous surface. The studies show that porous Ti surface has a significantly better biocompatibility than the other surface treatments and an excellent electrochemical performance [70].

As we can see Titanium alloys also present advantages and disadvantages over other metallic materials.

2. 5. 3 Tantalum

Porous tantalum, a new low modulus metal with a characteristic appearance similar to cancellous bone, is currently available for use in several orthopedic applications (hip and knee arthroplasty, spine surgery, and bone graft substitute) [71]. Tantalum trabecular metal offers several advantages over other current conventional materials used for implants by its uniformity and structural continuity, strength, low stiffness, high porosity, and high coefficient of friction [72]. This material is manufacture with the pyrolysis of a thermosetting polymer foam precursor to obtain a low density vitreous carbon skeleton which has a repeating dodecahedron array of pores interconnected by smaller openings or portals [73]. Commercially pure tantalum is deposited into and about the carbon skeleton using chemical vapor deposition/infiltration (CVD/CVI) to create a porous metal construct. The material can be produced at high volume porosity up to 75% to 80%. It can be machine-shaped into custom designs in situations of massive bone loss [74].

Tantalum has excellent biocompatibility and is safe to use in vivo as evidenced by its historical and current use in pacemaker electrodes, cranioplasty plates and as radiopaque markers. The bioactivity and biocompatibility of porous tantalum are due to its ability to form a self-passivating surface oxide layer [71]. Formation of a bone-like apatite coating in vivo affords strong fibrous ingrowth properties and allows for substantial soft-tissue attachment with the potential for use in cases such as mega-prostheses and patella salvage [75].

A few studies have been carried out to evaluate bone ingrowth and tissue attachment on this material. The bone ingrowth was evaluated in a simple transcortical canine model [73]. The extent of filling of the pores of the tantalum material with new bone increased from 13% at two weeks between 42% and 53% at four weeks. In a period of 16 and 52 weeks the average extent of bone ingrowth was found at a ranged from 63% to 80%.

Evidence of Haversian remodeling was present at the interface bone/implant. Mechanical tests at four weeks indicated a minimum value of shear fixation strength of 18.5 MPa, substantially higher than has been obtained with other porous materials with less volumetric porosity. The samples presented 75% to 80% porosity.

In another study eight dorsal subcutaneous implants (in two dogs) were used to evaluate the performance of tantalum [76]. The tissue attachment strength to porous tantalum was three- to six-fold greater than was reported in a similar study with porous beads. This study demonstrated that porous tantalum permits rapid ingrowth of vascularized soft tissue, and attains soft tissue attachment strengths greater than with porous beads.

Although porous tantalum is in its early stages of evolution, the initial clinical data and basic science studies support its use as an alternative to traditional orthopedic implant materials [75].

CHAPTER III. Objective

Porous Nickel Titanium alloys have shown a great potential in the fabrication of biomedical devices. Their porous structure in combination with their unique shape memory properties made them suitable for bone replacement, therefore useful in orthopedic and dental applications. However there are still some concerns for the use of this porous alloy for long term implants due to its high Ni content that might cause a possible Ni ion release. Considering that ion release is strongly related to the corrosion resistance of a material, this work aims to elucidate the electrochemical behaviour of these alloys.

The main purpose of this study is to evaluate by using new approaches the corrosion resistance of porous Nickel Titanium alloys for medical applications

In order to achieve this goal the specific objectives were:

a) To determine the physical properties and surface characteristics such as phase transformation, surface chemical composition and morphology of different samples.

b) To evaluate the influence of a heat treatment applied to optimize the behavior and the biocompatibility property of these materials in their characteristics

c) To evaluate the corrosion resistance of different types of porous NiTi alloys

d) To evaluate and compare the corrosion resistance of porous and solid NiTi alloys by using a new approach (Spectroelectrochemistry)

CHAPTER IV. Experimental Procedure

4. 1 Materials

The NiTi alloy samples were fabricated using the Self propagating High temperature Synthesis (SHS) method, also called ignition synthesis, is based on the utilization of the exothermic heat formation upon interaction of various elements. This technique is used to produce porous samples. The specimens present an interconnected porosity that will allow bone ingrowth and therefore a good fixation of implants.

The specimens used for this study were obtained by the Self-propagating High-temperature Synthesis (SHS) procedure. Four types of NiTi alloys to be denoted in the following by A, B, C and D, from different suppliers, were analyzed. The sample A was provided by Professor Victor E. Gjunter from the Institute of Medical Materials and Shape Memory Implants, Tomsk, Russia, and the sample B was provided by Dr. Tae-Hyun Nam Division of Materials Science & Engineering Gyeongsang National University, Korea. The sample C was provided by Professor B. Silberstein from the Institute of Medical Materials and Shape Memory Implants, Russia made in a laboratory in Israel, and the sample D was provided by Dr. John Moore from the Colorado School of Mines (Non equiatomic alloy 48Ti-51Ni).

4.2 Annealing process

One series of specimens from each sample were submitted to an annealing process at 550°C for 30 min in an air atmosphere. The main purpose of this treatment is to release internal stress created during the forming processes. The temperature of 550°C was

chosen because at that temperature the damping reaches its maximum value in the martensite phase [77].

4. 3 Thermal Analysis: Differential Scanning Calorimetry

4. 3. 1 Principle

Shape memory alloys have two different phases, martensite and austenite; each of them has its own physical properties. Depending on the application the user decides what state is suitable. The Differential Scanning Calorimetry technique is used to identify the phase transformation temperatures of the shape memory materials.

Differential Scanning Calorimetry is a quantitative technique that measures the difference in the amount of heat required to increase the temperature of a sample and an inert reference as a function of the temperature. To obtain an accurate measure it is important to keep both the sample and the reference at nearly as possible to the same temperature. Mostly all of the physical or chemical transformations are associated with heat absorption (endothermic) or heat liberation (exothermic) [78]. The differential heat flow between an inert reference and a sample upon heating or cooling at a particular rate or under isothermal conditions is measured, therefore it is possible to calculate the amount of heat that has been absorbed or released. Only in the case of a thermal event characteristic of a particular material, a difference exists and a signal will be registered. This technique is widely used to determine glass transitions, melting points, and any other phase transformation in metals and polymers.

This technique will be used to identify the martensite and austenite phases of the different samples.

4. 3. 2 Sample Preparation

The cylindrical specimens, with a thickness of 2 mm, and diameter of 10 mm were cut from porous rods with a diamond saw in order to maintain their internal structure. They were cleaned during 10 min by immersion in a bath containing first acetone, then methanol using an Ultrasonic cleaner (Branson, Model 2510) apparatus. A sample of 25 mg was sealed in an aluminum crucible.

4. 3. 3 Equipment

The analyses were carried out in a Perkin Elmer Pyris1 Calorimeter equipped with a CryoFill Liquid Nitrogen Cooling system. The apparatus has been calibrated into temperature interval 0°C – 200°C at a rate of 10°C, using Indium as reference materials. Each specimen with a mass of 25 mg approximately, have been cycled once within the range of 0°C to 190°C at a heating/cooling rate of 5°C, using He as purge gas. We have recorded two thermograms of the treated and non treated specimen of each material.

4. 4 Morphological Analysis: Scanning Electron Microscopy

4. 4. 1 Principle

The scanning electron microscopy (SEM) analyses were performed in order to determine the surface morphology and the porosity. The information is obtained from the interactions of an electron beam and the surface sample. The electron beam is generated from a tungsten filament. When the primary electron beam interacts with the sample, an electron emission and electromagnetic radiation is produced, and directed to a detector [79]. Two types of electrons are emitted from the surface. Low energy electrons are

detected with an Everhart-Thornley detector, a scintillator-photomultiplier device. The electric signal is amplified and used to produce an image. The size of the interaction depends on the beam electron energy, the atomic number of the sample and its density. The obtained image is well defined and has a three dimensional appearance. Using this technique, $\cong$ 5-10 nm resolution is possible. This resolution depends on different condition such as the nature of the sample and the equipment that is used. The other type of electrons that can be detected, are high energy electrons so called backscattered electrons. These electrons are reflected or back-scattered after its interaction from the surface sample. Backscattered electrons are useful to identify different chemical compositions. This is possible because the backscattered-electron coefficient increases with the atomic number. Therefore regions with different contrast are observed.

The morphological characteristics such as porosity and surface texture will be determined with the use of this technique.

4. 4. 2 Sample Preparation

Cylindrical specimens 5mm thickness and 10 mm diameter; were sonically cleaned during 10 min by immersion in acetone, follow by methanol using an Ultrasonic cleaner (Branson, Model 2510) apparatus. These cylinders were mounted in a copper sample holder with carbon paint.

4. 4. 3 Equipment

The micrographs were taken using a JEOL model JSM-840 Scanning Electron Microscope at 15.0 kV coupled to an ultra thin window (UTW) energy dispersive X ray spectrometer (EDS).

4.5 Surface Analysis: Electron Spectroscopy for Chemical Analysis (ESCA) or X-Ray Photoelectron Spectroscopy (XPS)

4. 5. 1 Principle

The Electron Spectroscopy for chemical analysis (ESCA), also called X-ray Photoelectron Spectroscopy (XPS) technique provides qualitative and quantitative information on the elements present at the surface of the sample; therefore it permits to identify the surface chemical composition. Some features are a elements detection at a >0.1 atomic % concentration, b) information about molecular environment (oxidation state, bonding atoms, etc.) c) depth profiles about several hundred nanometers in the sample with ion etching technique [80]. These characteristics among others make this technique the most powerful analytical tool available.

In order to carry out an analysis, the sample or surface to be analyzed is first place in a vacuum environment and then irradiated with photons. For ESCA, the photon source is in the X-ray energy range. The atoms comprising the surface emit electrons (photoelectrons) after direct transfer of energy from the photon to the core-level electron. These emitted electrons are subsequently separated according to energy and counted. The energy of the photoelectrons is related to the atomic and molecular environment from which they originated. The number of electrons emitted is related to the concentration of the emitting atom in the sample.

The chemical composition of the oxide layer of the sample will be determined with the use of this powerful technique.

4. 5. 2 Sample Preparation

Cylindrical samples with dimensions of 5 mm thickness and diameter of 10 mm were used. The specimens were degreased by a 10 min immersion in an ultrasound bath in acetone, followed by methanol using an Ultrasonic cleaner (Branson, Model 2510) apparatus to remove any surface contamination. These cylinders were mounted on a copper sample holder using a copper sticky tape.

4. 5. 3 Equipment

The measurements were made by using VG ESCALAB-3 Mark II system equipped with a non-monochromatic twin-anode X-ray source. The Al $K\alpha_{1-2}$ x-ray radiation with an energy of 1486.6 eV was used. The anode was operated at 14.7 kV and 20 mA, and the analyzer was operated at constant pass energy of 20 eV. The spectrometer was calibrated at the binding energy of Au ($4f_{7/2}$) (84 eV), Ag ($3d_{5/2}$) (368.3 eV) and Cu ($2p_{3/2}$) (932.4 eV) levels using pure metals. The resolution of the instrument is 0.8 eV. The adventitious C1s peak at 285.0 eV was taken as energy reference for charge compensation. The data shown were obtained at a take off angle of 0° with respect to the surface plane.

4. 6 Surface Analysis: Auger Electron Spectroscopy

4. 6. 1 Principle

Auger electron spectroscopy (AES) represents today the most important chemical surface analysis tool for conducting samples. The method is based on the excitation of so-called

'Auger electrons'. AES principle is based on the use on primary electrons with typical energies between 3-30 kV and the possibility to focus and scan the primary electron beam in the nanometer and micrometer range analyzing the top-most atomic layers of the matter [81]. The emitted Auger electrons are part of the secondary electron spectrum obtained under electron bombardment with a characteristic energy allowing one to identify the emitting elements. The experimental setup is very similar to that of a Scanning Electron Microscope, with the difference that electrons are not only used for imaging but also for chemical identification of the surface atoms, depth profile and measurement of the thickness of the oxide layer.

Auger electrons with energies up to 2000 eV, have a high probability to escape only from the first few monolayers because of their restricted kinetic energy. Consequently, they are much better suited for surface analysis.

The thickness as well as the elemental composition of the oxide layer will be determined by using this technique.

4. 6. 2 Sample preparation

The cylindrical specimens of 5 mm thickness and 10 mm diameter were mounted in a sample holder with silver paint. In order to avoid any surface contamination they were ultrasonically cleaned during 10 min in acetone, follow by methanol in an Ultrasonic cleaner (Branson, Model 2510) apparatus.

4. 6. 3 Equipment

The Auger analyses were performed in a JEOL JAMP-30 system equipped with a LaB_6 filament and at a background pressure of 10^{-7} Pa. The depth profile of chemical elements: Ni, Ti, Cr, and O, were acquired at an energy resolution of 0.1% using 10 kV, 0.5 μA argon ions. The argon etch rate was calibrated on a standard of thermally grown SiO_2 of 1000 Å of Si. These analyses were carried out before and after the heat treatment in order to compare the effect of heat processing on the samples.

4. 7 Electrochemical behavior evaluation: Voltammetry (Potentiodynamic mode)

4. 7. 1 Principle

In this technique the potential is varied between two defined limits E1 and E2

$$E(t)+ = E(t = 0) + It \quad \text{Where:} \quad I = dE/dt$$

The electric current is a function of the scan rate [I= f (E, I)]
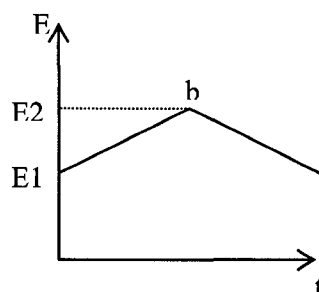
Figure 4.1 E/t diagram

The potentiodynamic tests or voltammetry consist in varying the potential from E1 to E2, or up to point b. In the cyclic polarization, the start potential and end potential are the same, so the scan takes place from E1 to E2 and goes back to E1. (Figure 4.1) This permits to observe the hysteresis loop which is an indicator of the crevice corrosion susceptibility.
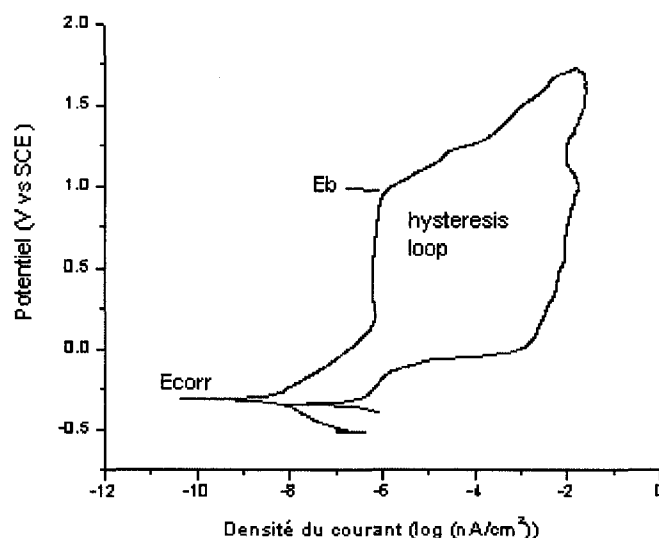
Figure 4.2 Typical corrosion curve

From both tests information is obtained in the corrosion curve (Figure 4.2). Several values and parameters are calculated in both tests: E_{corr} (the corrosion potential), I_{corr} (the

corrosion current), E_b (the breakdown potential of the passive film) and E_p (the repassivation potential). This last value is only calculated for the cyclic polarization tests. These parameters are defined as follows [82]:

E_{corr} is the value of potential at witch cathodic and anodic potentials equilibrate. This is an indicator of the stability of the surface.

I_{corr}, the corrosion current is associated to E_{corr}. It is a relative measure of corrosion. This value is necessary to calculate the corrosion rate that illustrates the quantity of material lost during corrosion

E_b, the breakdown potential, indicates at what point the passive oxide layer stops being protective; which permits the possible formation of pits. While the passive film is broke, the current increase rapidly. The higher the E_b, the more resistant the metal is to pitting corrosion

E_p is the potential of repassivation, and is define as the intersection between the reversed scan and the initial one.

Certain conditions are considered in the corrosion standard to analyse the results:

- The difference between E_p and E_b values is an indicator of the pitting corrosion resistance of the material. The smaller the difference, the greater is the resistance.

- The hysteresis between E_p and E_b is an indicator of crevice corrosion susceptibility. The smaller the hysteresis, the greater is the resistance.

- When the scan is reversed, if the curve goes over the curve done before application of the reversed scan, the metal shows total repassivation. In this case, no hysterisis is formed and the point where the scan is reversed is called the vertex potential (E_v). This point shall be reported instead of E_b and E_p if it happened.

- If E_b is not present on the curve, there is nor pitting nether crevice corrosion of the metal.

The critical parameters such as corrosion potential, breakdown potential and corrosion rate will be measured to evaluate the corrosion resistance of the different samples.

4. 7. 2 Cell

The electrochemical investigations were done using conventional so-called three electrodes cell (Ballon) provided by Gamble technology Inc. While the working electrode is our sample, in this case the NiTi, a graphite electrode and a saturated calomel electrode is used as a reference electrode (Figure 4.3). The corrosion tests were performed in potentiodynamic mode at 37°C using Hank's Balance Salt Solution as electrolyte according to the ASTM G5-94 procedure [83]. This electrolyte was deoxygenated with nitrogen gas before and during the experiments. After an initial delay (1h) which allows the stabilization of the open circuit potential (OCV), the test was started. A 0.17 mV/s scan rate was applied in the potential range from 250 mV to 1000mV. The density and porosity of the sample are used to calculate the surface of the sample.
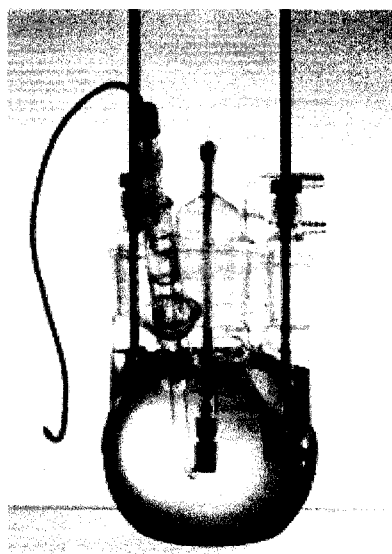
Figure 4.3 Corrosion cell set up for potentiodynamic tests

4. 7. 3 Electrode preparation

Cylindrical specimens 5mm thickness and 10 mm diameter were used. To insure a clean surface the samples were immersed for 10 min in acetone follow by methanol in an Ultrasonic cleaner (Branson, Model 2510) apparatus. A PPME holder was fabricated as show in the Figure 4.4 to expose only one side of the cylindrical sample.
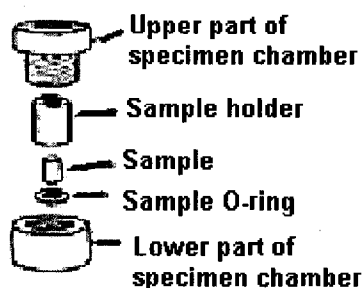
Figure 4.4 Sample's holder for the electrochemical evaluation.

4. 7. 4 Equipment

Potentiodynamic tests were performed in a Potentiostat/Galvanostat, Model 273, EG&G Princeton Applied Research.

4. 8 *In situ* Fourier Transformed Infrared Reflectance Spectroscopy

4. 8. 1 Principle

This method couples two different techniques: one electrochemical and the second optic spectroscopy. It allows the in-situ study of the interface electrode/solution under a variation of potential.

In the Optic spectroscopy reflexion the variations of the characteristics of the incident electromagnetic wave (wavelength, polarization, intensity) after reflexion by the surface electrode can be associated to its physical properties (optical, electric and magnetic) [84]. Therefore the identification, of species form at the surface and on the immediate surrounding of the electrode, is possible by the detection of their characteristic vibrational spectra.

The different electrochemical parameters (corrosion potential, breakdown potential and corrosion rate) will be measured as well as the relative reflectivity in order to identify the interactions between the electrode and the electrolyte.

4. 8. 2 Cell

This electrochemical cell was fabricated in Kel-F (a high density Teflon) mounted on an aluminum support. The cell is equipped with a calcium fluoride (CaF_2) transparent window on the studied range (1000-3000 cm^{-1}). It consists in a Saturated Calomel Electrode as reference, and a platinum counter electrode (Figure 4.5). The same procedure as in the potentiodynamic tests was followed. Two conditions were change, first the scan was started at a 500 mV more cathodic potential than the open circuit potential (OCP), increasing toward the anodic values at a constant rate of 0.17mV/s up to 2000mV/SCE, and then a reverse scan was carried out toward the cathodic value. Second, the Hank's Balanced Salt Solution was used without phenol red, to avoid any influences due to this chemical component.
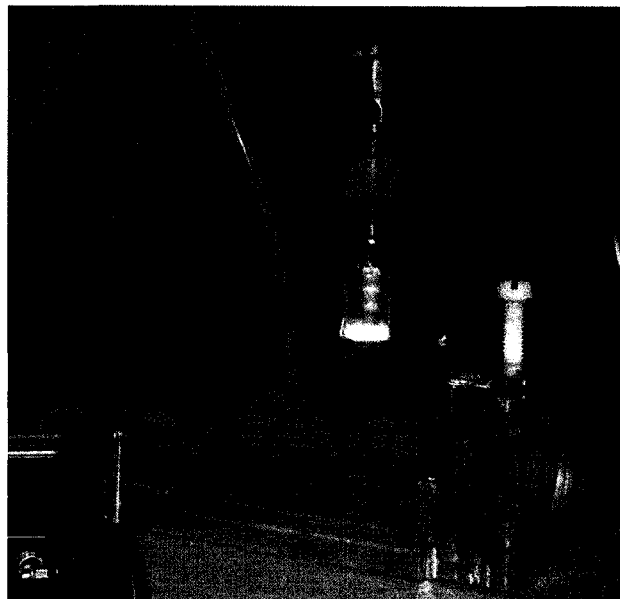
Figure 4.5 Corrosion cell set up for in-situ FTIR spectro-electrochemistry

4. 8. 3 Electrode preparation

The samples were mechanically polished through a series of silicon carbide papers up to a 600-grit surface finish and then finished mirror-like using a 1 μm diamond paste on an Ecomet 3 Grinder/Polisher. The sample was place in a Kel-F holder fix with resin to avoid any leakage. The sample holder was positioning in the middle of the cell as shown in the Figure 4.6. The working electrode is place against the CaF_2 window, in a way that the optic trajectory is minimized (a few micrometers), during the acquisition data.
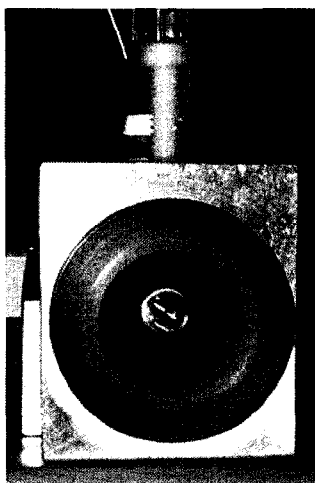
Figure 4.6 Sample detail for the UV spectro-electrochemistry cell

4. 8. 4 Equipment

Fourier Transformed Infra-Red system IFS 66/S Bruker Optics equipped with a MCT Mid-band D316 detector. The detection range is found on the range of 10000-600 cm^{-1} with a sensitivity D*>2.5x10^{10}cm Hz$^{1/2}$ W^{-1}. A middle infrared lamp was used as a source of light. The electrochemical equipment used was a Potentiostat/Galvanostat, Model 273, EG&G Princeton Applied Research.

CHAPTER V. Characteristics of porous Nickel-Titanium ALLOYS for medical applications

Hernández R.[1], Polizu S.[1], Turenne S.[2], Yahia L'H.[1]

1 Groupe de Recherche en Biomécanique/Biomatériaux (GRBB)

2 Département de génie physique et de génie des matériaux

École Polytechnique de Montréal, C.P. 6079, Succ. "Centre-Ville",

Montréal (QC) H3C 3A7, Canada

Status

5. 1 Abstract

We investigate the behavior of NiTi porous alloys, possessing the property of shape memory, by using different characterization methods XPS, Auger, DSC and SEM. The study mainly focuses on the determination of porosity, surface characteristics and the phase transformation. In the case of porous material the biomechanical compatibility is closely related to the internal structure and porosity distribution. To describe appropriately the influence of the properties of NiTi on the memory shape, two types of materials provided by different sources has been analyzed. Despite the fact that both materials present different pores size, they exhibit an open and interconnected porosity. Our measurements show that the temperature of the inception of the martensite-austenite phase transition occurs at 60°C, which is by 20°C greater than the body temperature. Moreover, we show that the surface characteristics can be greatly influenced by heat treatment. Furthermore, we observe that the R-phase occurs only for one of the used

materials after its heat treatment. The correlation between the composition and the other characteristics measured has been found.

5. 2 Introduction

NiTi alloys with a porous internal structure have already been used for approximately a decade, in maxillofacial surgeries [33] and other orthopedic procedures [5, 34-36] involving thousands of patients in Russia [6-7] and China [5, 8]. However, the interest for these materials is still increasing in many areas of the biomedical field, such as, in the development of shape memory implants of special design. Therefore, further knowledge is needed concerning the relationship between, on one hand, the phase constituents and the factors determining the internal structure of the material, and on the other, the fundamental material properties and the response of the biomedical device used.

The key factors identified to play a determinant role, for the use of these alloys as materials for implants, and their capillary property and biomechanical compatibility (low elastic modulus, damping capacity). The capillarity behaves in conjugation with internal structure. In fact, the capillary force controls the transport of fluid through interconnected pore channels and the material wetability influences the velocity and height of rise fluid in capillaries [37-38]. The optimal combination of both features encourages the bone marrow penetration within the internal structure of the implant. This results in a good attachment between any contacting tissue and the porous NiTi implant.

An interconnected porosity is very important because the bone will grow within the interconnected pore channels near the surface maintaining its vasculararity and long-term viability and providing a desirable firm fixation. It has been found that the optimal pore size is in the range of 100-400 μm [39]. Besides their opened porous structure allows

bone tissue ingrowth into the body of the implant and thus provides the desirable firm fixation.

The porosity affects also the mechanical behavior of the material [40]. A good matching between the elastic modulus of the bone (20 GPa) and that one of the implant is needed. The closer values have been shown by NiTi alloys in the martensite phase (28-41 GPa). Moreover, if the material has an internal structure of 50% porosity, it exhibits a lower modulus (14-20 GPa), which allows the possibility of significant bone ingrowth at this matching value.

Porous NiTi can be produced by various manufacturing processes. We can mention, for instance, Powder Metallurgy and Self-propagating High-temperature Synthesis (SHS). Powder metallurgy process NiTi alloys consist in the compactation and sintering of titanium and nickel powders [42]. The investigation of their properties and behaviors, including crystal structure, phase composition, mechanical properties and shape memory parameters, started to be carried out in the late 1970's [40]. From these studies, it has been reported that the properties of the sintered alloys are extremely sensitive to the sintering conditions. The SHS method, also called ignition synthesis, is based on the utilization of the exothermic heat of formation upon interaction of various elements. There exist two kinds of SHS: layer burning and heat explosion [40]. In the former, heat is initially released due to localized exothermic reaction in some regions. It is then absorbed by the neighboring layers of powder, causing reactions and thereby shifting the reaction zone. In this case, a chemical reaction takes place only in a thin-layer wave of burning but not in the whole volume at the same time. In the latter, the increase of the temperature in the whole volume of the reacting system leads to a self-ignition that is similar to an explosion. In the reacting zones the maximum temperature values reached in both techniques are similar. These temperatures can be lower, or higher than the melting point of NiTi. Both methods can be used efficiently to control the porosity range and thus

providing appropriately sized and interconnected pores, in order to create similar bone morphology.

Although the fact that the porous NiTi posses the biocompatibility property that has been found to be comparable of the stainless steel, cobalt-chromium and titanium material's, only a few studies have conducted for its investigation. Shabalovskaya *et al.*, have carried out an *in vitro* study and concluded that the porous as well as the solid phases of NiTi, are well accepted by human tissues as nearly as pure titanium is [49]. Based on *in vitro* and *in vivo* experiments, Rhalmi *et al.* arrived at the same result, and observed bone ingrowth within the pores of the implants three weeks after implantation [50].

Our objective in this paper is to provide, via different techniques, a systematic characterization of porous NiTi alloys for medical applications by determining the physical properties and surface characteristics. In this study we extend the investigation to two types of samples produced by two different sources. Since the internal stress created by processing may turn out to be very large, an annealing process is considered in order to optimize the behavior and the biocompatibility property of these materials.

5. 3 Materials and Methods

5. 3. 1 Materials

The selected samples consist of two types of NiTi alloys, to be denoted in the following by A and B, supplied by different sources. The sample A was provided by Professor Victor E. Gjunter from the Institute of Medical Materials and Shape Memory Implants, Tomsk, Russia, and the sample B was provided by Dr. Tae-Hyun Nam Division of Materials Science & Engineering Gyeongsang National University, Korea. Both specimens were obtained by the SHS procedure.

The specimens, each of a thickness of 5 mm, were cut from cylindrical porous rods with a diamond saw in order to maintain their internal structure. They were cleaned during 10 min by immersion in a bath containing a mixture of acetone and methanol using an Ultrasonic cleaner (Branson, Model 2510) apparatus.

5. 3. 2 Methods

The experimental techniques we have used led to a good characterization of our alloys with respect to the surface characteristics as well as to the transformation temperature. One series of specimen from each sample was submitted to an annealing process during 30 min at 550°C. The cleaning operation was carried out after the process.

Thermal Analysis: We used the Differential Scanning Calorimetry (DSC) technique, to identify the phase transformation behavior. The analyses were carried out in a Perkin Elmer Pyris1 Calorimeter equipped with a CryoFill Liquid Nitrogen Cooling system. The apparatus has been calibrated into temperature interval 0–200°C at a rate of 10°C, using Indium as reference materials. Each specimen with a mass of 25 mg approximately have been cycled once within the range of 0-190°C at a heating/cooling rate of 5°C, using He as purge gas. We have recorded two thermograms for each sample A and B, corresponding to treated and non-treated material.

Morphological Analysis: The scanning electron microscope (SEM) analyses were performed in order to determine the surface texture and the porosity. The micrographs were taken using a JEOL model JSM-840 Scanning Electron Microscope at 15.0 kV on the treated and non-treated specimens.

Surface Analysis: The X-ray Photoelectron Spectroscopy (XPS) technique permitted us to identify the surface chemical composition. The measurements were made by using ESCALAB-3 MKII system equipped with a non-chromatic twin-anode X-ray source. The

Al $K\alpha_{1-2}$ x-ray radiation with quantum energy of 1486.6 eV was used. The anode was operated at 14.7 kV and 20 mA, and the analyzer was operated at a constant pass energy of 20 eV. The spectrometer was calibrated at the binding energy of Au $(4_{f7/2})$(84 eV) and $Cu(2_{p3/2})$(932.4 eV) levels using pure metals. The resolution of the instrument is 0.8 eV. The advantageous C1s peak at 285.0 eV was taken as energy reference. The data shown were obtained at a take off angle of $0°$ with respect to the surface plane.

Auger analysis has been used to determine the thickness of the oxide layer created on the surface of the two types of samples after heat treatment. They were performed in a JEOL JAMP-30 system equipped with a field emission source under a pressure of 10^{-7} Pa. The depth profile of chemical elements: Ni, Ti, Cr and O, were acquired at an energy resolution of 0.1% using 3 kV, 0.5 μA argon ions. The argon etch rate was calibrated by using a standard of thermally grown SiO_2 of 1000 Å of Si. These analyses were carried out before and after the heat treatment in order to compare the effect of heat treatment on the samples.

5. 4 Results and Discussion

To describe the shape memory performance and other properties of NiTi shape memory alloys, our analysis takes into account not only the different sources of materials but consider also the effect of heat treatment. The later turns out to be necessary to release internal stress created during processing. We decided to carry out the heat treatment at $550°C$ since at this temperature the damping reaches its maximum value in the martensite phase [77].
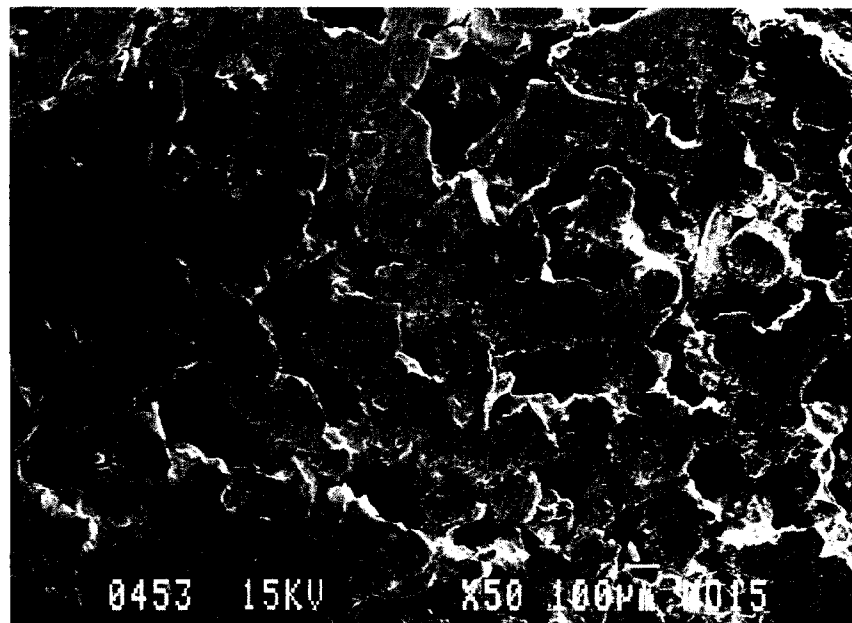
Figure 5.1 Scanning electron microscopy of porous NiTi material A
(Original magnification: x50).
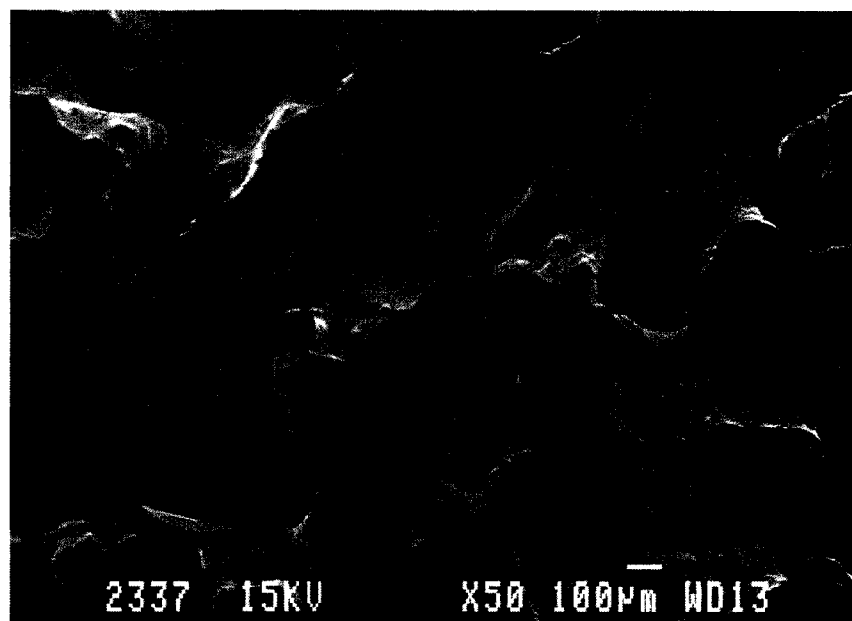
Figure 5.2 Scanning electron microscopy of porous NiTi material B
(Original magnification: x50).

Figure 5.3 Surface of the material B (Original magnification: x200).

The material A exhibited an interconnected and opened porosity with a pore size of 80-120 μm as revealed by SEM observation (Figure 5.1). No changes in the characteristic features of the surface or in the porosity have been detected after heat treatment. For the material B, we observed a homogeneous pore distribution with a pore size of 100 μm for the isolated pores. Moreover, as shown in Figure 5.2, the pores are opened and interconnected. The observed textured surface characterizes this sample (Figure 5.3). The mean pore size (100-120 μm) reveals an internal structure that promotes the capillary phenomena [39]. Both materials present an interconnected structure that enhance the bone tissue ingrowth and good fixation of the implant

The results of the DSC measurements for the material A revealed an austenite transformation with a broad peak of width of 16°C (As = 101°C) and an enthalpy of ΔH=3.5 J/g. The martensite phase limits are found at temperatures of 64°C (Ms) and 72°C (Mf) with a ΔH=7.3 J/g. The curve profile does not show any changes between 0-50°C as shown in Figure 5.4, indicating that the samples are in the martensite phase at the body temperature. After the heat treatment, we have observed a new peak arising at

104°C, which may correspond to the R-phase accompanied by an increment in the ΔH (twice the initial value).
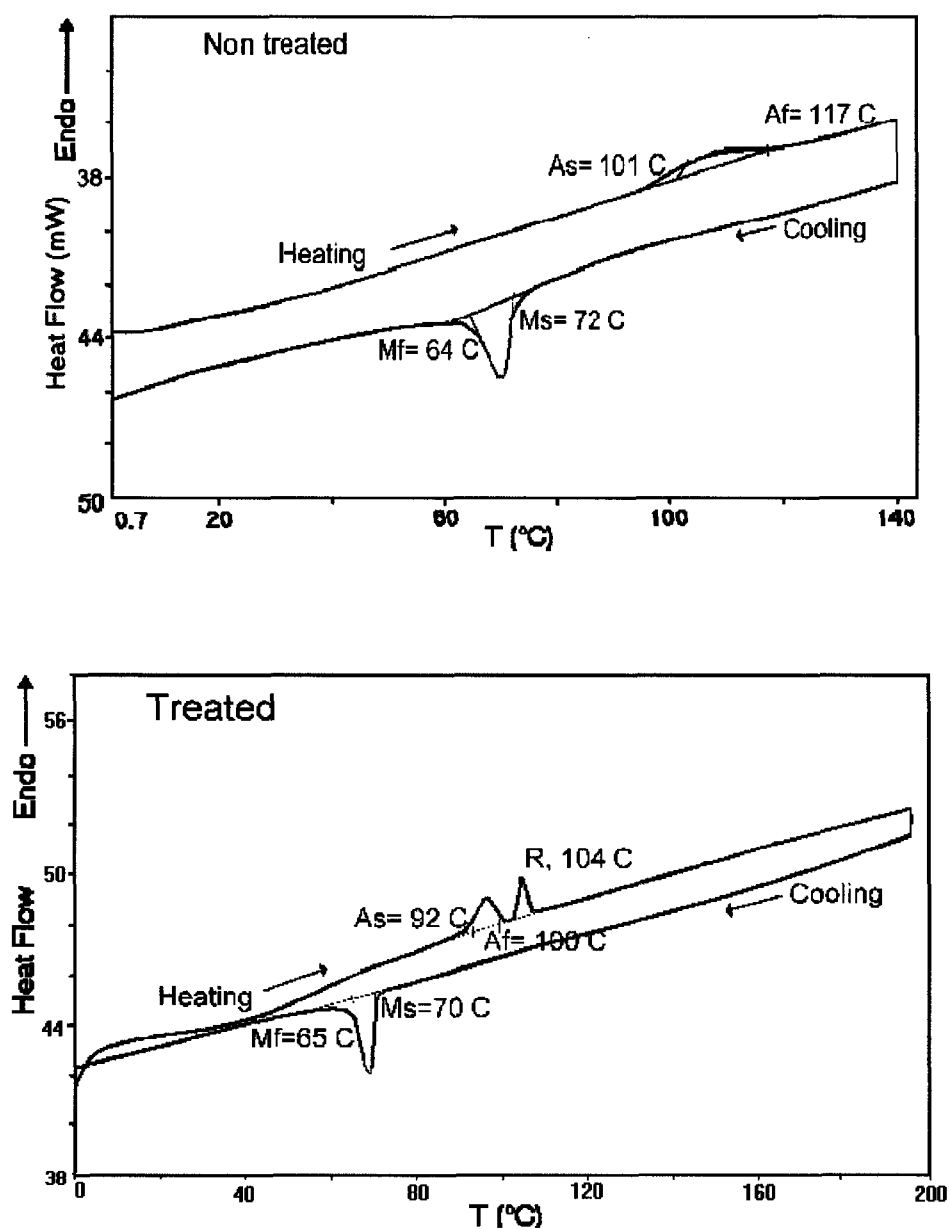
Figure 5.4 DCS-Thermal analysis curve of porous NiTi alloy A before and after treatment.

The DSC measurements for the material B show an austenite transformation with a broad peak of 17oC of width (As = 95°C) and a ΔH=2.2 J/g. The martensite phase peak limits are found, respectively, at the temperatures of 71°C (Ms) and at 63°C (Mf) with a ΔH=3.1 J/g. Similarly to the sample A, the material B remains in the martensite phase at the body temperature (Figure 5.5).

We have observed that the R-phase appears only in material A after the heat treatment. The thermal treatments or changes in the alloy chemical composition are the only conditions that may lead to its detection [85]. As both materials were submitted to the same heat treatment process, we presume that R-phase transformation becomes detectable due to chemical compositions of this material.

The XPS study indicates that the surface undergoes oxidation after heat treatment for both materials (Table 5.1, 5.2). The surface is mainly composed of titanium oxide and of nickel oxide in much less extended amount. The high resolution XPS spectra show the Ni peak at 852.22 eV for material A and at 851.75 eV for the material B for the non-treated series. Since the Ni was oxidized after heat treatment no trace of Ni in atomic state was found for these series as revealed by the presence of peaks at 855.82eV corresponding to material A and 855.56eV for material B.. For the material B we also found a peak at 575 eV which corresponds to chromium, the Cr/Ti ratio is 0.10%.
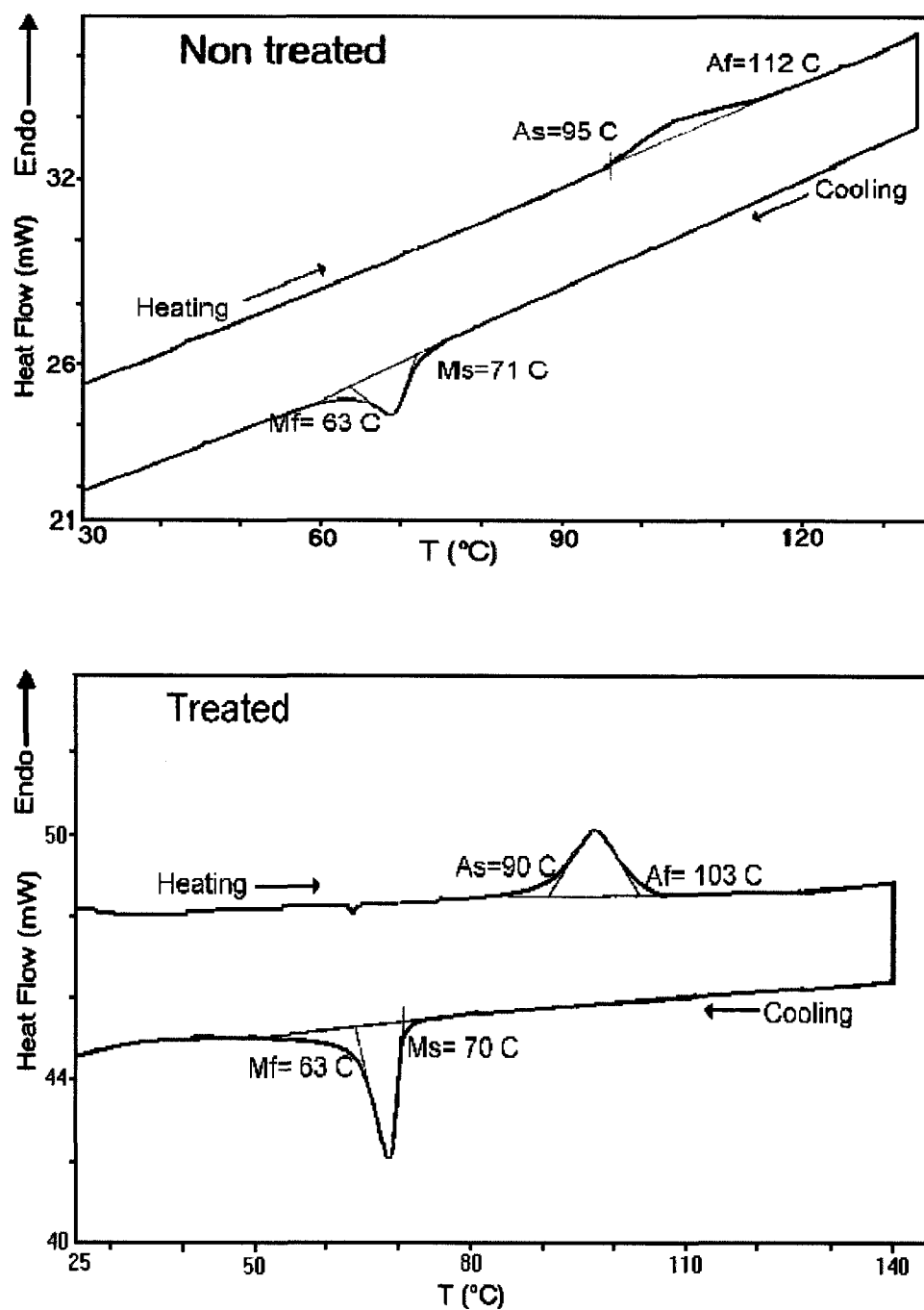
Figure 5.5 DCS-Thermal analysis curve of porous NiTi alloy B
before and after treatment.

Table 5.1 Surface chemical composition as obtained by XPS high-resolution analysis for material A

Non Treated		Treated	
Element	BE(eV)	Element	BE(eV)
Ni	852.22		
Ni-O	852.95		
Ni_2O_3	855.45	Ni_2O_3	855.82
shake-up Ni	*857.94*	*shakeup Ni_2O_3*	*861.73*
Shake-up NiO	*858.67*	*sat p1/2*	*861.5*
Shake-up Ni_2O_3	*861.4*	*sat p1/2*	*863.5*
Ti^{2+}	454.55		
p1/2 Ti^{2+}	*460.63*	Ti^{3+}	456.21
Ti^{3+}	456.33	*p1/2 Ti^{3+}*	*462.38*
p1/2 Ti^{3+}	*461.51*	Ti^{4+}	459.42
Ti^{4+}	458.79	*p1/2 Ti^{4+}*	*464.96*
p1/2 Ti^{4+}	*464.35*		

Table 5.2 Surface chemical composition as obtained by XPS high-resolution analysis for material B

Non treated		Treated	
Elements	BE(eV)	Elements	BE(eV)
Ni	851.75		
Ni_2O_3	854.94	Ni_2O_3	855.56
shake-up Ni	*853.85*	*shake-up*	*861.56*
shake-up Ni	*857.85*		
Shake-up Ni_2O_3	*861.4*		
		Cr	575
Ti^{4+}	458.05	Ti^{4+}	458.29
p1/2 Ti^{4+}	463.61	*p1/2 Ti^{4+}*	463.87

From the Auger results, we calculated the thickness of the oxide layer. We used as reference that each cycle corresponds to 71.6 Å. (specific characteristic of the instrument). For the non-treated series, we calculated for material A 16.3 cycles which correspond to 1171.4 Å and for material B, 4.3 cycles which correspond to 310.26 Å. After the annealing, the oxide layer for material A is 3977.5 Å and for material B is 2864.0 Å. We thus see that the oxide layer has been increased by the annealing. The surface profiles are shown in Figures 5.6 and 5.7.
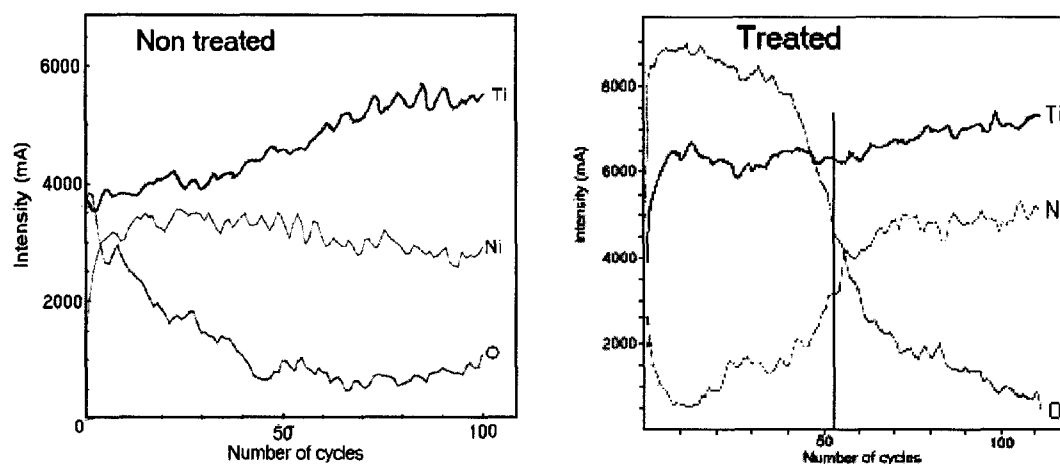
Figure 5.6 Surface's profile for the material A (y axe number of cycles).
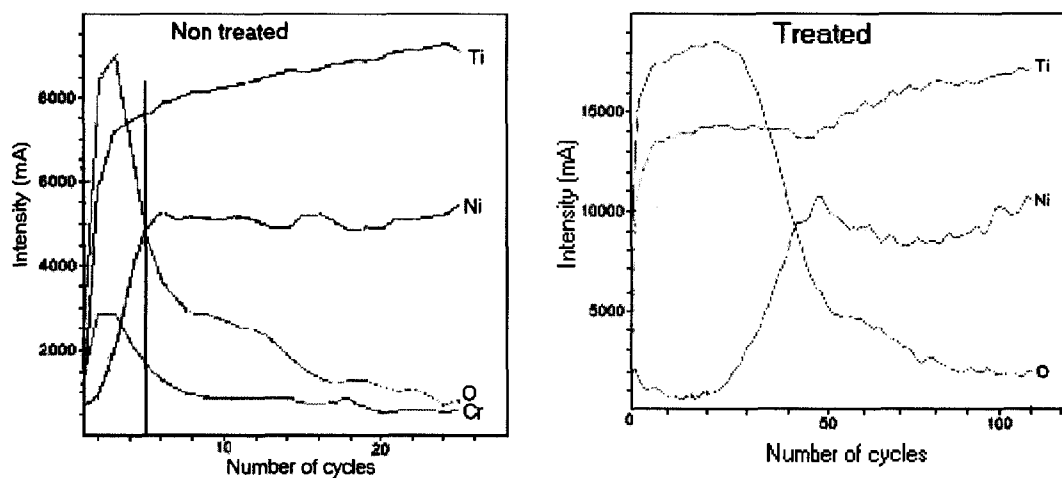
Figure 5.7 Surface's profile for the material B (y axe number of cycles).

5. 5 Future work

The capillary properties, damping capacity and corrosion behavior of these porous materials are now under investigation in view to attempt a fully characterization.

5.6 Acknowledgments

5.7 References

See chapter XI

CHAPTER VI. Corrosion Resistance of Porous Nickel-Titanium Alloys for Medical Applications

Hernández R.[1,2], Cisse O.[2], Polizu S.[1], Napporn T.[2], Savadogo O.[2], Yahia L'H.[1]

[1]Laboratoire d'Innovation et Analyse de Bioperformance

[2]Laboratoire de nouveaux matériaux pour l'énergie et l'électrochimie

École Polytechnique de Montréal, C.P. 6079, Succ. "Centre-Ville", Montréal (QC) H3C 3A7, Canada

Status

6.1 Abstract

The electrochemical behaviour of four different types of porous NiTi alloys was studied. The samples were produced by Self-propagating High-temperature Synthesis (SHS) procedure. The samples were analyzed by SEM, XPS, AES techniques and potentiodynamic tests. A heat treatment was performed to release stresses generated through processing. Its influence on the corrosion resistance of the samples was also evaluated. The results show that the treated samples exhibited a lower corrosion rate. However the highest breakdown potentials were observed on the non treated samples. In fact, the heat treatment improved the corrosion resistance of only one material. A correlation between the chemical composition and pore size and the electrochemical behavior was found. In particular it was found that the corrosion resistance is related to the surface chemical composition of the electrodes rather to their surface morphology.

Keywords: Porous NiTi alloys, corrosion resistance, SEM, XPS, potentiodynamic test.

6. 2 Introduction

Metallic materials are used extensively as orthopedics implants, dental materials and other medical applications [88]. Occasionally the interactions between these implants and the surrounding tissues lead to their degradation often induced by the corrosion. Therefore the electrochemical behavior of these devices needs to be studied in order to indicate the possible way for preventing ion release and thus improving the functional performance and durability of these implants, otherwise the primary factor governing their biocompatibility. Among the aspects affecting biocompatibility are the amounts and forms of released corrosion products and their disposition in the body after release.

Several metallic materials have been used to fabricate medical implants [88]. Nickel-Titanium alloys have developed a great interest due to its thermal shape memory, superelasticity and high damping properties, which make such alloys behave differently compare to other metals. Indeed, NiTi shape memory alloy has properties that could be very useful in surgical applications [89].

Solid NiTi alloys exhibit passive electrochemical behavior comparable to other clinically used alloys [22]. NiTi alloy derives its biocompatibility and good corrosion resistance from a homogenous oxide layer mainly composed of TiO_2, with a very low concentration of nickel [2]. The evaluation of the biocompatibility and corrosion resistance through the electrochemical investigations showed that NiTi behaves much like titanium. However in some cases the corrosion resistance of these alloys could be lower or unpredictable than that one of pure titanium [90]. This behaviour might be explained by the heterogeneity of the oxide layer containing nickel ions the surface. The release of these ions from the materials due to corrosion may cause unfavorable effects [91]. In order to prevent this problem, some solutions have been proposed as the application of surface treatments. It is well documented that surface treatments can improve the corrosion resistance of the materials [24].

The surface of the material plays an important role because of its interaction with the tissues. Thereby the roughness of the material defines the contact surface. In the case of NiTi for biomedical implants a rougher surface is managed to produce a porous permeable structure for some applications whereas in others a smoother surface is required [26]. In the literature some studies showed that the surface texture of the alloy affects both the corrosion resistance and cell response, therefore its biocompatibility [9]

In the latest decades a new generation of NiTi alloys has emerged. This alloy presents an interconnected porous structure fabricated by various techniques. This porous structure provides excellent ingrowth in living tissue and firm fixation. Due to their generally good biocompatibility these materials can serve in the body for a long time without being removed [40]. NiTi shape memory alloy porosint, is a promising artificial bone material [43]. Although, the porosity and the roughness of such materials enhance the reaction on the surface, it could promote the extent of corrosion [92]. Indeed, there is a lack of studies regarding the corrosion resistance of these alloys.

The objective of this work is to investigate the electrochemical behavior of porous NiTi alloys provided by different sources. The morphology and the chemical composition of the surface are correlated in order to explain this phenomenon.

6. 3 Experimental Procedure

6. 3. 1 Materials

The selected samples consist of four types of NiTi alloys supplied by different sources presented in Table 6.1 and denoted in the following by A, B, C and D. All specimens were obtained by the Self-propagating High-temperature Synthesis (SHS) procedure applied under different conditions by the suppliers. The cylindrical specimens, with a

thickness of 5 mm, and diameter of 10 mm were cut from porous rods with a diamond saw in order to maintain their internal structure. They were cleaned during 10 min by immersion in a bath of acetone and then methanol using an Ultrasonic cleaner (Branson, Model 2510) apparatus.

A heat treatment was applied in order to release internal stress created during forming processes, one series of specimens from each type was submitted to an annealing process during 30 min at 550°C in an air atmosphere. The samples will be denoted as X_T for the treated and X_{NT} for the non-treated, where X is A, B, C or D. The cleaning operation was carried out after the process.

Table 6.1 List of samples' suppliers

Sample	Supplier	Affiliation
A	Prof. Victor E. Gjunter	Institute of Medical Materials and Shape Memory Implants, Tomsk, (Russia)
B	Dr. Tae-Hyun Nam	Division of Materials Science & Engineering Gyeongsang National University, (Korea)
C	Prof. B. Silberstein	Institute of Medical Materials and Shape Memory Implants, (Russia) made in a laboratory in Israel
D	Prof. John Moore	Colorado School of Mines (Non equiatomic alloy 48Ti-51Ni), USA

6. 3. 2 Surface Analysis

The chemical composition of the surface was identified by using the X-ray Photoelectron Spectroscopy (XPS) technique. A VG ESCALAB-3 Mark II system equipped with a non-chromatic twin-anode X-ray source the measurements were made. The Al $K\alpha_{1-2}$ x-ray radiation with quantum energy of 1486.6 eV was used. The anode was operated at

14.7 kV and 20 mA, and the analyzer was operated at constant pass energy of 20 eV. The spectrometer was calibrated at the binding energy of Au $(4f_{7/2})(84\,eV)$ and Cu $(2p_{3/2})(932.4\,eV)$ levels using pure metals. The resolution of the instrument is 0.8 eV. The advantageous C1s peak at 285.0 eV was taken as energy reference.

Auger analysis (AES) has been used to determine the thickness of the oxide layer created on the surface of the two types of samples after heat treatment. They were performed in a JEOL JAMP-30 system equipped with a field emission source under a pressure of 10^{-7} Pa. The depth profile of chemical elements: Ni, Ti and O, were acquired at an energy resolution of 0.1% using 3 kV, 0.5 μA argon ions. The argon etch rate was calibrated by using a standard of thermally grown SiO_2 of 1000 Å of Si. These analyses were carried out before and after the heat treatment in order to emphasis the effect of heat treatment on the samples.

6. 3. 3 Morphological Analysis

The morphological analysis of the samples provides a structural profile of material and its surface relief. Information concerning the surface texture and the porosity of the samples as well as the effects of the corrosion evaluation were obtained by scanning electron microscope (SEM) analyses. The micrographs were taken using a JEOL model JSM-840 Scanning Electron Microscope at 15.0 kV on the treated and non-treated specimens.

6. 3. 4 Electrochemical Corrosion Test

The electrochemical investigations were done using conventional so-called three electrodes cell (Ballon) provided by Gamble technology Inc. While the working electrode is one of the 4 materials, the counter electrode is in graphite electrode and saturated calomel electrode is used as a reference electrode (Figure 6.1). The corrosion tests were

performed in potentiodynamic mode at 37°C using Hank's solution as electrolyte according to the ASTM G5-94 procedure [83]. This electrolyte was deoxygenated with nitrogen gas before and during the experiments. After an initial delay (1h) which allows the stabilization of the open circuit potential (OCV), the test was started. A 0.17 mV/s scan rate was applied in the potential range from 250 mV to 1000mV. The density and porosity of the sample are used to calculate its surface.
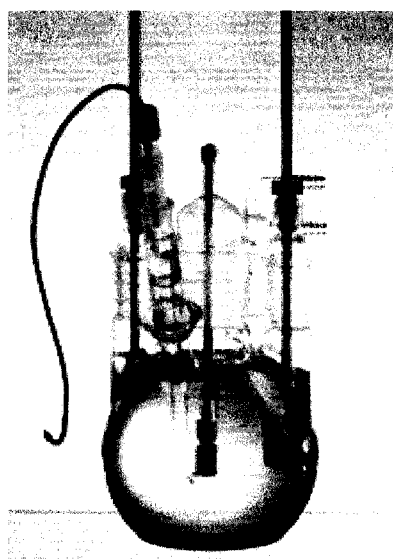
Figure 6.1 Corrosion cell set up for potentiodynamic tests

6. 4 Results

Figure 6.2 shows the potentiodymamic curves obtained with samples A_T and A_{NT}. The values of the breakdown potential, as listed in Table 6.2, confirm that the non treated sample exhibits higher potential than the treated sample. On the other hand, the corrosion potential of the sample A_{NT} is significantly different than that one of the treated sample as summarized in Table 6.3.
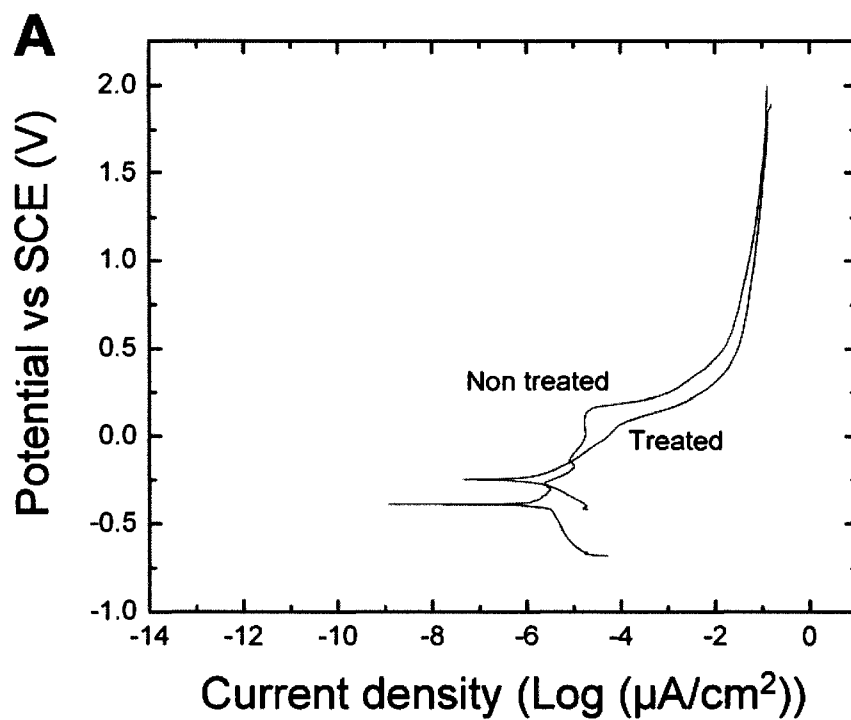
Figure 6.2 Potential/current density curves for sample A

Table 6.2 Breakdown values for the studied samples

Breakdown potential (mV)				
Sample	A	B	C	D
Non Treated	163.00	-32.80	173.00	-136.30
Treated	61.40	-18.30	15.62	14.70

Table 6.3 Corrosion potential values obtained for the samples

Corrosion potential (mV)				
Sample	A	B	C	D
Non Treated	0.3901	0.2109	0.2770	0.2860
Treated	0.1454	0.2220	0.2806	0.1532

The results in Table 6.2, 6.3 exhibit that the material B displays a more stable behaviour in comparison to those of type A. Indeed, we can see on the Figure 6.3 that both curves are almost superposed, indicating that the non-treated and the treated samples follow the same behavior. Accordingly, the difference between the values of the breakdown potential of material B is negligible and less pronounced compared to the other materials (Table 6.2). These samples exhibit the same corrosion potential.
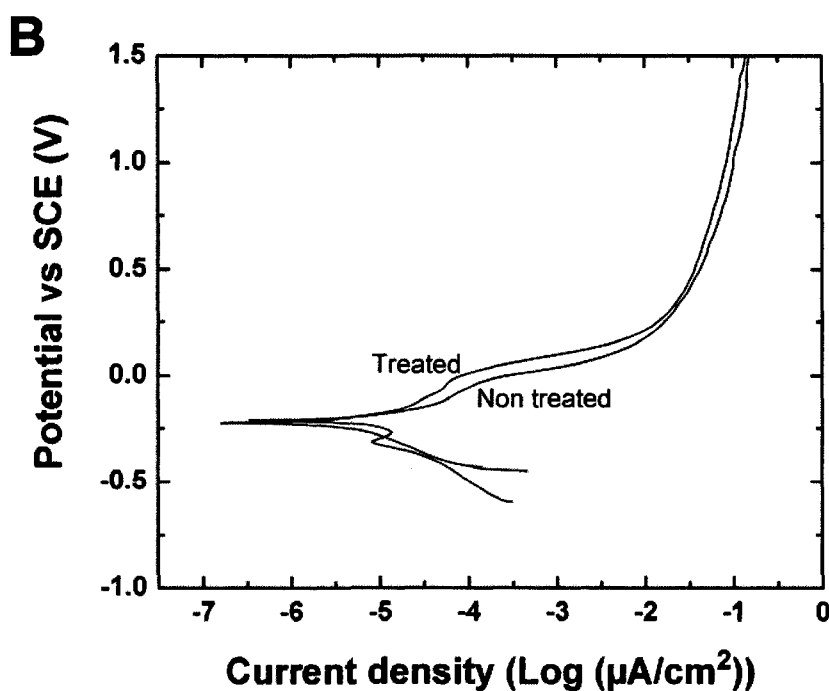
Figure 6.3 Potential/current density curves for sample B

Regarding the material C, we observe that its behavior is comparable to that one of the type A as shown in figure 6.4. In fact the breakdown potential is lower for the treated sample (Table 6.2) and easier to identify. However their corrosion potentials are almost superposed (Table 6.3).

C
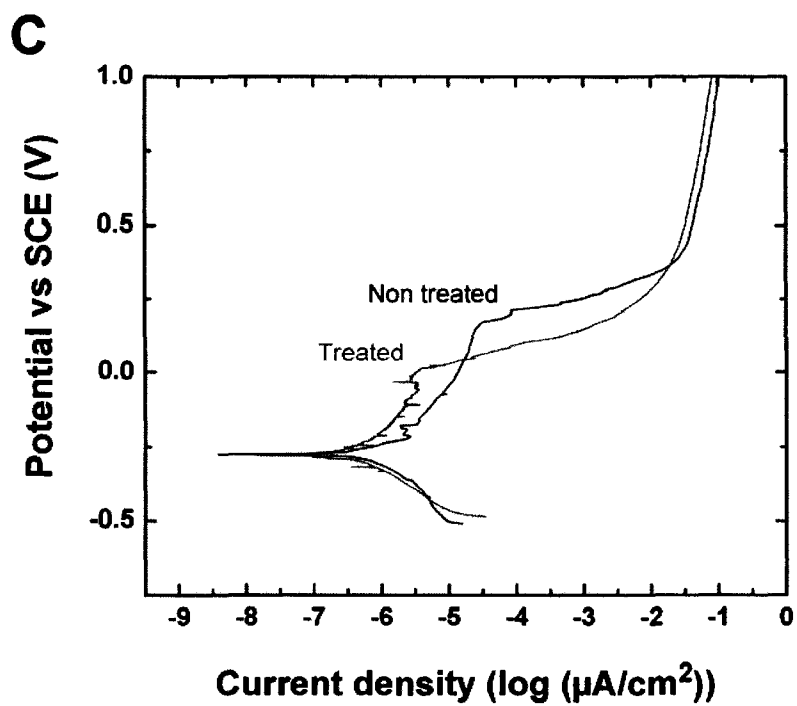
Figure 6.4 Potential/current density curves for sample C

D
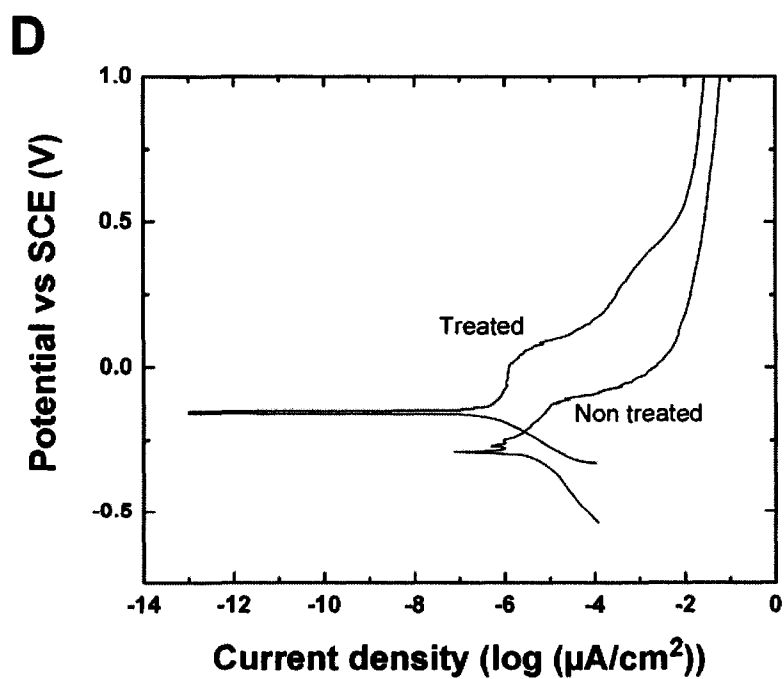
Figure 6.5 Potential/current density curves for sample D

The sample D_T shows a breakdown potential at a higher value (Figure 6.5) contrary to the preceding samples. The material D did not follow the same behaviour in terms of breakdown and corrosion potentials. Indeed, the corrosion potential of the sample D_{NT} is lower than that of the sample D_T.

The microscopic analysis for the samples revealed that the heat treatment did not generate any morphological changes. Thereby same characteristics were observed on non-treated and treated samples. Then non-treated samples were chosen to represent the morphology without any preference.
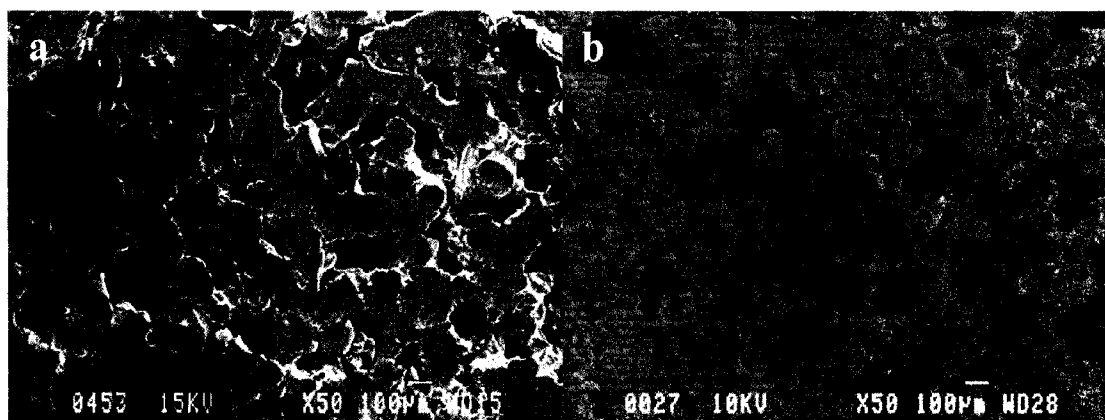
Figure 6.6 Scanning electron microscopy of porous NiTi material A;

a) as received and b) after corrosion test

The material A presents and interconnected porosity, with a pore size of 80-120μm (Figure 6.6a). The changes on its porosity are obvious after the electrochemical evaluation. The surface shows a higher roughness (Figure 6.6b).
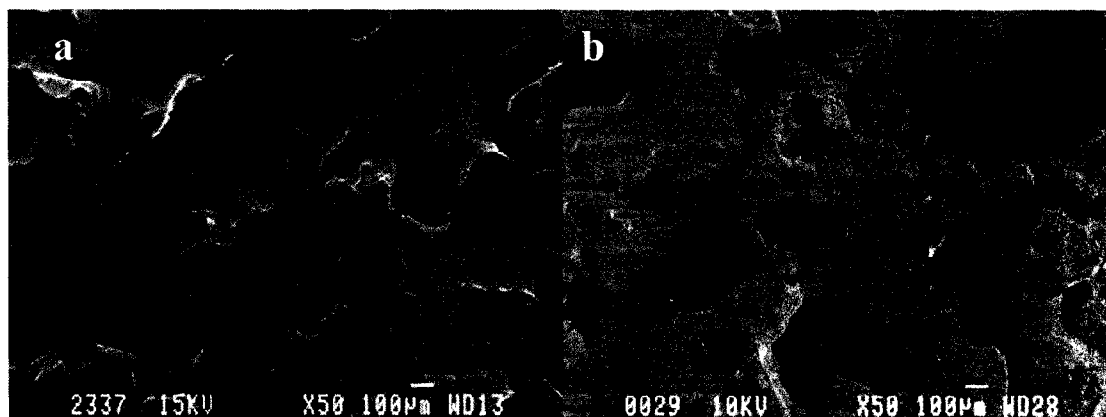
Figure 6.7 Scanning electron microscopy of porous NiTi material B;

a) as received and b) after corrosion test

Figure 6.7a shows that material B exhibit a mean pore size in the range of 100-120μm. Moreover, the pore size of 100μm for isolated pores could be observed. The corroded surface is shown in figure 6.7b. As it can be observed the corrosion took place not only at the surface but at deeper levels too.
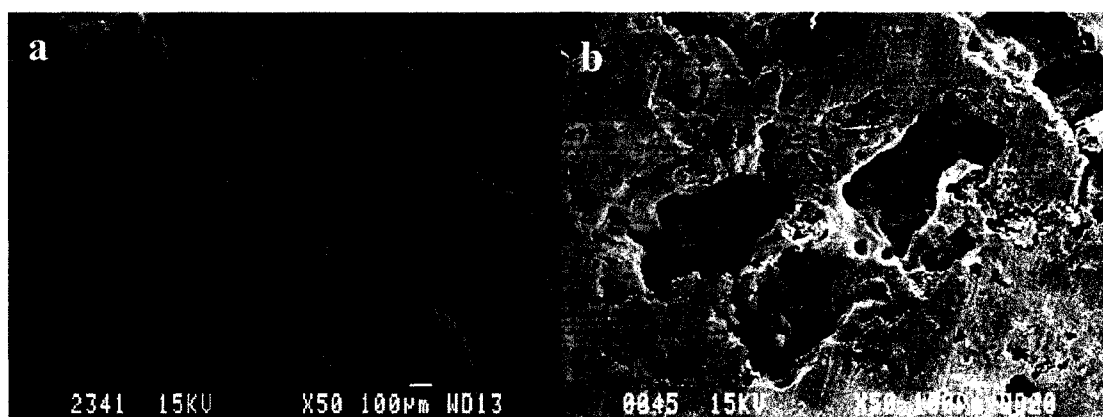
Figure 6.8 Scanning electron microscopy of porous NiTi material C;

a) as received and b) after corrosion test

The material C exhibited an interconnected and opened porosity with a pore size of 100 μm as revealed by SEM observation (Figure 6.8a). A change in the pores size and their distribution is visible after corrosion test (Figure 6.8b). In fact the edges of the pores were

more susceptible for corrosion as we can see in the micrographs (Figures 6.6b, 6.7b and 6.8 b).
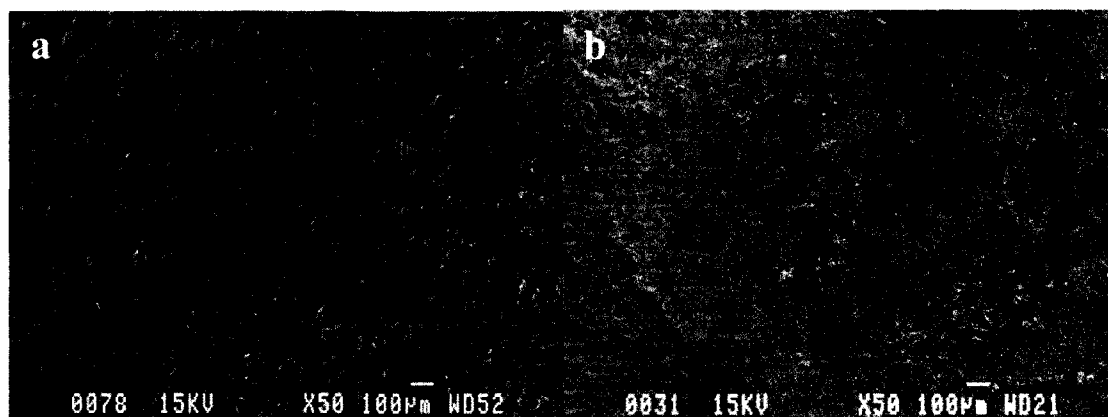
Figure 6.9 Scanning electron microscopy of porous NiTi material D;

a) as received and b) after corrosion test

These morphological characteristics are different in the case of material D; the pores with 35-50μm diameter are interconnected to form an opened structure (Figure 6.9a). After performing the potentiodynamic test we observed a different pore size distribution as well as an increment on the pore diameter (Figure 6.9b).

6. 5 Discussion

Table 6.2 shows clearly that the highest values for the breakdown potentials were measured in the A_{NT} and C_{NT}. However these values decrease after the sample treatment. Therefore the effect of the treatment reduces the corrosion resistance of materials A and C. Three negative values of the breakdown potential are observed for samples B_T, B_{NT} and D_{NT}. Thereby the break of the protective layer occurs at an early stage, even on non treated samples for materials B and D. The less noble breakdown potential was obtained for sample D_{NT}. This might be and indication that its passive film is less protective than

the passive layer on sample A. However all the samples show a breakdown potential which can be attributed to a chemical breakdown of the passive layer.

The slowly increase of the breakdown potential value after treatment does not show any improvement in the corrosion behavior in the case of sample B.

As has been already pointed out, sample D is the only one which breakdown potential is significantly increased due to the treatment. One of the determining factors of such increase is the presence of smaller pores which provide a smoother surface. This is in agreement with the investigations of Trepanier *et al.* [22], who showed that samples with smoother surfaces exhibit higher corrosion resistance than those with irregular layers.

This is also supported by the work of Abiko *et al.* [9] which showed that porous NiTi treated by chemical etching has a breakdown potential of 60 mV. This is due to its reduce passivity. Therefore the reduce passivity for this porous sample could be attributed to the inhomogeneous surface structure. The breakdown potential measured for the treated samples in our work are lower except for sample A_T which value is very close to the one obtained in their study.

Our results seem in contradiction to those who showed that the corrosion resistance of porous NiTi decreased with the increase of porosity [11], because we observed higher breakdown potentials for bigger pores. But it is important to notice that the porous samples used in their work were fully filled with resin. This resin can inhibit the propagation of the corrosion through the pores. This can explain the difference between the two studies.

Even though, materials A, B and C exhibit a high porosity, the samples A_{NT} and C_{NT} showed the highest breakdown potentials among the other samples. Therefore the size of the pores is not the only parameter which affects the corrosion resistance. Surface

composition might be another key factor influencing the corrosion behaviour of the sample.

The corrosion rates of the various samples are summarized in Table 6.4. The results show that the treated samples lead to the decrease of the corrosion rate. The specimens C_T and D_T exhibit the lowest values whereas the highest value was obtained for the B_{NT}. The corrosion rate of the sample decreases in the order: B>A>C>D for the non treated and treated samples. The ratio of the corrosion rate of the non treated samples on those of the treated electrodes increases in the order: D<A<C<B. This evaluation indicates that the treatment has a more pronounced effect on sample B than on sample D. This behaviour might be strongly related to the surface of the sample. Furthermore, XPS studies can sustain the correlation between the corrosion rates and surface composition.

Table 6.4 Measurements of the corrosion rate for the studied materials

Material	Corrosion rate (mmpy)	
	Non treated	Treated
A	0.1183	0.0359
B	0.9340	0.1680
C	0.0760	0.0221
D	0.0505	0.0202

The XPS analysis carried out before the treatment of the samples reveals the presence of Ni ions. After the heat treatment the surface undergoes oxidation for all the materials, no trace of Ni in atomic state (Table 6.5 to 6.8) is observed. This is in agreement with previous data [93] showing that there is a Ni-zone free in the oxide layer when treated at a temperature between 500°C and 600°C. Furthermore the oxidation treatment of NiTi in air at temperatures close to 500°C produce a smooth protective nickel-free oxide layer

which enhances the biocompatibility of this alloy. However the corrosion resistance was not evaluated.

The low corrosion rates observed on treated samples are an indication of the high corrosion resistance compare to those non-treated. The data presented in the table 6.6 does not indicate the presence of intermediate titanium oxides on material B. This absence could be related to the higher corrosion rate measured for this material. Therefore the presence of intermediate titanium oxides on surface chemical composition of the samples results on better corrosion rates and improved corrosion resistance. This is the case of materials A, C and D which exhibit significant lower corrosion rates than B because their surface contains intermediate titanium oxides.

Table 6.5 Surface chemical composition obtained by XPS high-resolution analysis for material A

Non Treated			Treated		
Element	Before corrosion test	After corrosion test	Element	Before corrosion test	After corrosion test
	Concentration (%)			Concentration (%)	
C	61.50	37.54	C	41.90	42.76
O	30.20	42.83	O	45.80	49.84
Ni	1.87	--	Ni	--	--
Ni-O	0.31	3.40	Ni-O	--	0.13
Ni_2O_3	0.42	0.78	Ni_2O_3	3.80	0.50
Ti^{2+}	0.21	--	Ti^{2+}	--	--
Ti^{3+}	0.59	6.36	Ti^{3+}	1.08	5.52
Ti^{4+}	2.90	0.74	Ti^{4+}	4.72	0.80

The oxygen concentration before and after treatment remains almost the same value for materials C and D as shown in tables 6.7 and 6.8. On the contrary for materials A and B the oxygen concentration decreases after the treatment. As the value of the total oxide concentration does not necessarily indicated a difference in the corrosion rates of these materials we can conclude that the difference on the corrosion rate might be attributed to the types of oxides of the chemical composition.

Small concentrations of other elements such as: Na, Cl, Ca (<2%) after the corrosion evaluation tests were found. This is attributed to the contamination of the sample surfaces by the hank's solution.

Table 6.6 Surface chemical composition obtained by XPS high-resolution analysis for material B

Non treated			Treated		
Element	**Before corrosion test**	**After corrosion test**	**Element**	**Before corrosion test**	**After corrosion test**
	Concentration (%)			**Concentration (%)**	
C	55.10	35.72	C	29.30	44.69
O	35.00	60.70	O	54.10	46.67
Ni	1.20	--	Ni	--	--
Ni-O	--	--	Ni-O	--	0.85
Ni_2O_3	0.80	0.98	Ni_2O_3	1.90	0.67
Ti^{2+}	--	--	Ti^{2+}	--	--
Ti^{3+}	--	--	Ti^{3+}	--	6.30
Ti^{4+}	5.9	2.60	Ti^{4+}	12.50	0.82

The presence of NiO after the corrosion tests was observed in treated samples B, C and D (Table 6.6-6.8). These concentrations are in agreement with those already reported in the literature where the concentrations were: oxygen 27-50%, carbon 25-69%, titanium 2-22% and nickel 0-6% [3].

Table 6.7 Surface chemical composition obtained by XPS high-resolution analysis for material C

Non Treated			Treated		
Element	Before corrosion test	After corrosion test	Element	Before corrosion test	After corrosion test
	Concentration (%)			Concentration (%)	
C	33.57	29.51	C	24.67	30.48
O	54.18	53.89	O	54.05	54.34
Ni	0.35	0.13	Ni	--	--
Ni-O	0.14	--	Ni-O	--	0.30
Ni_2O_3	0.28	0.14	Ni_2O_3	4.83	0.05
Ti^{2+}	0.55	--	Ti^{2+}	--	--
Ti^{3+}	0.50	--	Ti^{3+}	0.89	--
Ti^{4+}	6.44	14.36	Ti^{4+}	14.03	8.43

AES spectra surveys were carried out before and after corrosion evaluation. They showed the presence of Ti, Ni, O and C. We found also traces of Na, Ca, and Cl after the corrosion test, the presence of these elements was observed before in the XPS study. A depth profile was carried out to determine the element distribution for Ti, Ni and O. It can be observed that the contamination carbon layer disappears almost immediately after Ar^+

sputtering. The oxide layer was measured for the samples and the results are found in table 6.9. From these measurements it is obvious that a passivation layer was formed at the surface. Due to the nature of the sample we cannot conclude if we are in the presence of a homogenous oxide layer. It seems to have a homogenous chemical composition, but in the pore borders the oxide layer might have some defects.

Table 6.8 Surface chemical composition obtained by XPS high-resolution analysis for material D

	Non treated			Treated	
Element	Before corrosion test	After corrosion test	Element	Before corrosion test	After corrosion test
	Concentration (%)			Concentration (%)	
C	40.9	37.15	C	36.28	33.49
O	50.22	49.93	O	43.32	52.93
Ni	0.64	--	Ni	--	--
Ni-O	--	--	Ni-O	--	0.22
Ni_2O_3	0.96	0.60	Ni_2O_3	3.8	0.28
Ti^{2+}	0.40	--		--	--
Ti^{3+}	0.38	3.18	Ti^{3+}	0.36	--
Ti^{4+}	4.82	1.40	Ti^{4+}	5.44	4.21

Table 6.9 Oxide layer thickness from AES measurements

Oxide layer thickness (nm)				
	Non treated		**Treated**	
Material	**Before**	**After**	**Before**	**After**
A	12	10	40	82
B	3	7	29	73
C	7	12	33	58
D	7	9	20	54

6. 6 Conclusions

The corrosion resistance of porous Nickel-titanium alloys was investigated. The results showed higher breakdown potentials were observed among the non treated samples. These samples presented also bigger pores. The impact of the surface treatment varies with the type of sample. While in the case of sample B, there is not a visible effect; a decrease of the breakdown potential value was measured for materials A and C. However an important improvement is evident for material D, which surface is characterized by the presence of smaller pores. Thus, we can conclude, that the surface treatment used in our investigations led to an improvement of the corrosion resistance for small pores whereas a decrease was observed for bigger pores. The presence of the intermediate Ti oxide results on better corrosion rates. In fact no traces of Ni ions were observed at the surface. This treatment showed also the role of the surface composition besides the pore size on the corrosion resistance.

6. 7 Acknowledgements

6.8 References

See Chapter XI

CHAPTER VII. In situ Fourier Transformed Infrared Reflectance Spectroscopy applied to Porous and Solid NiTi alloys for their electrochemical evaluation

R. Hernández [1,2], T. Napporn[2], O. Savadogo[2 *], L'H. Yahia[1]

[1]Laboratoire d'Innovation et Analyse de la Bioperformance

[2]Laboratoire de nouveaux matériaux pour l'énergie et l'électrochimie

École Polytechnique de Montréal, C.P. 6079, Succ. "Centre-Ville", Montréal (QC) H3C 3A7, Canada

Status

7.1 Abstract

Spectroelectrochemistry method was used to investigate the corrosion behaviour of porous and solid NiTi in Hank's solution. The effect of the surface preparation on the corrosion resistance of the sample was studied. The results showed that solid electropolished sample and solid mechanopolished samples exhibited a better corrosion resistance than porous mechanopolished sample. However the solid mechanopolished sample exhibited a higher corrosion rate almost as high as the one showed by the porous sample. On the other hand a higher breakdown potential was measured porous samples compared to previous studies. A higher susceptibility for pitting and crevice corrosion was observed. This behaviour could be explained by its internal structure. The FTIR results showed the interactions between the solution and the samples. It can be observed that each sample exhibit a particular behaviour. The porous sample as well as the solid samples showed Ti-OH interactions. Moreover both solid samples exhibited another peak corresponding to the OTi(OH)CCH interaction, which is explained by the chemical

composition of the electrolyte, in this case the Hank's solution that has a certain amount of glucose. However an inversion of the peak is observed in both samples, this direction change can be attributed to the surface treatment. The electropolished sample showed a more stable behaviour mean while the mechanopolished sample exhibited a change during the reverse scan. .

Keywords: corrosion, FTIR, Nickel-Titanium alloy, porosity, surface treatment

7. 2 Introduction

Nickel-Titanium alloy is a promising biomaterial its unique properties provide a large variety of medical applications. Despite the numerous studies performed to evaluate this material, its utility as a superelastic, shape-memory alloy implant material has yet to be fully investigated [39]. The results on the corrosion characteristics of NiTi alloy have ranged from "it behaves much like titanium" to "its corrosion resistance is either low or unpredictable" [90]. The results are governed by the surface interactions that occurs the interface between a material and its surroundings. Therefore, the surface of the implant plays an important role on its corrosion resistance. In fact, it most acts as a barrier protection at the metal/tissue interface. Their properties such as roughness, chemical composition, an even its mechanical properties are important.

Original NiTi surface has revealed a tendency towards preferential oxidation of titanium [94]. Different treatments such as, electropolishing, heat treatment, acid passivation have been applied to NiTi surfaces to improve its corrosion resistance. This improvement is attributed to the plastically deformed native oxide layer removal and replacement by a newly grown; more uniform one [24]. There are few corrosion studies dealing with the study of the surface composition, for example the use of XPS and AES to characterized Nitinol surfaces [3]. The results showed that the oxide layer at the surface of NiTi alloys is mainly composed by TiO_2 and smaller amounts of NiO and Ni_2O_3 [2, 14, 95]. The

conditions of the treatments can vary from one study to another, because there are no standards on this matter. The variation of a few parameters on different treatments, for example oxidation media, temperature and electrical potential can significantly change the surface composition [3]. The results obtained can be either a Ti-base surface with TiO_2 the only oxide or Ni-base surface built from less stable Ni oxides and hydroxides. Therefore a particular interest most be paid to the chemical composition of the surface. In the literature the electrochemical behaviour of the NiTi material in physiological environments is not clearly established and is rather controversial. In order to improve its corrosion behaviour different surface treatments have been proposed, such as electropolishing, acid passivation, etc. Corrosion evaluation performed on treated samples indicated that the employed treatments range in their importance from minimal to strong [23]. Several studies agreed that electropolishing improves the corrosion resistance of NiTi alloys [2, 23-24, 96]. NiTi alloys can present a different behavior due to small changes in the chemical composition or surface in consequence its behavior lacks of predictability

The objective of this study is to better understand the influence of the sample surface treatment on the electrode/environment interactions on the corrosion resistance of NiTi alloys. Further more our study aimed to better understand the electrochemical behaviour of NiTi alloys. Specifically, we will study the effect of the sample surface treatment on the corrosion behaviour. In particular the studies were done using the following treated samples: a porous mechanopolished sample, a solid mechanopolished sample and a solid electropolished sample. These samples will be studied by the In situ Fourier Transformed Infrared Reflectance Spectroscopy coupled to the voltammetry technique or spectrooelectrochemistry to identify the interactions between the surface and the environment in this case the Hank's solution.

7. 3 Experimental procedure

7. 3. 1 Materials

Porous NiTi cylindrical specimens 5mm thickness and 10 mm diameter were used. These samples were provided by Dr. Moore, from the Colorado School of Mines. The solid samples were provided by Dr. Ming Wu from Memry Corporation. Two different samples were received mechanopolished and electropolished; these treatments were carried out in their facilities. The porous samples were mechanically polished through a series of silicon carbide papers up to a 600-grit surface finish and then finished mirror-like using a 1 m diamond paste on an Ecomet 3 Grinder/Polisher. To insure a clean surface the samples were immersed for 10 min in acetone follow by methanol in an Ultrasonic cleaner (Branson, Model 2510) apparatus. The samples will be denoted as PMP for the porous mechanopolished sample, SMP for the solid mechanopolished specimen and SEP for the solid electropolished sample.

7. 3. 2 Methods

The electrochemical equipment used was a Potentiostat/Galvanostat, Model 273, EG&G Princeton Applied Research. The working electrode is our sample, in this case the NiTi, the counter electrode is platinum and a saturated calomel electrode is used as reference electrode. The corrosion tests were performed in potentiodynamic mode at 37°C using Hank's Balance Salt Solution as electrolyte according to the ASTM G5-94 procedure [83]. However, the solution was used without phenol red, to avoid any reflections due to this component. This electrolyte was deoxygenated with nitrogen gas before and during the experiments. After an initial delay (1h) which allows the stabilization of the open circuit potential (OCP), the test was started. The scan was started at a 500 mV more

cathodic potential than the OCP, increasing toward the anodic values at a constant rate of 0.17mV/s up to 2000mV/SCE, and then a reverse scan was carried out toward the cathodic value.

Fourier Transformed Infra-Red system IFS 66/S Bruker Optics equipped with a MCT Mid-band D316 detector cooled by liquid nitrogen. The detection range is found on the range of 10000-600 cm^{-1} with a sensitivity D*>2.5x10^{10}cm Hz$^{1/2}$ W^{-1}. A middle infrared lamp was used as a source of light. For the purposes of this study a CaF_2 window was used. The FTIR spectra were measured every 15 mV through the scan. At each potential, 100 interferograms were collected, Fourier-transformed and added. Each set of 100 averaged spectra was used to calculate the relative change of the electrode reflectivity defined as:

$$DR/R= Ro-R/Ro,$$

where Ro is the reference reflection [97]. According to the authors, the reference is arbitrary and must be taken at a no absorption region or where the value of the current remains constant.

7. 3. 3 Morphological Analysis

The morphological evaluation of materials provides a structural profile of material and its surface relief. Information concerning the surface texture and the effect of the corrosion on the surface samples were obtained by scanning electron microscope (SEM) analyses. The micrographs were taken using a JEOL model JSM-840 Scanning Electron Microscope at 15.0 kV and 20.0 kV.

7. 4 Results and Discussion

The electrochemical behaviour of the porous sample is shown in Figure 7.1. The sample exhibits a breakdown potential at 142.16 mV and a corrosion potential at -268.01 mV. The hysteresis on this sample is higher than those of the other samples. The high hysteresis of the sample is an indication of the high sensitivity of the interface to corrosion.

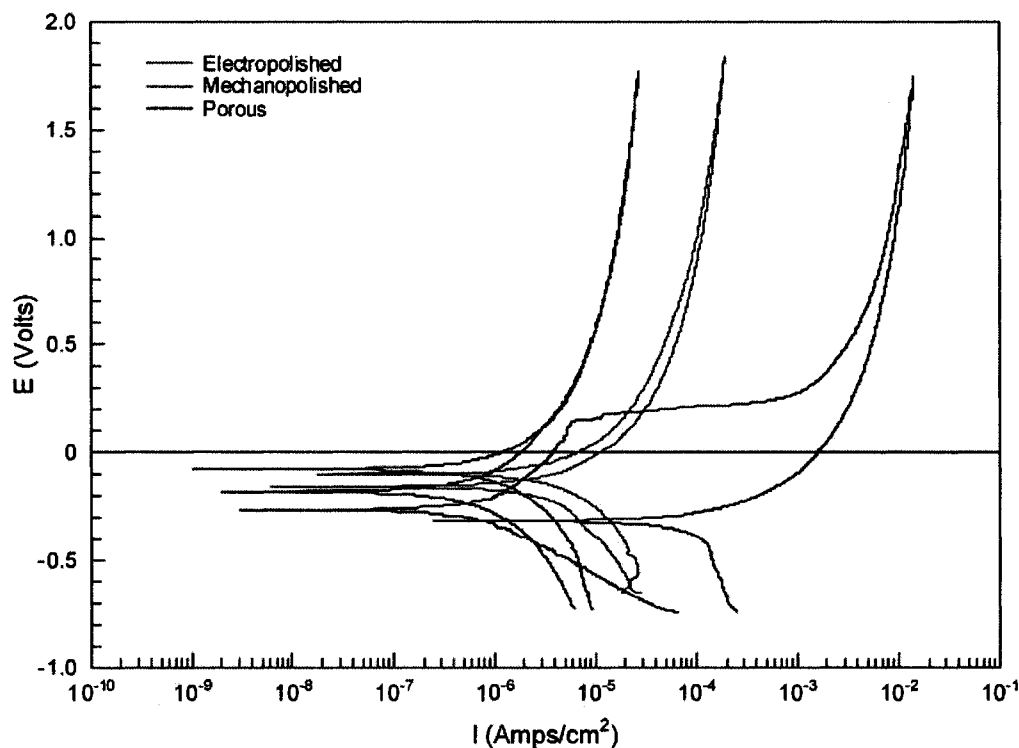Figure 7.1 Cyclic Polarization curves for the different samples: solid electropolished, solid mechanopolished and porous mechanopolished.

The mechanical polished sample does not exhibit a breakdown potential, but the corrosion potential is observed at -156.93 mV. The repassivation potential is not visible because the initial scan and the reverse scan are superposed. However the SMP sample presents a small hysteresis (Figure 7.1).

The electropolished sample shows the same behaviour as the mechanopolished sample. It can be observed, that there is no hysteresis for this sample. The corrosion potential was obtained at -180.06mV (Figure 7.1).

The corrosion rates are summarized on Table 7.1. The porous sample presents the higher corrosion rate, followed by the SMP and SEP. There is almost no difference between the corrosion rate of the porous sample and the solid mechanopolished. The solid electropolished sample show a lower corrosion rate almost 5 times smaller than that one of the porous sample.

Table 7.1 Corrosion rates as measured for the different samples

Sample	Corrosion rate (mmpy)
Porous mechanopolished	0.10593
Solid mechanopolished	0.080569
Solid electropolished	0.025879

The corrosion effect is visible only on the edge of the porous sample as it can be observe in Figure 7.2. The pores that are found in the rest of the surface do not present signs of corrosion.
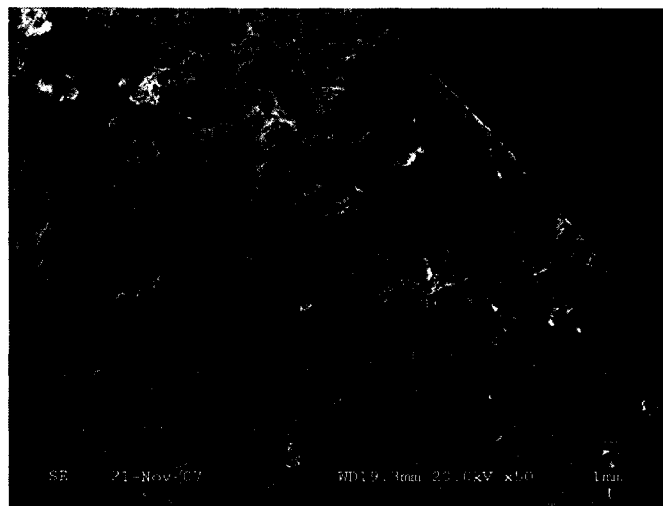
Figure 7.2 Porous mechanopolished sample after the corrosion evaluation

The mechanopolished sample does not exhibit the edge effect (Figure 7.3). The presence of pits on the surface is observed (Figure 7.4). However they were already present on the surface sample before the corrosion evaluation (Figure 7.5). Traces of the mechanical polishing are observed on the sample as received and after corrosion.
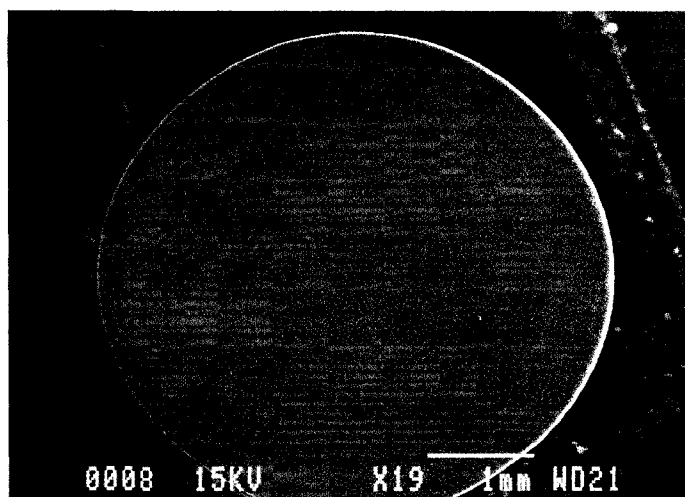
Figure 7.3 Solid mechanopolished sample following corrosion evaluation
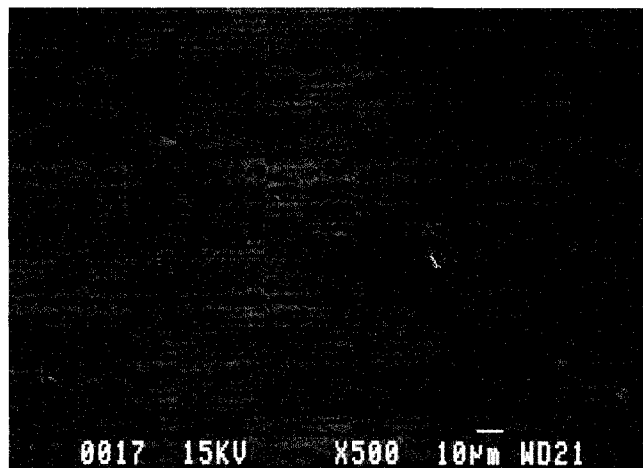
Figure 7.4 Detail on the corrode surface of the solid mechanopolished sample

Figure 7.5 Detail of the solid mechanopolished sample as received

The electropolished sample exhibit a smoother surface and does not show any signs of corrosion (Figure 7.6). There are some micro pores (less than 1μm) at the surface of the sample (Figure 7.7). As it can be observed in Figure 7.8, these pores were already visible before the electrochemical evaluation.
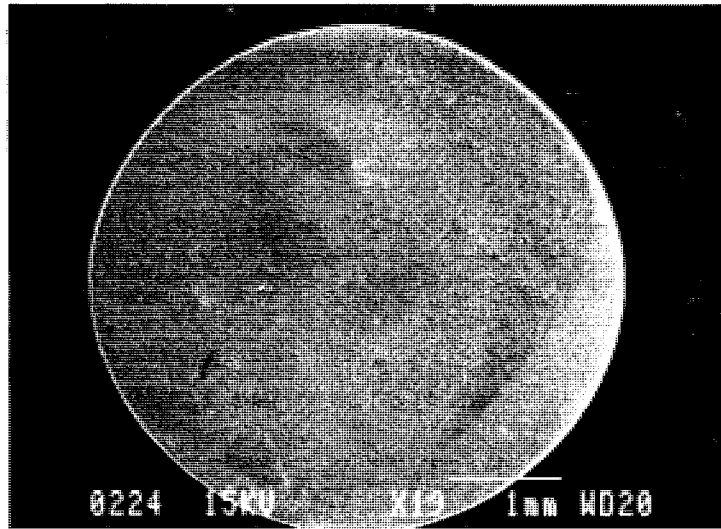
Figure 7.6 Solid electropolished sample following corrosion evaluation
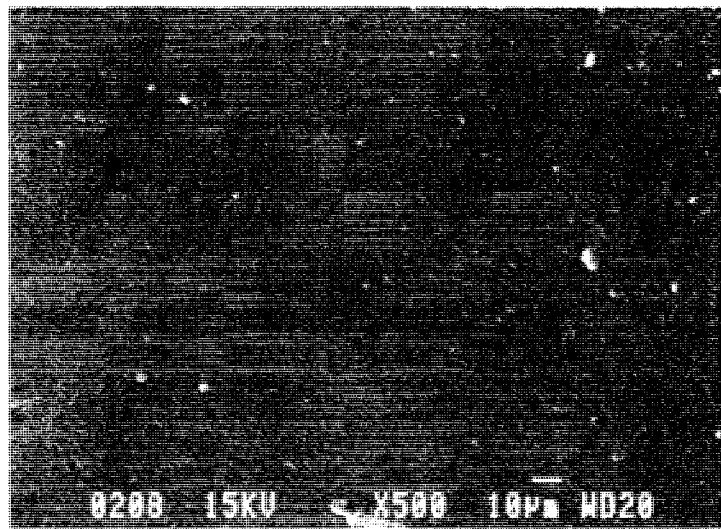
Figure 7.7 Detail on the corrode surface of the solid electropolished sample
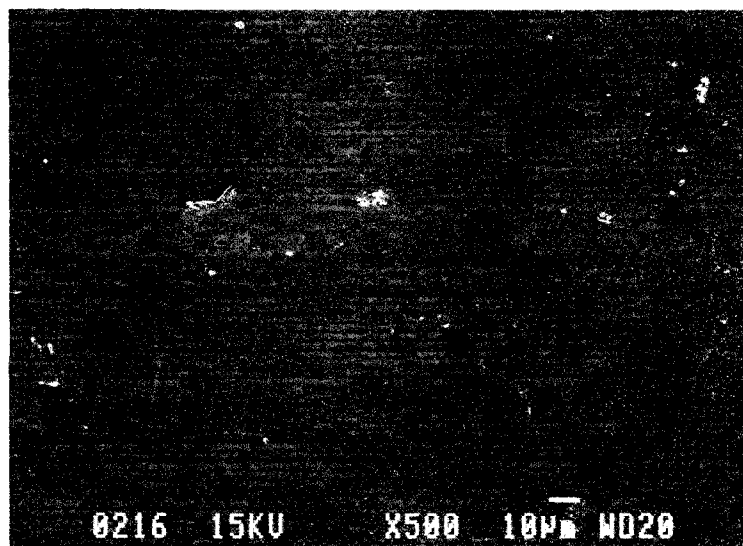
Figure 7.8 Detail of the surface of the solid electropolished sample as received

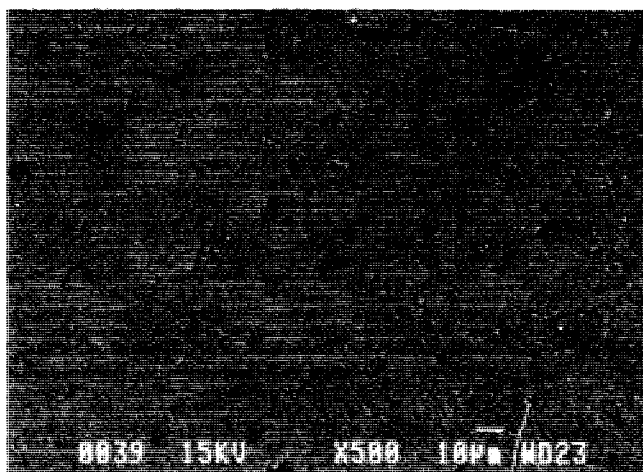According to these results, solid electropolished sample and solid mechanopolished samples show better corrosion resistance than porous mechanopolished samples. As samples SEP and SMP does not show any hysteresis (Figure 7.1), we can conclude that both specimens showed a complete repassivation and a great resistance to crevice corrosion. However the solid mechanopolished sample exhibits a higher corrosion rate almost as high as the one showed by the porous sample. It has been reported that contradictory results for mechanical polished samples can be attributed to the variability of the protective layer on NiTi, due to grain boundaries defects and surfaces stress [2]. Figure 7.5 and 7.7 showed smoother surfaces for the corrode samples.

On the other hand porous samples exhibit a breakdown potential value higher that others reported on the literature [9, 98], but lower than those ones published for solid samples, indicating the susceptibility of these samples for pitting corrosion. This sample also showed the highest corrosion rate; which can be explained from Figure 7.2 where it is clearly showed that the surface undergoes corrosion particularly on the edges. The hysteresis exhibit by the porous sample indicates that it is more susceptible for crevice corrosion.

The FTIR obtained for the porous sample exhibit the appearance of five bands; these can be related to the formation of corrosion products and their interaction with the solution (Figure 7.9). In each band the presence of a peak is observed at $1627cm^{-1}$, $2096cm^{-1}$, $2323cm^{-1}$, $3101cm^{-1}$ and $3650cm^{-1}$ respectively. A change of the intensity is evident for the scan at to 0.2387 V, which correspond to that one of the corrosion potential. According to the literature [99-100, 104-105] three of the bands can be attributed to Ti-OH interactions except for the peaks that appear at $2096cm^{-1}$ and $2323cm^{-1}$ that we were not able to identify. All these bands are found on the positive direction of the IR band. There is an important intensity increment observed at the corrosion potential, which can be attributed to the electrochemical reaction occurring at this stage. On the reverse scan it can be observed that the same bands appeared however the wavelength present a shift in the values compared to those ones of the initial scan. They appeared at $1240cm^{-1}$, $1619cm^{-1}$, $2102cm^{-1}$, $2356cm^{-1}$, $3076cm^{-1}$ and $3644cm^{-1}$ (Figure 7.10). On the basis of the literature results it can be attributed to Ti-OH interactions [99-100, 104-105] as well as another peak at $1240cm^{-1}$, attributed to PO_2 interactions [102]. The intensity of the bands appears to be lower for the reverse scan.

Figure 7.9 FTIR spectra of the surface of the porous mechanopolished sample during the
initial scan

Figure 7.10 FTIR spectra of the surface of the mechanopolished sample during the
reverse scan

The FTIR spectra for the SMP sample towards the anodic direction during are shown in Figure 7.11. It is possible to observe a band in the range of 800-1000 cm^{-1}, on the positive direction that can be attributed to TiO_2 and P-OH interactions [101-102]. Another band at 1446-1741 cm^{-1}, on the negative direction, attributed to Ti-OH interactions [99]. A single peak is found at 2358 cm^{-1}, on the positive direction, which we not able to identified. Two farther bands are identified at the range of 2910-3351cm^{-1} on the negative direction an interaction OTi(OH)CCH appeared due to the chemical composition of the Hank's solution [101]; and the other one at 3351-3648cm^{-1} on the positive direction, attributed to Ti-OH interactions [99-100, 104-105]. Through the cathodic direction the first band does not appear (Figure 7.12) showing a difference on the surface/solution interactions. The second band becomes a defined peak at 1643cm^{-1} from Ti-OH interactions [99] and another single peak is found at 2341cm-1. The two farther bands are observed at 2921-3390cm^{-1} and 3390-3629cm^{-1}, (Ti-OH interactions) a shift on the values compared to that one of the anodic direction scan is observed [99-100, 104-105]. The intensity is reduced at lower potentials.
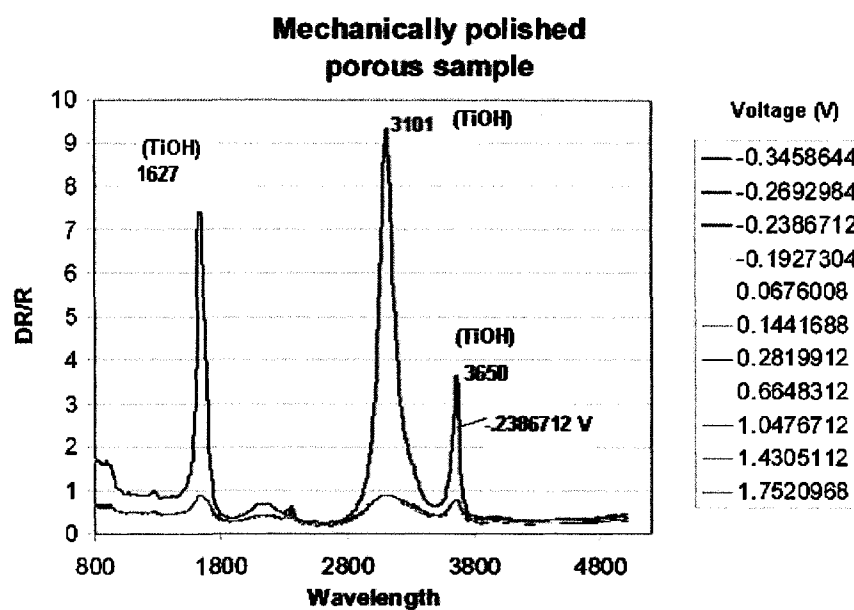

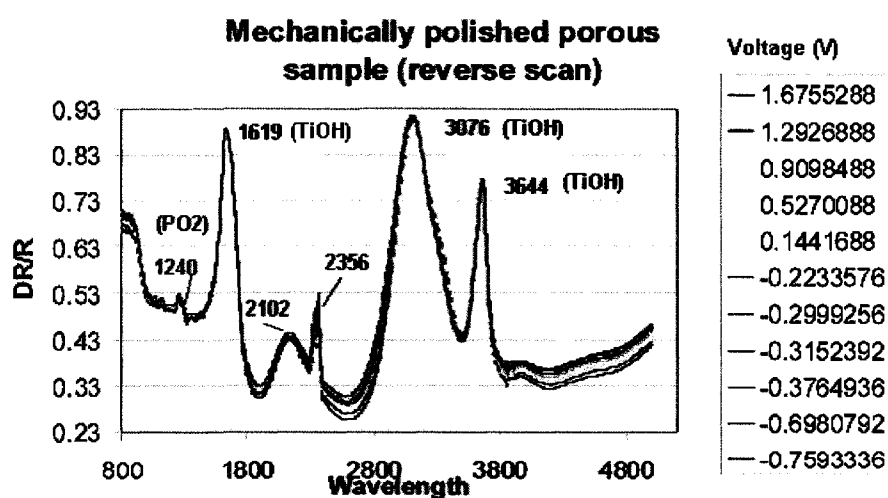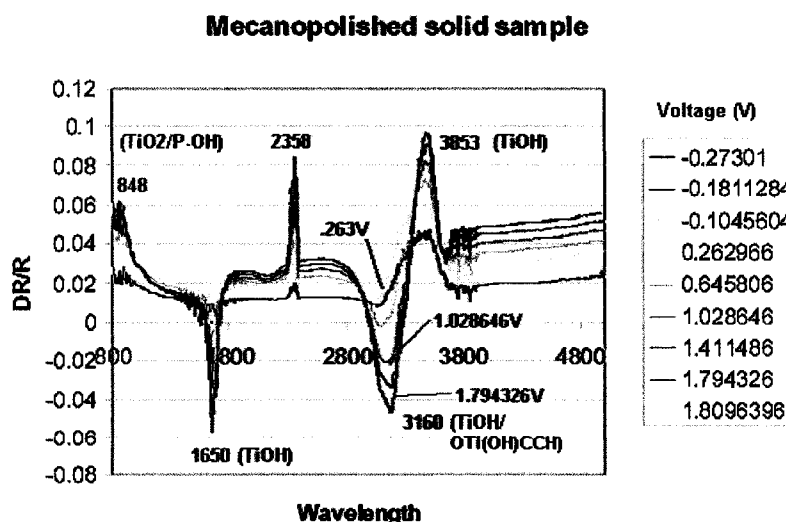Figure 7.11 FTIR spectra of the surface of the solid mechanopolished sample during the initial scan
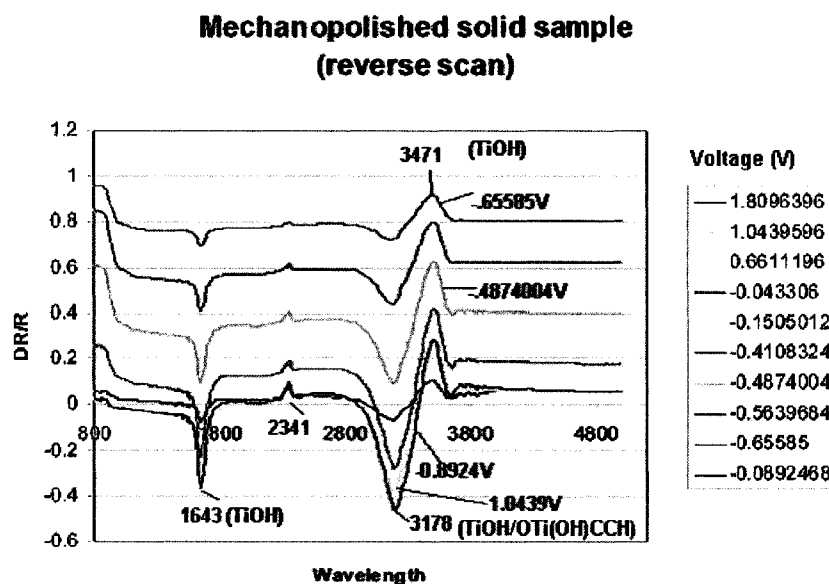
Figure 7.12 FTIR spectra of the surface of the solid mechanopolished sample during the reverse scan

The FTIR spectra for the SEP sample that correspond to the initial scan are shown in Figure 7.13. Similar spectra to that one of the SMP sample is observed. Four bands are observed at a different range, the first one 800-1000cm^{-1} on the positive direction, that can be attributed to the presence of TiO_2 and P-OH interactions [101-102]. The second band 1359-1805cm^{-1} on the negative direction, attributed to Ti-OH interactions [99]. The third band 2946-3654cm^{-1} on the positive direction, originated from the interaction OTi(OH)CCH due to the chemical composition of the Hank's solution is observed [101]. The last band on the negative direction, at 3610-3907cm^{-1}, that can be attributed to Ti-OH interactions [99-100, 104-105]. A single peak is observed at 2339 cm^{-1} that we were not able to identify. An increment on the intensity is observed for higher potentials; particularly the highest intensity corresponds to the vertex potential. Figure 7.14 shows the FTIR spectra for the reverse scan as it can be observed the four bands are present at a range 800-935cm^{-1}(TiO2/P-OH), 1336-1893cm^{-1}, 2844-3677cm^{-1} and 3608-3943cm^{-1} respectively from Ti-OH interactions [99-100, 104-105]. A single peak is found at

2335cm^{-1}. The variation of the intensity is smaller and the bands are shifted. The spectra of the reverse scan show a lower intensity of the peaks than that one of the initial scan.

Electropolished solid sample

3176 (TiOH/ OTi(OH)CCH)

(TiO2/P-OH)
848

2339

1.760V

.5975V

27822V

1695
(TiOH)

DR/R

Wavelength

800   1800   2800   3800   4800   5800

0.1
0.08
0.06
0.04
0.02
0
-0.02
-0.04
-0.06

Voltage (V)

—-0.2782208
—-0.1986013
—-0.1826774
-0.1189818
0.1994962
0.5975937
—0.9956912
—1.3937887
—1.7600384
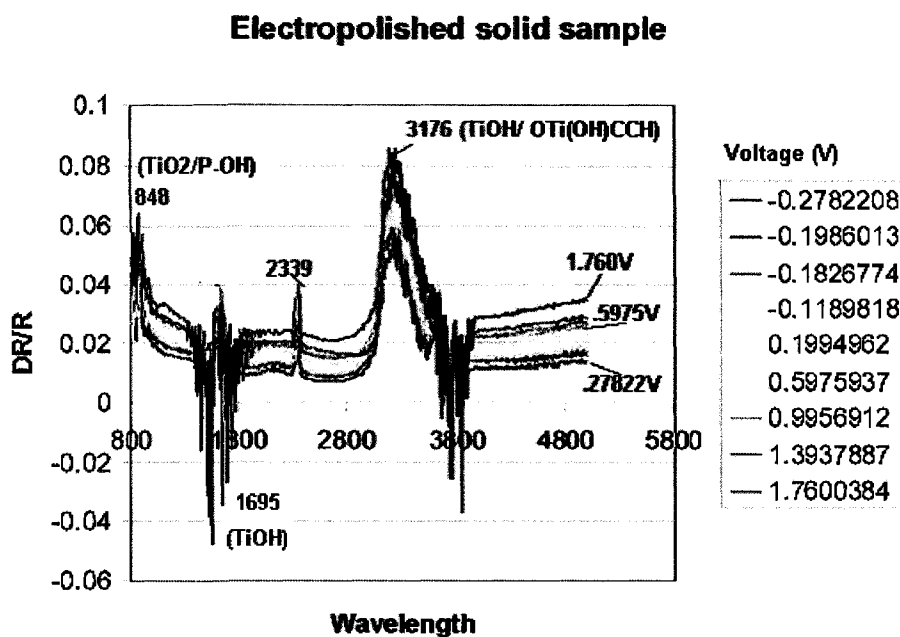
Figure 7.13 FTIR spectra of the surface of the solid electropolished sample during the initial scan

It was observed that each sample exhibited a particular behaviour. The porous sample as well as the solid samples showed Ti-OH interactions. Moreover both solid samples exhibited another peak corresponding to the OTi(OH)CCH interaction, which is explained by the chemical composition of the electrolyte, in this case the Hank's solution that has a certain amount of glucose. However an inversion of the peak is observed in both samples, this direction change can be attributed to the surface treatment. The electropolished sample showed a more stable behaviuor mean while the mechanopolished sample exhibited a change during the reverse scan. .
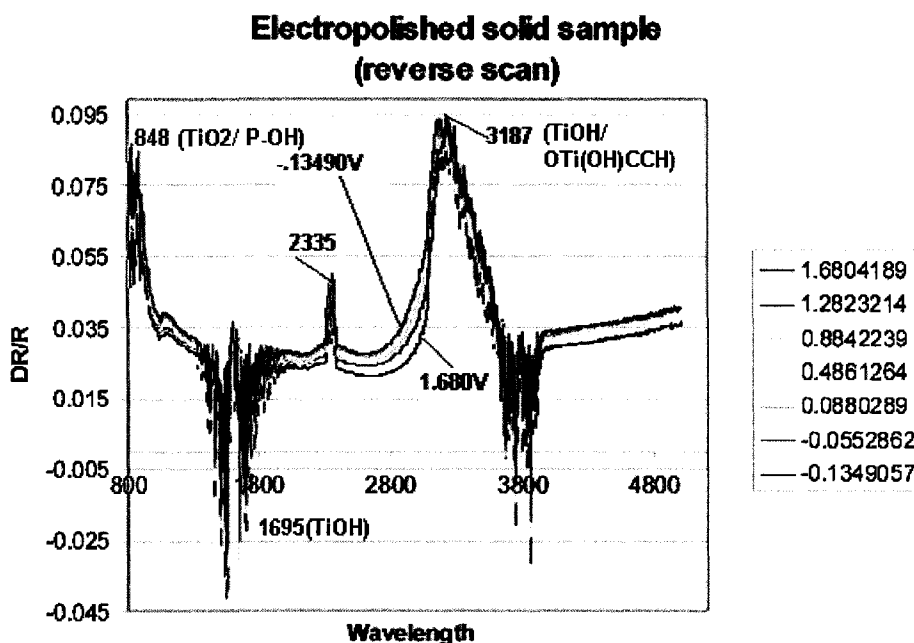
Figure 7.14 FTIR spectra of the surface of the solid electropolished sample during the reverse scan

7.5 Conclusions

The corrosion resistance of a porous NiTi was evaluated and its behaviour was compared to that one of solid samples. The results showed that the porous sample exhibits a higher susceptibility towards pitting and crevice corrosion than the solid samples. However the corrosion rate exhibited by the mechanopolished samples both porous and solid were similar and lower than one of the electropolished sample. The FTIR confirmed that the three different samples had a different behaviour and interact in different ways with the Hank's solution used in this study. There were no visible interactions observed at critical potentials except for an intensity increment exhibited by the porous sample at the corrosion potential.

7.6 Acknowledgments

7. 7 References

See Chapter XI

CHAPTER VIII. General Discussion

The aim of this study was to provide a better understanding of the electrochemical behaviour of porous NiTi alloys. At the beginning of this study four different materials were evaluated, their physico-chemical characteristics were identified. In fact all the samples exhibited an open and interconnected porosity in the range of 100-400 μm. The material D presented a lower value of the isolated pores however the interconnected pores were in the same range as the other materials. According to the literature a pore size on this range enhance bone ingrowth, therefore a better fixation [39]. This condition is required for materials that are candidates for orthopedic and dental implants in general for bone replacement.

The porosity has an effect not only on the bone ingrowth but also on the mechanical properties of the material. Therefore, these properties must match those ones of the bone. It has been reported in the literature that NiTi alloys in the martensite phase (28-41 GPa) match the elastic modulus of the bone. Moreover, if the material has an internal structure of 50% porosity, it exhibits a lower modulus (14-20 GPa), which allows the possibility of significant bone ingrowth at this matching value. The thermal analyses showed that all the samples are found on the martensite phase.

The interactions between the surface of the implant and the surrounding tissues depend on the porosity and the mechanical properties, but also on the chemical composition of the sample. These interactions have an influence on the biocompatibility and the corrosion resistance of the implant. The good biocompatibility and good corrosion resistance of solid NiTi alloys comes from a homogeneous oxide layer mainly composed of TiO_2 with a very low concentration of Ni [2]. However, there is a concern about the possibility of Ni-ion release due to the high content of Ni [14]. Therefore, it is important to avoid the presence of Ni-ions at the surface. The surface analyses on our samples showed that a surface oxidation occurs following the heat treatment. The surface is

mainly composed of titanium oxide and of nickel oxide in much less extended amount. Since the Ni was oxidized after heat treatment no trace of Ni in atomic state was found.

Despite the extensive research on the corrosion resistance of solid NiTi alloys, this property is not clearly established and is rather controversial. The results on these evaluations can varied due to numerous factors such as chemical composition and roughness of the surface. Surface treatments have been proposed to improve the corrosion resistance of solid NiTi alloys. These treatments are effective and the choice of treatment has to be done according to the desired properties. In the last few years a new emerging NiTi alloy with a porous structure has gained a particular interest. This alloys show the superelastic properties of solid alloys and their mechanical properties present values closer to those of the bones. As mentioned before its porous structure allows bone ingrowth. The biocompatibility and corrosion resistance is assumed to be as good as that one of the solid NiTi. However the porous structure could have an influence on its performance. The corrosion resistance of porous NiTi alloys has not been yet fully investigated. In particular its surface characteristics need special attention. An electrochemical evaluation was carried out on the different materials. The results show that the different materials present different behaviours. In particular, for materials A and C, that exhibited a lower corrosion resistance after the treatment. The highest breakdown potentials were obtained for the non-treated samples, but still lower to those ones of solid NiTi. These results are in agreement with those ones published by Abiko and Li [9, 11] where they showed that the corrosion resistance of porous alloys is found to be lower than that one of solid alloys. The morphology of the samples presents a visible change after the corrosion evaluation. An increment on the pore size is observed as well as a different pore size distribution. Furthermore the edges of the pores were more susceptible for corrosion. This can be confirmed by the values of the corrosion rates, where they decrease in the order: B>A>C>D. Therefore the smallest value is observed for material D. The value of the corrosion rate illustrates the quantity of material lost during corrosion. Therefore, the more corroded the sample the highest corrosion rate. The results

shown in Figures 6.6 to 6.9 confirm this behaviour. It was expected to observed higher effect due to the corrosion on samples with higher porosities as reported [11]. On the contrary the samples with higher porosities exhibited the highest breakdown potentials for the non-treated samples. Therefore the size of the pores is not the only parameter which affects the corrosion resistance of the materials. The surface analyses show the presence of a surface with no traces of Ni-ions after the treatment. Furthermore, after the corrosion evaluation only the non-treated sample C exhibits the presence of Ni at a concentration of 0.13%, but its titanium oxide concentration is higher. The chemical composition of materials A, C and D exhibited the presence of intermediate oxides and also lower corrosion rates to those shown by material B. Therefore the presence of intermediate titanium oxides on the surface chemical composition of samples results on better corrosion rates and improved corrosion resistance. Moreover, the low corrosion rates observed on treated samples are an indication of high corrosion resistance compare to those non-treated. However these values are still low in comparison to those ones obtained for solid samples.

Table 8.1 Summary Results

	Oxide layer thickness (nm)				Corrosion rate (mmpy)	
	Non treated		Treated		Non treated	Treated
Material	Before Corrosion	After Corrosion	Before Corrosion	After Corrosion		
A	12	10	40	82	0.1183	0.0359
B	3	7	29	73	0.934	0.168
C	7	12	33	58	0.076	0.0221
D	7	9	20	54	0.0505	0.0202

In the quest for a better understand of the electrochemical behaviour and the interactions of the oxide layer and the environment, an investigation using the Spectroelectrochemistry method for the first time. Our results showed that the solid

samples exhibited a higher corrosion resistance. Moreover the lowest corrosion rate was observed for the electropolished sample. As has been reported electropolished NiTi exhibits a good biocompatibility and corrosion resistance [2-3, 24, 97]. The porous sample exhibited a higher susceptibility to pitting and crevice corrosion. However its corrosion rate showed a value closer to that one of the solid mechanopolished sample. The FTIR measurements permitted to identify certain interactions (Ti-OH) that were present for all the samples. However the solid samples exhibited also other interactions not present in the porous sample. This could be explained by the different surfaces of the samples.

The corrosion resistance of solid NiTi alloys is still controversial and there are no standards to determine an acceptable value for this material. The mechanism of corrosion need to be better evaluated with techniques such as XPS, AES and SEM to identify any changes of the surface. However there are not many studies that have been published dealing with this specific surface characterization. The study of porous NiTi has only started a few decades ago and its electrochemical behaviour is still unknown due to the porous nature of the material. That on one hand is necessary to promote bone ingrowth but on the other might increase its corrosion resistance.

The use of new techniques such as FTIR *in situ* was proposed to elucidate the interactions that were taking place at the interface of the sample and the electrolyte. We need to understand that the human body is unique and there are certain conditions that we cannot simulate in the laboratory. This technique was the first step to understand the mechanisms of corrosion resistance for the NiTi alloys solid and porous, and also for the different treatments that are widely used. Electropolished samples have proved to have a better corrosion resistance than mechanical polished, however there are no studies trying to understand this behaviour.

We propose to further study the Porous NiTi alloys which remain a promising material for bone replacement due to their unique properties. Other porous materials such as Titanium and Tantalum do not offer the same advantages. Titanium alloys are biocompatible but their mechanical properties are higher than those ones of the bone, their porosity is limited to a few layers, and do not has the superelasticity or shape memory properties. Moreover the porous NiTi alloys have the damping capacity, which is suitable for different applications, for example disc replacement. On the other hand there is evidence that the porous NiTi also have capillarity properties which enhances the bone ingrowth within the implant [59]. These characteristics have been observed neither in Titanium nor in Tantalum.

CHAPTER IX. Conclusions

The morphological evaluation confirmed that no visible changes were observed on the characteristics of the samples due to the heat treatment. In fact all the samples exhibited an open and interconnected porosity in the range of 100-400 µm.

The electrochemical behaviour of porous Nickel-titanium alloys was investigated. The results showed that the corrosion resistance of these materials is related not only to their morphology but also to their surface chemical composition. Moreover, the presence of the intermediate Ti oxide results on better corrosion rates.

The corrosion resistance of a porous NiTi was investigated and compared to that one of solid samples. The results showed that the porous sample exhibits a higher susceptibility towards pitting and crevice corrosion than the solid samples. However the corrosion rate exhibited by the mechanopolished samples both porous and solid were similar and lower than one of the electropolished sample. The FTIR confirmed that the three different samples had a different behaviour and interact in different ways with the Hank's solution used in this study. There were no visible interactions observed at critical potentials except for an intensity increment exhibited by the porous sample at the corrosion potential.

CHAPTER X. Limits and Recommendations

This study did not aim to produce any statistic information; the interest was to understand the mechanism of corrosion. Therefore, the Spectroelectrochemistry method was used for the first time to elucidate these mechanisms.

There are few studies of the corrosion resistance of porous biomaterials in general, and thus it was difficult to compare our results with the literature.

We suggest performing the spectroelectrochemistry investigation using polarized light, in order to assess and differentiate the adsorbed species and also those produced in the electrolyte.

We recommend the use of different electrolytes such as Ringer solution, artificial saliva, etc, in order to identify other interactions between the surface of the electrode and the electrolyte.

It will be important to perform the spectroscopy measurements at different wavelengths for example, in the near infrared or UV-visible regions where the oxide species can be detected during the corrosion test.

We suggest applying different surface treatments to porous samples such as electropolishing, acid passivation, in order to improve its corrosion resistance.

We recommend confirming the appearance of the R-phase on sample A with Transmission Electron Microscopy observations.

We recommend using this approach to study porous Tantalum and Titanium in terms of corrosion resistance.

It will be useful to perform this study under cyclic stress to evaluate its influence on the electrochemical behaviour.

CHAPTER XI. References

1. W. J. Buehler and F. E. Wang, "A summary of recent research on the Nitinol alloys and their potential application in ocean engineering, *Ocean Eng*, vol. 1, pp. 105-120, 1967.

2. B. Thierry, M. Tabrizian, C. Trepanier, O. Savadogo and L'.H. Yahia, "Effect of the surface treatment and sterilization processed on the corrosion behavior of NiTi shape memory alloy", *Journal of Biomedical Materials Research*, vol. 51, no. 3, pp.685, 2000.

3. S. A. Shabalovskaya, "Surface, corrosion and biocompatibility aspects of NiTinol as an implant material", *Bio-Medical Materials and Engineering*, vol. 12, pp. 69, 2002.

4. G. Riepe, C. Heintz, L. Birken, E. Kaiser, N. Chakfé, M. Morlock, G. Delling and H. Imig, "Degradation of Stentor devices after implantation in human beings", in: *SMST-2000 Proceedings of the third conference on Shape Memory and Superelastic Technologies*, Edited by: A. R. Pelton and T. Duering, Menlo Park, CA: SMST Society Inc., 2000, pp. 279-283.

5. P.P.F. Kuo, P.J. Yang, Y.F. Zhang, H.B. Yang, Y.F. Yu, K.R. Dai, W.Q. Hong, M.Z. Ke, T.D. Cai, and J.C. Tao, "The Use of Nickel-Titanium Alloy in Orthopedic Surgery in China", *Orthopedics*, vol. 12, no. 1, pp.111-116, 1989.

6. V. Brailovski and F. Trochu, "Review of shape memory alloys medical applications in Russia", *Bio-Medical Materials and Engineering*, vol. 6, no. 4, pp. 291-298, 1996.

7. V.E. Gjunter, "Medical application of SMA in Russia", in: *Proceedings of the First International Symposium on Advanced Biomaterials (ISAB)*, Montreal, Canada, 1997, p.3.

8. K. Dai, "Studies and applications of NiTi shape memory alloys in the medical field in China", *Bio-Medical Materials and Engineering*, vol. 6, no. 4, pp. 233-240, 1996.

9. Y. Abiko, R. Sachdeva, K. Endo, Y. Araki, T. Kaku and H. Ohno, "Corrosion resistance and biological evaluation of Ni-Ti alloys with varied surface textures" in: *SMST-1994 Proceedings of the first conference on Shape Memory and Superelastic Technologies*, Edited by: A. R. Pelton and T. Duering, Menlo Park, CA: SMST Society Inc., 1994, pp. 203-208.

10. Y.-H. Li, G.-B. Rao, L.-J. Rong, Y. Li and W. Ke, "Effect of pores on corrosion characteristics of porous NiTi alloy in simulated body fluid", *Materials Science and Engineering,* vol. A 363, pp. 356-359, 2003.

11. Y.-H. Li, G.-B. Rao, L.-J. Rong, Y. Li, and W. Ke, "The influence of porosity on corrosion characteristics of porous NiTi alloy in simulated body fluid", *Materials Letters*, vol. 57, pp. 448-451, 2002.

12. J. Van Humbeeck, R Stalmans and P. A. Besselink, "Shape Memory Alloys" in: *Metals as biomaterials*, 1st ed., Edited by: J.A Helsen and H.J Breme, England, John Wiley and Sons, 1998, pp. 73-100.

13. K. Bhattacharya, "Theory of martensitic microstructure and the shape-memory effect", Unpublished notes, pp.70.

14. J. Ryhanen, "Biocompatibility Evaluation of Nickel-Titanium shape memory alloy", PhD, University of Oulu, Oulu, Finland, 1999.

15. D. Scharnweber, "Degradation (*in vitro- in vivo* corrosion)" in: *Metals as biomaterials*, 1st ed., Edited by: J.A Helsen and H.J Breme, England, John Wiley and Sons, 1998, pp. 108-112.

16. N.D. Spencer and M. Textor, "Surface modification, Surface analysis and Biomaterials", in: *Materials in Medicine*, Edited. M.O. Speidel, P.J. Uggowitzer, vdf Hochschulverlag AG, ETH Zürich, Zurich, 1998, pp. 165-189.

17. G. Rondelli, B. Vicentini, "Evaluation by electrochemical tests of the passive film stability of equiatomic Ni-Ti alloy also in presence of stress-induced martensite", *Journal of Biomedical Materials Research,* vol. 51, pp. 47-54, 2000.

18. G. Rondelli, B. Vicentini, and A. Cigada, "The corrosion behavior of nickel titanium shape memory alloys", *Corrosion Science*, vol. 30, pp. 805-812, 1990.

19. G. Rondelli, "Corrosion resistance tests of NiTi shape memory alloys", *Biomaterials*, vol. 17, pp. 2003-2007, 1996.

20. F. Villermaux, M. Tabrizian, L'H Yahia, G. Czeremuszkin, and D. Piron, "Corrosion resistance improvement of NiTi osteosynthesis staples by plasma polymerized tetrafluoroethylene coating", *Bio-Medical Materials and Engineering,* vol. 6, pp. 241-254, 1996.

21. F. Villermaux, M. Tabrizian, L'H.Yahia, M. Meunier, and D. Piron, "Excimer laser treatment of NiTi shape memory alloy biomaterials", *Applied Surface Science*, vol. 109/110, pp. 62-66, 1997.

22. D. Wever, A. Velderhuizen, J de Vries, H. Buscscher, D. Uges, and J.R. van Horn, "Electrochemical and surface characterization of a nickel-titanium alloy", *Biomaterials*, vol. 19, pp. 761-769, 1998.

23. S. Shabalovskaya, G. Rondelli, V. Itin, and J. Anderegg, "Surface and Corrosion Aspects of NiTi Alloys", in: *SMST-2000 Proceedings of the third conference on Shape Memory and Superelastic Technologies*, Edited by: A. R. Pelton and T. Duering, Menlo Park, CA: SMST Society Inc., 2000, pp. 299-308.

24. C. Trepanier, M.Tabrizian, L'H. Yahia, L. Bilodeau, and D. Piron, "Effect of modification of oxide layer on NiTi stent corrosion resistance", *Journal of Biomedical Materials Research,* vol. 43, pp. 433-440, 1998.

25. Y.Y. Su and V. Raman, "The Quest for Nitinol wire surface quality for medical applications", in: *SMST-1997 Proceedings of the Second conference on Shape Memory and Superelastic Technologies*, Edited by: A. R. Pelton and T. Duering, Menlo Park, CA: SMST Society Inc., 1997, pp. 389-394.

26. S. Trigwell and G. Selvaduray, "Effects of the surface finish on the corrosion of NiTi alloy for biomedical applications", in: *SMST-1997 Proceedings of the Second conference on Shape Memory and Superelastic Technologies*, Edited by: A. R. Pelton and T. Duering, Menlo Park, CA: SMST Society Inc., 1997, pp. 383-388.

27. A. Michiardi, C. Aparicio, J.A. Planell and F.J. Gil, "New oxidation treatment of NiTi shape memory alloys to obtain Ni-free surfaces and to improve biocompatibility", *Journal of Biomedical Materials Research part B: Applied biomaterials*, vol. 77, no. 2, pp. 249-256, 2006.

28. M. Berger-Gobet, B. Broxup, C. Rivard and L'H. Yahia, "Biocompatibility testing of NiTi screws using immunohistochemistry on sections containing metallic implants", *Journal of Biomedical Materials Research*, vol. 32, pp. 243-248, 1996.

29. D. J. Wever, A.G. Veldhuizen, M.M. Sanders, J.M. Schakenraad and J. R. van Horn, "Citotoxic, allergic and genotoxic activity of a nickel-titanium alloy", *Biomaterials*, vol. 18, no. 16 pp. 1115-1120, 1997.

30. C. Trepanier, T.K. Leung, M. Tabrizian, L.'H. Yahia, J.-G. Bienvenu, J.-F. Tanguay, D.L. Piron and L. Bilodeau, "Preliminary investigation of the effects of surface treatments on biological response to shape memory NiTi stents", *Journal of Biomedical Materials Research part B: Applied biomaterials*, vol. 48, pp. 165-171, 1999.

31. D.A. Armitage, D.M. Grant, T.L. Parker and K.G. Parker, "Haemocompatibility of surface modified NiTi", in: *SMST-1997 Proceedings of the Second conference on Shape Memory and Superelastic Technologies*, Edited by: A. R. Pelton and T. Duering, Menlo Park, CA: SMST Society Inc., 1997, pp. 411-416.

32. B. Thierry, Y. Merhi, L. Bilodeau, C. Trepanier and M. Tabrizian, "Nitinol versus stainless steel stents: acute thrombogenenicity study in an ex vivo porcine model", *Biomaterials*, vol. 23, no. 14, pp. 2997-3005, 2002.

33. V.E. Gjunter, *Superelastic Shape Memory Implants in Maxillofacial Surgery, Traumatology, Orthopaedics and Neurosurgery*, Tomsk, Russia: Tomsk University Publishing House (TUP), 1995.

34. B.M. Silberstein, "Porous nickel-titanium implants for spinal anterior fusion", in: *Proceedings of the First International Symposium on Advanced Biomaterials (ISAB)*, Montreal, Canada, 1997, pp. 164.

35. J.O. Sanders, A.E. Sanders, R. More, and R.B. Ashman, "A Preliminary Investigation of Shape Memory Alloys in the Surgical Correction of Scoliosis", *Spine*, vol. 18, no. 12, pp. 1640-1646, 1993.

36. P.A. Savchenko, V.A. Lazarev, I.V. Sokulov, V.E. Gjunter, and A.V. Proskurin, "Correction of scoliotic deformities of the vertebral column with superelastic designs", in: *Proceedings of the First International Symposium on Advanced Biomaterials (ISAB)*, Montreal, Canada, 1997, pp. 163.

37. V. K. Sheleg and V. V. Sabich, "Effect of the method of production of porous metallurgy materials on their capillary properties (Review)", *Powder Metallurgy and Metal Ceramics*, vol. 35, no. 5-6, pp. 244-252, 1996.

38. A. G. Kostornov, N. E. Skrynskaya and M. Kh. Akhmedov, "Laws of capillary transport in porous materials prepared from titanium alloy VT6 fibers", *Powder Metallurgy and Metal Ceramics*, vol. 36, no. 1-2, pp. 60-66, 1996.

39. R. A. Ayers, T. A. Bateman and S. J. Simske, "Porous NiTi and a Material for Bone Engineering, Basic Properties", in: *Shape Memory Implants*, 1st ed., Edited by: L'Hocine Yahia, New York: Springer-Verlag, 2000, pp. 73-86.

40. V. I. Itin, V. E. Gjunter, S. A. Shabalovskaya and R. L. C. Sachdeva, "Mechanical Properties and Shape memory of Porous Nitinol", *Materials Characterization*, vol. 32, pp. 179-187, 1994.

41. H. C. Yi and J. J. Moore, "The combustion synthesis of NiTi shape memory alloys", *Journal of Minerals, Metals and Materials Society*, vol. 42, pp. 31-35, 1990.

42. S. M. Green, D. M. Grant and N. R. Kelly, "Powder metallurgical processing of Ni-Ti shape memory alloy", *Powder Metallurgy*, vol. 40, no. 1, pp. 43-47, 1997.

43. C. Chenglin, L. Bo, Q. Shan, W. Shidong, Z. Shuge and Y. Xiaoxi, "TiNi shape memory alloy porosint", in: *SMST-1997 Proceedings of the Second conference on Shape Memory and Superelastic Technologies*, Edited by: A. R. Pelton and T. Duering, Menlo Park, CA: SMST Society Inc., 1997, pp.71-76.

44. S.A. Shabalovskaya, V.I. Itin and V.E. Gyunter, "Porous Ni-Ti –A new material for implants and prostheses", in: *SMST-1994 Proceedings of the first conference on Shape Memory and Superelastic Technologies*, Edited by: A. R. Pelton and T. Duering, Menlo Park, CA: SMST Society Inc., 1994, pp. 7-12.

45. I. Martynova, V. Skorohod, S. Solonin and S. Goncharuk, "Shape memory and superelasticity behaviour of porous NiTi material", *Journal de physique IV, colloque C4, supplément au Journal de physique III*, vol. 1, no. C4, pp. C4-421-C4-426, 1991.

46. Y.-H. Li, G.-B. Rao, L.-J. Rong and Y-Y Li, "Compressive property of porous NiTi alloy synthesized by combustion synthesis", *Journal of Alloys and Compounds*, vol. 345, pp. 271-274, 2002.

47. B.S. Becker and J.D. Bolton, "Potentiodynamic anodic polarization behavior of three porous sintered surgical alloys" in: Proceedings of the Fifth World Biomaterials Congress, May 29- June 2, Toronto, Canada, 1996, pp. 475.

48. S.L. Wu, P.K. Chu, X.M. Liu, C.Y. Chung, J.P.Y. Ho, C.L. Chu, et al., "Surface characteristics, mechanical properties and cytocompatibility of oxygen plasma-implanted porous nickel titanium shape memory alloy", *Journal of Biomedical Materials Research*, vol. 79, no.1, pp. 139-146, 2006.

49. S. Shabalovskaya, J. Anderegg, and J. Cunnick, "X-ray spectroscopic and in vitro study of porous TiNi, Biological Responses of NiTi Alloys", in: *SMST-1997 Proceedings of the Second conference on Shape Memory and Superelastic Technologies*, Edited by: A. R. Pelton and T. Duering, Menlo Park, CA: SMST Society Inc., 1997, pp. 401-406.

50. S. Rhalmi, M. Odin, M. Assad, M. Tabrizian, C.H. Rivard, L'H. Yahia, "Hard, soft tissue and in vitro cell response to porous nickel-titanium: a biocompatibility evaluation", *Bio-Medical Materials and Engineering*, vol. 9, pp. 151-162, 1999.

51. S-B. Kang, K-S. Yoon, J-S. Kim, T-H. Nam and V.E. Gjunter, "In vivo result of porous TiNi Shape Memory Alloy: Bone response and growth", *Materials Transactions*, vol. 43, no. 5, pp. 1045-1048, 2002.

52. S.J. Simske and R. Sachdeva, "Cranial bone apposition and ingrowth in a porous nickel-titanium implant", *Journal of Biomedical Materials Research*, vol. 29, pp.527-533, 1995.

53. R. A. Ayers, S. J. Simske, T. A. Bateman, A. Petkus, R. Sachdeva, V.E. Gyunter, "Effect of nitinol implant porosity on cranial bone ingrowth and apposition after 6 weeks", *Journal of Biomedical Materials Research*, vol. 45, pp. 42-47, 1999.

54. B. Berthierville, "Porous single-phase NiTi processed under Ca reducing vapor for use as a bone graft substitute". *Biomaterials*, vol. 27, pp. 1246-1250, 2006.

55. R. Venugolapan, and C. Trepanier, "Assessing the corrosion behavior of Nitinol for minimally - invasive device design", *Minimally Invasive Therapy & Allied Technologies,* vol. 9, pp. 67-75, 2000.

56. G. Airoldi and G Riva, "Innovative materials: the NiTi alloys in orthodontics", *Bio-Medical Materials and Engineering,* vol. 6, pp. 299-305, 1996.

57. L. Jordan, K. Goubaa, M. Masse and G. Bouquet, "Comparative study of mechanical properties of various Ni-Ti based shape memory alloys in view of dental and medical applications", *Journal de physique IV, colloque C4, supplément au Journal de physique III,* vol. 1, no. C4, pp. C4-139- C4-144, 1991.

58. F. Libiki, M. Assad, C. Coillard, and C.H. Rivard, "Bone integration and apposition of porous and non porous metallic orthopaedic biomaterials", Annales de chirurgie, vol. 130, no. 4, pp. 235-241, 2005.

59. M. Assad, P. Jarzem, M.A. Leroux, C. Coillard, A.V. Chernyshov, S. Charette *et al.,* "Porous titanium-nickel for intervertebral fusion in a sheep model: Part 1. Histomorphometric and radiological analysis", *Journal of Biomedical Materials Research (Applied Biomaterials),* vol. 64B, pp. 107-120, 2003.

60. M. Assad, A.V. Chernyshov, P. Jarzem, M.A. Leroux, C. Coillard, S. Charette *et al.,* "Porous titanium-nickel for intervertebral fusion in a sheep model: Part 2. Surface analysis and nickel release assessment", *Journal of Biomedical Materials Research (Applied Biomaterials),* vol. 64B, pp. 121-129, 2003.

61. S. Ulrich, *Endoluminal Stenting,* London, Saunders 1996, pp. 249-250.

62. D. Krupa, J. Baszekiewicz, J.A. Kozubowski, A. Barcz, J.W. Sobezak, A. Bilinski, M. Lewandowska-Szumiel and B. Rajchel, "Effect of phosphorous-ion implantation on the corrosion resistance and biocompatibility of titanium", *Biomaterials,* vol. 23, pp. 3329-3340, 2002.

63. A. Arys, C. Philippart, N. Dourov, Y. He, Q.T. Le, and J.J. Pireaux, "Analysis of Titanium Dental Implants after Failure of Osseointegration : Combined Histological, Electron Microscopy and X-Ray Photoelectron Spectroscopy Approach", *Journal of Biomedical Materials Research part B: Applied biomaterials,* vol. 43, no. 3, pp.300-312, 1998.

64. M. Takemoto, S. Fujibayashi, M. Neo, J. Suzuki, T. Kokubo and T. Nakamura, "Mechanical properties and osteoconductivity of porous bioactive titanium", *Biomaterials,* vol. 26, no. 30, pp. 6014-6023, 2005.

65. M. Kotate, N. Wakabayasi, M. Ai *et al.,* "Fatigue resistance of Titanium-Nickel cast clasps", *International Journal of Prosthodontics,* vol. 10, pp. 547-552, 1997.

66. M. Wong, J. Eulengerger, R. Schenk and E. Hunziker, "Effect of surface topology on the osseointegration of implant materials in trabecular bone", *Journal of Biomedical Materials Research,* vol. 29, pp. 1567-1575, 1995.

67. M. Takemoto, S. Fujibayashi, M. Neo, K. So, N. Akiyama, T. Matsushita, T. Kokubo and T. Nakamura, "A porous bioactive titanium implant for spinal interbody fusion: an experimental study using a canine model", *Journal of Neurosurgical Spine,* vol. 7, no. 4, pp. 435-443, 2007.

68. J.L. Ong and L.C. Lucas, "Auger electron spectroscopy and its use for the characterization of titanium and hydroxyapatite surfaces", *Biomaterials,* vol. 19, pp. 455-464, 1998.

69. J.B. Brunski, D.A. Puleo and A. Nanci, "Biomaterials and Biomechanics of Oral and Maxillofacial Implants: Current Status and Future Developments", *The International Journal of Oral and Maxillofacial Implants,* vol. 15, no. 1, pp. 15-46, 2000.

70. M. Simon, C. Lagneau, J. Moreno, M. Lissac, F. Dalard and B. Grosgogeat, "Corrosion reistance and biocompatibility of a new porous surface for titanium implants", *European Journal Oral Science,* vol. 113, no. 6, pp.537-545, 2005.

71. B. R. Levine, S. Sporer, R.A. Poggie, C.J. Della Valle and J.J. Jacobs, "Experimental and clinical performance of porous tantalum in orthopedic surgery", *Biomaterials,* vol. 27, pp. 4671-4681, 2006.

72. R. Cohen, "A porous tantalum trabecular metal: basic science", *American Journal of Orthopedics,* vol. 31, no. 4, pp. 216-217, 2002.

73. J.D. Bobyn, G.J. Stackpool, S.A. Hacking, M. Tanzer and J.J. Krygier, "Characteristics of bone ingrowth and interface mechanics of a new porous tantalum biomaterial", *The Journal of Bone and Joint Surgery (Br),* vol. 81-B, no. 5, pp. 907-914.

74. M.J. Christie, "Clinical applications of trabecular metal", *American Journal of Orthopedics,* vol. 31, no. 4, pp. 219-220, 2002.

75. B. Levine, S. Sporer, C.J. Della Valle, J.J. Jacobs and W. Paprosky, "Porous tantalum in reconstructive surgery of the knee: a review", *Journal of Knee Surgery,* vol. 20, no. 3, pp. 185-194, 2007.

76. S.A. Hacking, J.D. Bobyn, K. Toh, M. Tanzer and J.J. Krygier, "Fibrous tissue ingrowth and attachment to porous tantalum", *Journal of Biomedical Materials Research,* vol. 52, no. 4, pp. 631-638, 2000.

77. J. Van Humbeeck and Y. Liu, "The high damping capacity of shape memory alloys, Basic Properties" in: *Shape Memory Implants,* 1st ed., Edited by: L'Hocine Yahia, New York: Springer-Verlag, 2000, pp. 46-60.

78. Y.P. Khanna, "Thermal Characterization of Materials", in *A guide to materials characterization and chemical analysis,* Second edition, Edited by: J. P. Sibilia, England, John Wiley and Sons, Inc., 1996, pp. 267-271.

79. A.S. Frumento, *Biofísica,* Third edition, Spain, Mosby/Doyma libros, 1995.

80. B. Ratner and D. Castner, "Electron Spectroscopy for Chemical Analysis", in: *Surface Analysis*, Third edition, Edited by: J. C. Vickerman, England, John Wiley and Sons, Inc., 1999, pp. 43-98.

81. H.J. Mathieu, "Auger Electron Spectroscopy", in: *Surface Analysis*, Third edition, Edited by: J. C. Vickerman, England, John Wiley and Sons, Inc., 1999, pp. 99-133.

82. Annual Book of American Society for Testing Materials, "Standard Reference test method for making potentiostatic and potentiodynamic anodic polarization measurements", ASTM G15-99b, vol. 03.02, Philadelphia, Pennsylvania: American Society for Testing and Materials, 1999.

83. Annual Book of American Society for Testing Materials, "Standard Reference test method for making potentiostatic and potentiodynamic anodic polarization measurements", ASTM G5-94, vol. 03.02, Philadelphia, Pennsylvania: American Society for Testing and Materials, (1999).

84. INEX: Nanotechnology Exploitation website, "Fourier transformed infrared spectrometer", *INEX: Nanotechnology Exploitation website*, [on line] available at: http://www.inex.org.uk/page.asp?pageid=99 [December, 2005]

85. K. Goubaa, M. Masse and G. Bouquet, "Detection of the R-phase in Ni-Ti shape memory alloys", *Journal de physique IV, colloque C4, supplément au Journal de physique III*, vol. 1, no. C4, pp. C4-361- C4-366, 1991.

86. D.E. Hodgson and J.W. Brown, "Using Nitinol Alloys", Tech. Rep., Shape Memory Applications, Inc., Pacific Groove, California, 2000.

87. L'H. Yahia and J. Ryhanen, "Bioperformance of shape memory alloys", in: *Shape Memory Implants*, 1st ed., Edited by: L'H. Yahia, New York: Springer-Verlag, 2000, pp.3-23.

88. K. J. Bundy, "Corrosion and Other electrochemical aspects of Biomaterials", *Critical Reviews in Biomedical Engineering*, vol. 22, no. 3-4, pp. 139-251, 1994.

89. J. Ryhänen, M. Kallioinen, J. Tuukkanen, J. Junila, E. Niamelä, P. Sandvik, and W. Serlo, "*In vivo* biocompatibility evaluation of Nickel-titanium shape memory

metal alloy: Muscle and perineural tissue responses and encapsule membrane thickness", *Journal of Biomedical Materials Research*, vol. 41, no. 3, pp. 481, 1998.

90. S.A. Brown, "On the methods used for corrosion testing of NiTi", in: *SMST-2000 Proceedings of the third conference on Shape Memory and Superelastic Technologies*, Edited by: A. R. Pelton and T. Duering, Menlo Park, CA: SMST Society Inc., 2000, p 271.

91. J. Ryhänen, J. Tuukkanen, P. Sandvik, E. Niamelä, T. Jämsä, A. Pramila and P. Perämäki, "Surface corrosion and trace-metal determination of NiTi in biological environment alter long-term implantation", in: *SMST-2000 Proceedings of the third conference on Shape Memory and Superelastic Technologies*, Edited by: A. R. Pelton and T. Duering, Menlo Park, CA: SMST Society Inc., 2000, pp. 333-346.

92. J.L Ma and K. Wu, "The corrosion behavior of NiTi-Ta shape memory alloy", in: *SMST-2000 Proceedings of the third conference on Shape Memory and Superelastic Technologies*, Edited by: A. R. Pelton and T. Duering, Menlo Park, CA: SMST Society Inc., (2000) pp. 291-298.

93. G.S. Firstov, R.G. Vitchev, H. Kumar, B. Blanpain and J. Van Humbeeck, "Surface oxidation of NiTi shape memory alloy", *Biomaterials*, vol. 23, pp. 4863, 2002.

94. Chan C-M, Trigwell S, Duerig T. Oxidation of a NiTi alloy. Surface Interface Anal. 1990; 15:439-354.

95. Shabalovskaya SA. On the nature of the biocompatibility and on medical applications of NiTi shape memory and superelastic alloys. Biomed Mater Eng. 1996; 6:267-289.

96. T. Iwasita and F.C. Nart, "In situ infrared spectroscopy at electrochemical interfaces" *Progress in Surface Science*, vol. 55, no.4, pp. 271-340, 1997

97. O. Cisse, O. Savadogo, M. Wu and L'H. Yahia, "Effect of surface treatment of NiTi alloy on its corrosion behavior in Hanks' solution", *Journal of Biomedical Materials Research,* vol. 61, no. 3 , pp. 339 – 345, 2002.

98. R. Hernandez, O. Cisse, S. Polizu, T. Napporn, O. Savadogo and L'H. Yahia, "Corrosion resistance of porous Nickel-Titanium alloys for medical applications: Preliminary study", submitted.

99. T. Eliades, G. Eliades, A.E. Athanasiou and T.G. Bradley, "Surface characterization of retrieved NiTi orthodontic archwires", *Eur J of Orthodontics,* vol. 22, pp. 317-326, 2000.

100. C.-L. Chu, T. Hu, J. Zhou, Y.-P. Pu, L.-H. Yin, Y.-S. Dong, P.-H. Lin, JC.-Y. Chung and P.-K. Chu, "Effects of H2O2 pretreatment on surface characteristics and bioactivity of NaOH-treated NiTi shape memory alloy" *Trans Nonferrous Met Soc China,* vol. 16, pp.1295-1300, 2006.

101. L. Miao, J. Dong, L. Yu and M. Zhou, "Reactions of Titanium Dioxides with Acetylene Molecules. A Matrix Isolation FTIR and Density Functional Study", *J Phys Chem A,* vol. 107, pp. 1935-1940, 2003.

102. A. Michelmore, W. Gong, P. Jenkins and J. Ralston, "The interaction of linear polyphosphates with titanium dioxide surfaces" *Phys Chem Chem Phys,* vol. 2, pp. 2985-2992, 2000.

103. D.V. Kozlov, E.A. Paukshtis, E.N. Savinov, "The comparative studies of titanium dioxide in gas-phase ethanol photocatalytic oxidation by FTIR in situ method", *Appl Catalysis B: Environmental,* vol. 24, pp. L7-L12, 2000.

104. Bukovec P, Bukovec N, Orel B, Wissiak KS. Thermal analysis of Nickel oxide films. J of Thermal Analysis, 1993; 40:1193-1196.

105. Nakamura R, Nakato Y. Primary Intermediates of Oxygen Photoevolution Reaction on TiO2 (Rutile) Particles, Revealed by in Situ FTIR Absorption and Photoluminenscence Measurements. J Am Chem Soc. 2004; 126:1290-1298.

ANNEXE A. Characterization of Porous Nickel-Titanium Alloys for Medical Applications

Hernández R.[1], Polizu S.[1], Turenne S.[2], Yahia L'H.[1]

[1]Groupe de Recherche en Biomécanique/Biomatériaux (GRBB)

[2] Département de génie physique et de génie des matériaux

École Polytechnique de Montréal, C.P. 6079, Succ. "Centre-Ville",

Montréal (QC) H3C 3A7, Canada

Status

A. 1 Abstract

The importance of the porous NiTi alloys proposed as materials for implants lies in their two useful features: bio compatibility and bio functionality, that are necessary for bio implantable materials. Their super-elastic permeable structure makes them useful for many biomedical applications, such as substitutes for thin bones.

Combined chemical and physical analyses with two different samples of NiTi shape memory alloys were performed. The martensitic and the austenitic transformations induced by heat treatment (550°C) [77].were quantified by thermal analysis for one of the samples. The second one, treated for a longer time, did not display this behaviour.

The studied materials show an interconnected and opened structure with different pore size as revealed by SEM observations. The DSC measurements show an increment in the ΔH after heat treatment in the case of C sample. As the curve profile does not change between 0 and 50 °C, we conclude that the C sample is in the martensite phase. The XPS study indicates that the surface oxidation occurs after the heat treatment. This oxidized layer has a different thickness for the materials in the range of 2000 - 3280 Å.

Keywords: NiTinol, porous NiTi, Medical applications, damping capacity, capillarity.

A. 2 Introduction

The applications of NiTi in biomedical field are very wide. Several equiatomic and near equiatomic NiTi alloys with a porous internal structure have already been used for approximately a decade, in maxillofacial surgeries [33] and other orthopedic procedures [5-6] involving thousands of patients [6, 8]. However, the interest for these materials is still increasing in many areas of the biomedical field, such as the development of shape memory implants of special design. Therefore, further knowledge is needed concerning the relationship between, on one hand, the phase constituents and the factors determining the internal structure of the material, and on the other, the fundamental material properties and the response of the biomedical device used.

Numerous considerations need to be made in order to realize a full characterization of NiTi alloys. The influence of various parameters should be analyzed in view to explain the shape memory effect and the state of the structure. Quantitative and qualitative techniques are useful for this study.

A.3 Materials and Methods

A. 3. 1 Materials

The selected samples consist of two types of NiTi alloys, to be denoted in the following by C and D, supplied by different sources. The sample C was provided by Professor Victor E. Gjunter from the Institute of Medical Materials and Shape Memory Implants, but made in a laboratory in Israel (Equiatomic alloy 50-50), and the sample D was provided by Colorado School of Mines (Non equiatomic alloy 48Ti-51Ni). Both specimens were obtained by the Self-propagating High-temperature Synthesis (SHS) procedure.

Cylindrical specimens were cut from porous rods with a diamond saw in order to maintain their internal structure, with a thickness of 5 mm and diameter of 10 mm. They were cleaned for 10 min by immersion in a bath with acetone and methanol using an Ultrasonic cleaner (Branson, Model 2510) apparatus.

A. 3. 2 Methods

One series of specimen from each sample was submitted to an annealing process for 30 min at 550°C for C and D. The cleaning operation was carried out aging after the process. Moreover, a second heat treatment was carried out at the same temperature but for different periods of time, respectively 60 min and 90 min, for the material D.

Morphological Analysis: The morphological evaluation of materials provides a structural profile of material and its surface relief. Information concerning the surface texture and the porosity of the samples were obtained by scanning electron microscope (SEM) analyses. The micrographs were taken using a JEOL model JSM-840 Scanning Electron Microscope at 15.0 kV on the treated and non-treated specimens.

Thermal Analysis: Shape memory effect is usually attributed to the contribution of temperature effect. We used the Differential Scanning Calorimetry (DSC) technique, to identify the phase transformation behavior. The analyses were carried out in a Perkin Elmer Pyris1 Calorimeter equipped with a CryoFill Liquid Nitrogen Cooling system. The apparatus has been calibrated into temperature interval $0°C - 200°C$ at a rate of $10°C$, using Indium as reference materials. Each specimen with a mass of 20 mg approximately have been cycled once within the range of $0°C$ to $190°C$ at a heating/cooling rate of $10°C$, using He as purge gas. Two thermogrames were recorded for each sample, non-treated and treated.

Surface Analysis: Since the chemical composition control various properties, the concentration of particular species of atom need to be quantified on the surface of material. The X-ray Photoelectron Spectroscopy (XPS) technique permitted us to identify the surface chemical composition. By using ESCALAB-3 MKII system equipped with a non-chromatic twin-anode X-ray source the measurements were made. The Al $K\alpha_{1-2}$ x-ray radiation with quantum energy of 1486.6 eV was used. The anode was operated at 14.7 kV and 20 mA, and the analyzer was operated at a constant pass energy of 20 eV. The spectrometer was calibrated at the binding energy of Au $(4f_{7/2})(84 \text{ eV})$ and Cu $(2p_{3/2})(932.4 \text{ eV})$ levels using pure metals. The resolution of the instrument is 0.8 eV. The advantageous C1s peak at 285.0 eV was taken as energy reference. The data shown were recorded at a take off angle of $0°$ with respect to the surface plane.

Auger analysis (AES) has been used to determine the thickness of the oxide layer created on the surface of the two types of samples after heat treatment. They were performed in a JEOL JAMP-30 system equipped with a field emission source under a pressure of 10^{-7} Pa. The depth profile of chemical elements: Ni, Ti, Cr and O, were acquired at an energy resolution of 0.1% using 3 kV, 0.5 μA argon ions. The argon etch rate was calibrated by using a standard of thermally grown SiO_2 of 1000 Å of Si. These analyses were carried

out before and after the heat treatment in order to emphasis the effect of heat treatment on the samples.

A. 4 Results

Two different sources of materials and the effect of heat treatment were taken into account in order to describe the shape memory performance and other properties of NiTi shape memory alloys during our analysis. The main purpose for carrying out a heat treatment in the samples is to release internal stress created during forming processes. The temperature of 550°C was chosen because at that temperature the damping reaches its maximum value in the martensite phase [77].

The material C exhibited an interconnected and opened porosity with a pore size of 100 μm as revealed by SEM observation (Figure A.1a). This sample is characterized by a textured surface (Figure A.1b). The porosity aspect of material D is different. The pores with 35-50μm diameter are interconnected to form an opened structure (Figure A.2a). More details about this aspect could be observed in figure A.2b.
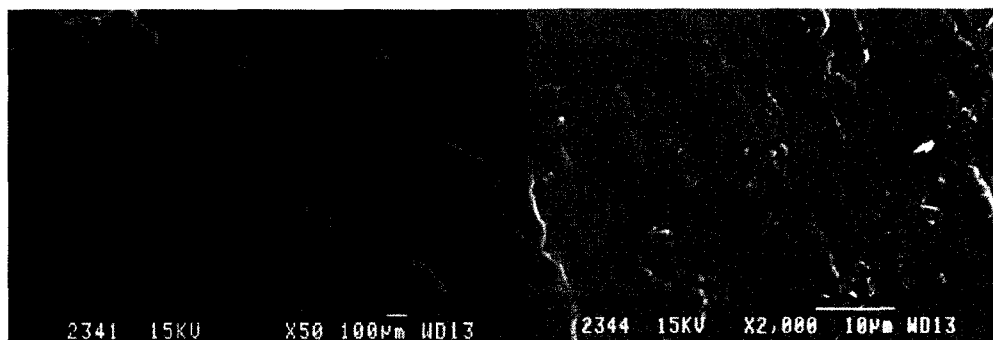

Figure A.1 Scanning electron microscopy of porous NiTi material C (Original magnification: a) x50 and b) x2000).
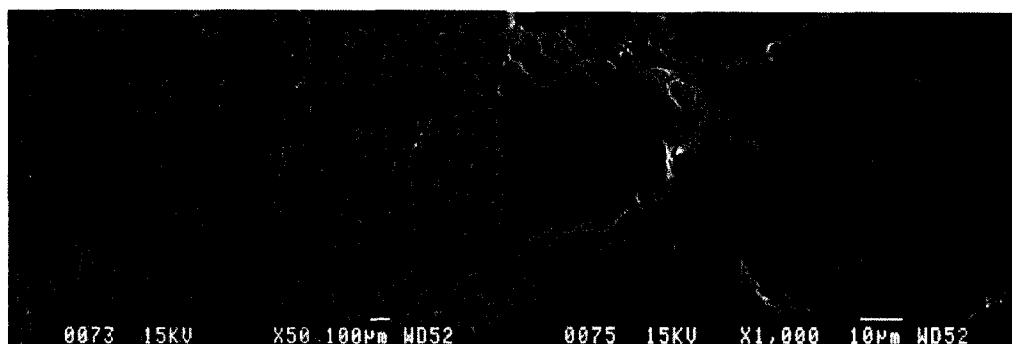
Figure A.2 Scanning electron microscopy of porous NiTi material D (Original magnification: a) x200 and b) x2000).

The changes in thermal behavior, occurred by heat treatment, have been estimated by DSC measurements. As can be seen in Figure A.3, the thermogram profile of C sample shows an austenite transformation with a broad peak of with $16.1^{\circ}C$ (As = $91.5^{\circ}C$) and a $\Delta H=5.373$ J/g. The martensite phase peak limits are found, respectively, at the temperatures of $70.2^{\circ}C$ (Ms) and at $64.5^{\circ}C$ (Mf) with a $\Delta H=5.622$ J/g. Any changes are displayed between $0\text{-}50^{\circ}C$, indicating that the material is in the martensite phase at the body temperature. The measurements carried out for original sample did not reveal any phase transformation between $0\text{-}190^{\circ}C$. Heat treatment seems to modify the molecular structure, resulting in phase transformation appearance.

No significant difference in thermal behavior could be observed before and after heat treatment for the material D. Both treated and no-treated samples did not exhibit the phase transformation temperatures. The material keeps this behavior even after performing the heat treatments for longer time. The DSC thermogrames are not representative for this case.
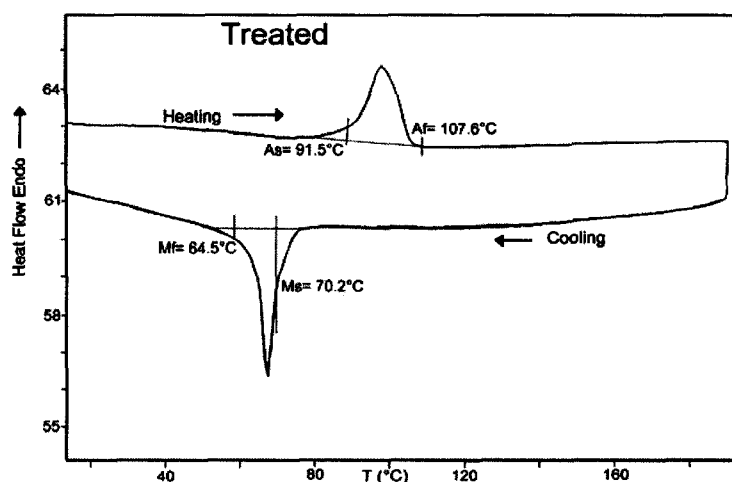
Figure A.3 DCS-Thermal analysis curve of porous NiTi alloy C after treatment.

The XPS study indicates that the surface undergoes oxidation after heat treatment for both materials (Table A.1, A.2). The surface is mainly composed of titanium oxide and of nickel oxide in much less extended amount. The high-resolution XPS spectra show the Ni peak at 852.22 eV for material C and at 851.75 eV for the material D for the non-treated series. Since the Ni was oxidized after heat treatment no trace of Ni in atomic state was found for these series as revealed by the presence of peaks at 855.82eV corresponding to material C and 855.56eV for material D. The presence of chromium is specific for the material D after heat treatment - at 577 eV.

Table A.1 Surface chemical composition obtained by XPS high-resolution analysis for material C

Non Treated		Treated	
Element	BE(eV)	Element	BE(eV)
Ni	852.22		
Ni-O	852.95		
Ni_2O_3	855.45	Ni_2O_3	855.82
Ti^{2+}	454.55		
p1/2 Ti^{2+}	*460.63*		
Ti^{3+}	456.33	Ti^{3+}	456.21
p1/2 Ti^{3+}	*461.51*	*p1/2 Ti^{3+}*	*462.38*
Ti^{4+}	458.79	Ti^{4+}	459.42
p1/2 Ti^{4+}	*464.35*	*p1/2 Ti^{4+}*	*464.96*

The thickness of the oxide layer has been estimated from the Auger measurements. As reference, we considered that each cycle corresponds to 66.67 Å. (specific characteristic of the instrument). The number of cycles is specific for each analyzed sample. For the non-treated series, we calculated 10.3 cycles for material C, which correspond to 740.85 Å and for material D, 10 cycles, which correspond to 666.7 Å. After the annealing, the oxide layer for material C is 3274.4 Å and for material D is 2002.73 Å. We thus see that the annealing has increased the oxide layer. The surface profiles are shown in Figures A.4 and A.5.

Table A.2 Surface chemical composition obtained by XPS high-resolution analysis for material D

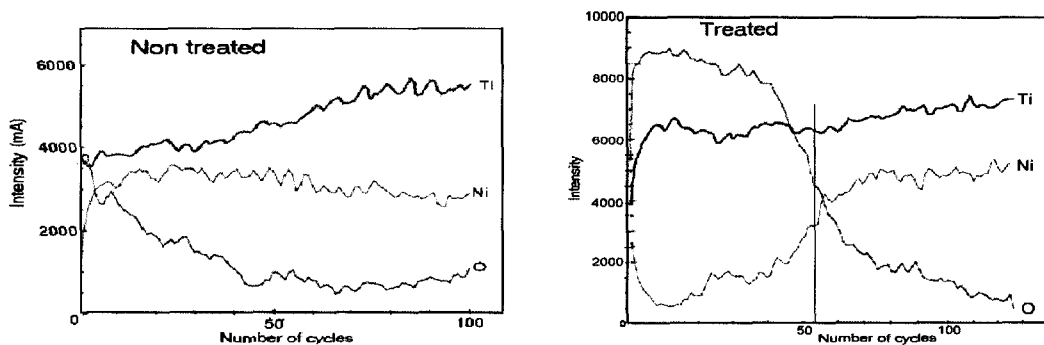| Non treated		Treated	
Elements	BE(eV)	Elements	BE(eV)
Ni	851.75		
Ni_2O_3	854.94	Ni_2O_3	855.56
		Cr	575
Ti^{2+}	454.55		
$p1/2\ Ti^{2+}$	460.63		
Ti^{3+}	456.33	Ti^{3+}	456.21
		$p1/2\ Ti^{3+}$	462.38
Ti^{4+}	458.05	Ti^{4+}	458.29
$p1/2\ Ti^{4+}$	463.61	$p1/2\ Ti^{4+}$	463.87

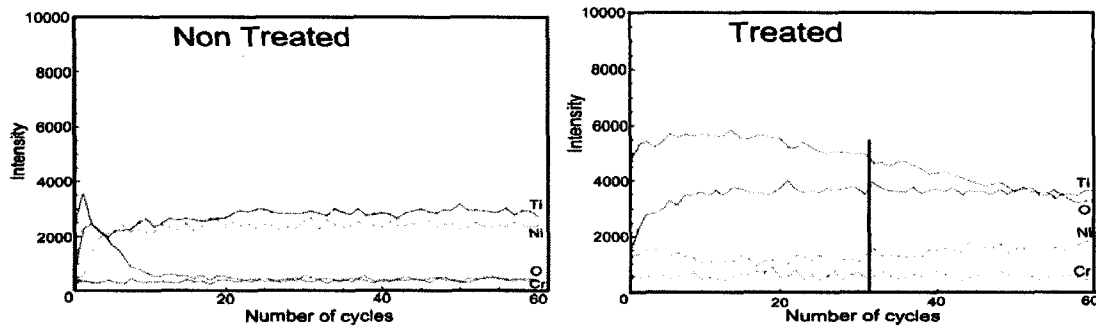Figure A.4 AES element distribution from the surface of material C.

Figure A.5 AES element distribution from the surface of material D.

A.5 Conclusions

The results showed different features of C and D samples. The mean pore size for material C (100μm) reveals an internal structure that enhances the capillary phenomena. Although the pore size is diminished (30-55μm), the interconnection is maintained in the case of material D [39]. Both materials present an interconnected structure that enhances the bone tissue ingrowth and good fixation of the implant.

The material D has a different chemical composition; the presence of Ni in a percentage of 51%, and the addition of chromium (0.5%) has a direct influence on the characteristics of the material. The excess of nickel can change the transformation temperature; it can be lowered from above 100°C to below 0°C [86]. The addition of chromium could control not only the phase transformation temperature but also improve the superelasticity of the alloy.

The Ni oxidation on the surface was confirmed after heat treatment for both samples. An important increment in the oxide layer thickness also was observed for material C.

A.6 References

See chapter XI